5-2023

Impact of Gamma Secretase Activating Protein on End-Organ Dysfunction in the Aftermath of Pneumonia in a Novel Gamma Secretase Activating Protein Knockout Rat

Meredith S. Gwin

Impact of Gamma Secretase Activating Protein on End Organ Dysfunction in the Aftermath of Pneumonia in a Novel Gamma Secretase Activating Protein Knockout Rat

A Dissertation

Submitted to the Graduate Faculty of the
University of South Alabama
in partial fulfillment of the
requirements for the degree of

Doctor of Philosophy

in

Basic Medical Science

by
Meredith S. Gwin
B.S., Biology University of Mobile, 2016 Summa Cum Laude
A.A., Liberal Arts Coastal Alabama Community College, 2014 Summa Cum Laude
A.A., Liberal Arts Coastal Alabama Community College, 2014 Summa Cum Laude

May 2023

ACKNOWLEDGEMENTS

I'd like to thank my mentor Troy Stevens for his enthusiasm of my dissertation work, his innate ability to crack a dad joke at any given moment, his punniness, and for great conversations about sports, science, politics, and life. I am very grateful for all that you have taught me. To my committee members, Drs. Balczon, Lee, Lin, Morrow, and Richter for your constant support and encouragement throughout this work and to Dr. Lee specifically, for having those tough conversations - I know they weren't easy for you have or for me to hear but they were necessary. Dr. Michelle Schuler and Leigh Ann Wiggins thank you for taking time to show me all the things related to animal husbandry and surgical skills - it has been my favorite part of this work and I am so grateful. To my cohort, Jennifer, Mika, Marzieh, Lina, Althea, Rebecca, and Kierra, I wouldn't have made it through the first semester without you all. To my science sister Dr. Sarah Voth, thank you for everything. To my sister January, thank you for being the one I can always count on. To my dad, thank you for showing me that I can do all things through spite which strengthens me. To my mom, thank you for your unconditional love, for your

selflessness, and for allowing me space to grow in the way I want; I know it hasn't been easy, but I am so thankful.

For my niece Selby and nephews Henry and Will - You are capable of anything you put your mind to. I hope that you see that it is possible to be successful while being true to yourself and not conforming to what the world says you should be. Growth is uncomfortable and pressure is a privilege. I love you all so big and being your aunt is the greatest joy of my life. Do not let the bastards get you down.

For Denise - I will never be able to put into words what you mean to me or the immense impact you've had on my life. I, without a doubt, would not be writing this dissertation if it were not for you. You believed in me and saw things in me when I could not see them in myself, and I am immeasurably grateful for you.

For Rebekah - For exposing me to the beauties and tragedies that are science, for your raw honesty in all situations, for believing in me, for sharing the same sense of humor and taste in music, for allowing me to be a part of your children's lives, for your delicious baked goods, and for giving me one of my greatest friendships.

TABLE OF CONTENTS

Page

LIST OF TABLES

LIST OF FIGURES

LIST OF ABBREVIATIONS

Aβ	=	Amyloid beta
GSAP	=	Gamma secretase activating protein
APP	=	Amyloid precursor protein
HAP	=	Hospital-acquired pneumonia
ICU	=	Intensive care unit
VAP	=	Ventilator associated pneumonia
ARDS	=	Acute respiratory distress syndrome
PICS	=	Post-intensive care unit syndrome
T3SS	=	Type-3 secretion system
ExoY	=	Exoenzyme Y
ExoU	=	Exoenzyme U
ExoT	=	Exoenzyme T
ExoS	=	Exoenzyme S
$ExoY^+$	=	*P. aeruginosa* mutant expressing only the exoenzyme Y
cAMP	=	Cyclic adenosine monophosphate
cGMP	=	Cyclic guanosine monophosphate
cUMP	=	Cyclic uridine monophosphate
cCMP	=	Cyclic cytosine monophosphate

cNMPs = Cyclic nucleotide monophosphates

PMVECs = Pulmonary microvascular endothelial cells

TGN = trans-Golgi network

APP_{695} = Amyloid precursor protein isoform containing 695 amino acids

APP_{751} = Amyloid precursor protein isoform containing 751 amino acids

APP_{770} = Amyloid precursor protein isoform containing 770 amino acids

APPsα = Amyloid precursor protein soluble alpha. Soluble N-terminal fragment formed after APP cleavage by α-secretase

C83 = Membrane bound C-terminal fragment formed after APP cleavage by α-secretase

P3 = Cleavage product of γ-secretase cleavage of C83 fragment

APPsβ = Amyloid precursor protein soluble beta. Soluble N-terminal fragment formed after β-secretase cleavage of APP

C99 = Membrane bound C-terminal fragment formed after β-secretase cleavage of APP

AICD = Amyloid intracellular domain

PS1/PS2 = Presenilin 1 or 2

NCT = Nicastrin

APH1 = Anterior pharynx defective 1

PEN2 = Presenilin enhancer 2

PION = Pigeon homolog protein

Fe65 = Cytosolic adapter protein and an important binding partner of amyloid precursor protein

kDa	=	Kilodaltons
cDNA	=	Complementary DNA
NTF	=	Amino (N)-terminal fragment
CTF	=	Carboxyl (C)-terminal fragment
WT	=	Wild-type
KO	=	Knockout
γ	=	Gamma
$A\beta_{40}$	=	Amyloid beta x-40 with regards to the length of the protein
$A\beta^{42}$	=	Amyloid beta x-42 with regards to the length of the protein
CRISPR	=	Clustered regularly interspaced palindromic repeats
Cas9	=	CRISPR associated protein 9
CFU	=	Colony forming units
BALF	=	Bronchoalveolar lavage fluid
RBC	=	Red blood cell(s)
WBC	=	White blood cell(s)
Hct	=	Hematocrit
Hgb	=	Hemoglobin
SSC-A	=	Side scatter area
FSC-A	=	Forward scatter area
FSC-H	=	Forward scatter height
FSC-W	=	Forward scatter width
K_f	=	Filtration coefficient
BPM	=	Beats per minute

IL-10 = Interleukin 10 – anti-inflammatory cytokine

GM-CSF = Granulocyte-macrophage colony-stimulating factor

MCP-1 = Monocyte chemoattractant protein-1

IL-6 = Interleukin-6 – anti-inflammatory cytokine

CD68 = Cluster of Differentiation 68 – expressed in cells of myeloid lineage including monocytes, macrophages and dendritic cells

CD11b/c = Cluster of Differentiation 11b/c – expressed in monocytes, macrophages, and granulocytes

CD45 = Cluster of Differentiation 45 – expressed on hematopoietic cells

RP1 = Marker of blood and peritoneal neutrophils

CD43 = Cluster of Differentiation 43 – leukocyte marker

His48 = Granulocyte marker

H & E = Hematoxylin and eosin

H_2O = Water

LTP = Long term potentiation

E-LTP = Early long term potentiation

L-LTP = Late long term potentiation

CA3 = comu Ammonis. Hippocampal subfield 3

CA1 = comu Ammonis. Hippocampal subfield 1

AMPA = α-amino-3-hydroxy-5-methyl-4-isoxazole propionic acid receptor

NMDA = N-methyl-D-aspartate receptor

fEPSP = Field excitatory post-synaptic potential

TBS	=	Theta burst stimulation
DNA	=	Deoxyribonucleic acid
STEMI	=	ST-elevation myocardial infarction
Non-STEMI	=	Non-ST elevation myocardial infarction
PCR	=	Polymerase chain reaction
PBS	=	Phosphate buffered saline
OD_{540}	=	Optical density at 540 nanometer wavelength
NaCl	=	Sodium chloride
KCl	=	Potassium chloride
$MgSO_4$	=	Magnesium sulfate
KH_2PO_4	=	Potassium dihydrogen phosphate
$NaHCO_3$	=	Sodium bicarbonate
$CaCl_2$	=	Calcium chloride
NaH_2PO_4	=	Sodium dihydrogen phosphate monohydrate
$MgCl_2$	=	Magnesium chloride
DMEM	=	Delbecco's modified eagles media
FBS	=	Fetal bovine serum
aCSF	=	Artificial cerebrospinal fluid
kHz	=	Kilohertz
Hz	=	Hertz
RPM	=	Rotations per minute
mL	=	Milliliters
cm	=	Centimeter

ms	=	Milliseconds
mmol	=	Millimole

ABSTRACT

Meredith S. Gwin, B. S., University of South Alabama College of Medicine, May 2023. Impact of Gamma Secretase Activating Protein on End-Organ Dysfunction in the Aftermath of Pneumonia in a Novel Gamma Secretase Activating Protein Knockout Rat. Chair of Committee: Dr. Troy Stevens, Ph.D.

Pneumonia elicits the production of cytotoxic beta amyloid (Aβ) that contributes to end-organ dysfunction, yet the mechanism linking infection to production of cytotoxic Aβ is unknown. Here, we tested the hypothesis that γ-secretase activating protein (GSAP), which promotes Aβ production, contributes to end-organ dysfunction following bacterial pneumonia. First-in-kind GSAP knockout rats were generated. Wild type and knockout rats possessed similar body weights, organ weights, circulating blood cell counts, arterial blood gases, and cardiac indices at baseline. Intratracheal *Pseudomonas aeruginosa* infection caused acute lung injury and a hyperdynamic circulatory state. Whereas infection led to arterial hypoxemia in wild type rats, the alveolar-capillary barrier integrity was preserved in GSAP knockout rats. Infection provoked neutrophil recruitment to the airways, yet neutrophils in the knockout rats appeared immature. Infection potentiated myocardial infarction following ischemia-reperfusion injury, and this potentiation was abolished in knockout rats. In the hippocampus, GSAP contributed to both pre- and postsynaptic neurotransmission, increasing the presynaptic action potential recruitment, decreasing neurotransmitter release probability, decreasing the

postsynaptic response, and preventing postsynaptic hyperexcitability, resulting in greater early long-term potentiation but reduced late long-term potentiation. Infection abolished early and late long-term potentiation in control rats, whereas the late long-term potentiation was preserved in GSAP knockout rats. Furthermore, hippocampi from the knockout rats exhibited a GSAP-dependent increase in neurotransmitter release probability and postsynaptic hyperexcitability. These results elucidate an unappreciated role for GSAP in innate immunity and highlight the contribution of GSAP to end-organ dysfunction during infection.

CHAPTER I

INTRODUCTION

Pneumonia accounts for ~2.4 million deaths each year, and among surviving patients, the 1-5 year morbidity and mortality rates are staggering[1-4]. Pneumonia is the world's leading cause of death among children under the age of 5 and is the second most common cause of hospital admissions for adults in the United States[4]. Nosocomial pneumonia is the second most common nosocomial infection and the most common nosocomial infection that leads to death in critically ill patients[5-10]. Patients in the intensive care unit that have nosocomial pneumonia suffer increased incidences of morbidity, including neurocognitive decline, increased risk of heart attack and stroke, prolonged muscle weakness and decreased quality of life, and mortality post discharge[11-22]. Mechanisms responsible for infection-dependent end-organ dysfunction during and in the aftermath of bacterial infection are unknown.

Pneumonia leads to the generation of cytotoxic beta amyloid (Aβ) by the pulmonary endothelium that can be retrieved from the bronchoalveolar lavage fluid (BALF), blood, and cerebrospinal fluid of human and animal subjects[23-33]. Aβ is produced via consecutive cleavages of amyloid precursor protein by beta and then gamma secretases, and it has both physiologic and pathologic roles[34-37]. Mechanisms

responsible for this infection-dependent increase in cytotoxic Aβ have not been addressed.

Gamma secretase activating protein (GSAP) is a newly discovered component of the gamma secretase complex[38]. Data suggest that GSAP functions as a structural switch between two forms of gamma secretase that have different affinities for amyloid precursor protein (APP) compared to other substrates by altering the active site of gamma secretase, thus providing effector specificity[39]. GSAP contributes to Aβ production by increasing the affinity of the gamma secretase complex for APP without impacting other gamma secretase substrates such as NOTCH[39].

Here we sought to uncover the impact of GSAP in bacterial infection-induced end-organ dysfunction. Using a novel GSAP knockout rat generated with help from Drs. Mikhail Alexeyev and Aron Geurts, we introduced *P. aeruginosa* bacteria intratracheally to induce pneumonia. Forty-eight hours post-infection cardiopulmonary ultrasonography was performed with the help of Dr. Ji Young Lee, arterial blood was collected for complete blood counts and an electrolyte panel, plasma was separated for Aβ quantification, bronchoalveolar lavage fluid was collected to assess cell infiltration into the airspace, and the hippocampus was dissected to measure changes in long-term potentiation, as performed by Dr. Mike Lin. In separate experiments, rats were infected, and 48-hours later open chest myocardial infarction experiments were done by Dr. Xi-Ming Yang to assess the impact of GSAP on ischemia reperfusion injury. In other sets of experiments, Dr. Chun Zhou performed isolated perfused lung experiments to assess the

impact of GSAP on the filtration coefficient in the presence and absence of *P. aeruginosa*.

Mechanisms responsible for infection-dependent end-organ dysfunction during and in the aftermath of bacterial infection are unknown. Here, we reveal that *P. aeruginosa* bacterial pneumonia utilizes GSAP to promote end-organ dysfunction, including impacting the severity of ischemia reperfusion injury, increasing the presynaptic action potential recruitment, and preventing post-synaptic hyperexcitability. These results incriminate GSAP in the host-pathogen response during pneumonia, and they provide a previously unappreciated role for GSAP as a mechanistic link between bacterial infection and end-organ dysfunction.

1.1 References

1 El Solh, A. A., Alhajhusain, A. Update on the Treatment of *Pseudomonas aeruginosa* Pneumonia. *J Antimicrob Chemother.* **64**, 229-238 (2009). https://doi.org:10.1093/jac/dkp201

2 *Pseudomonas aeruginosa* in healthcare settings*. Centers for Disease Control and prevention.* (2019). https://www.cdc.gov/hai/organisms/pseudomonas.html

3 Dick, A., Liu, H., Zwanziger, J., Perencevich, E., Furuya, E. Y., Larson, E., Pogorzelska-Maziarz, M. & Stone, P. W. Long-term Survival and Healthcare Utilization Outcomes Attributable to Sepsis and Pneumonia. *BMC Health Ser Res.* **12**, 432 (2012). https://doi.org:10.1186/1472-6963-12-432

4 Dadonaite, B. & Roser, M. Pneumonia. *Our World in Data* (2019). https://ourworldindata.org/pneumonia

5 Chevret, S., Hemmer, M., Carlet, J. & Langer, M. Incidence and Risk Factors of Pneumonia Acquired in Intensive Care Units. Results from a Multicenter Prospective Study on 996 Patients. European Cooperative Group on Nosocomial Pneumonia. *Intensive Care Med* **19**, 256-264 (1993). https://doi.org:10.1007/BF01690545

6 Dandagi, G. L. Nosocomial Pneumonia in Critically Ill Patients. *Lung India* **27**, 149-153 (2010). https://doi.org:10.4103/0970-2113.68321

7 Fagon, J. Y., Chastre, J., Hance, A. J., Montravers, P., Novara, A. & Gibert, C. Nosocomial Pneumonia in Ventilated Patients: A Cohort Study Evaluating Attributable Mortality and Hospital Stay. *Am J Med* **94**, 281-288 (1993). https://doi.org:10.1016/0002-9343(93)90060-3

8 Langer, M., Mosconi, P., Cigada, M. & Mandelli, M. Long-term Respiratory Support and Risk of Pneumonia in Critically Ill Patients. Intensive Care Unit Group of Infection Control. *Am Rev Respir Dis* **140**, 302-305 (1989). https://doi.org:10.1164/ajrccm/140.2.302

9 Nielsen, S. L., Røder, B., Magnussen, P., Engquist, A. & Frimodt-Møller, N. Nosocomial Pneumonia in an Intensive Care Unit in a Danish University Hospital: Incidence, Mortality and Etiology. *Scand J Infect Dis* **24**, 65-70 (1992). https://doi.org:10.3109/00365549209048402

10 Rice, L. B. Federal Funding for the Study of Antimicrobial Resistance in Nosocomial Pathogens: No ESKAPE. *J Infect Dis* **197**, 1079-1081 (2008). https://doi.org:10.1086/533452

11 Fan, E., Dowdy, D. W., Colantuoni, E., Mendez-Tellez, P. A., Sevransky, J. E., Shanholtz, C., Himmelfarb, C. R., Desai, S. V., Ciesla, N., Herridge, M. S., Pronovost, P. J. & Needham, D. M. Physical Complications in Acute Lung Injury Survivors: A Two-Year Longitudinal Prospective Study. *Crit Care Med* **42**, 849-859 (2014). https://doi.org:10.1097/CCM.0000000000000040

12 Hopkins, R. O. & Jackson, J. C. Assessing Neurocognitive Outcomes after Critical Illness: Are Delirium and Long-Term Cognitive Impairments Related? *Curr Opin Crit Care* **12**, 388-394 (2006). https://doi.org:10.1097/01.ccx.0000244115.24000.f5

13 Hopkins, R. O., Suchyta, M. R., Snow, G. L., Jephson, A., Weaver, L. K. & Orme, J. F. Blood Glucose Dysregulation and Cognitive Outcome in ARDS Survivors. *Brain Inj* **24**, 1478-1484 (2010). https://doi.org:10.3109/02699052.2010.506861

14 Hopkins, R. O., Weaver, L. K., Collingridge, D., Parkinson, R. B., Chan, K. J. & Orme, J. F., Jr. Two-year Cognitive, Emotional, and Quality-of-Life Outcomes in Acute Respiratory Distress Syndrome. *Am J Respir Crit Care Med* **171**, 340-347 (2005). https://doi.org:10.1164/rccm.200406-763OC

15 Hopkins, R. O., Weaver, L. K., Pope, D., Orme, J. F., Bigler, E. D. & Larson-Lohr, L. V. Neuropsychological Sequelae and Impaired Health Status in Survivors of Severe Acute Respiratory Distress Syndrome. *Am J Respir Crit Care Med* **160**, 50-56 (1999). https://doi.org:10.1164/ajrccm.160.1.9708059

16 Jackson, J. C., Pandharipande, P. P., Girard, T. D., Brummel, N. E., Thompson, J. L., Hughes, C. G., Pun, B. T., Vasilevskis, E. E., Morandi, A., Shintani, A. K., Hopkins, R. O., Bernard, G. R., Dittus, R. S., Ely, E. W., & Bringing to Light the Risk Factors and Incidence of Neuropsychological Dysfunction in I. C. U. Survivors (BRAIN-ICU) Study Investigators. Depression, Post-Traumatic Stress Disorder, and Functional Disability in Survivors of Critical Illness in the Brain-ICU Study: A Longitudinal Cohort Study. *Lancet Respir Med* **2**, 369-379 (2014). https://doi.org:10.1016/S2213-2600(14)70051-7

17 Mikkelsen, M. E., Christie, J. D., Lanken, P. N., Biester, R. C., Thompson, B. T., Bellamy, S. L., Localio, A. R., Demissie, E., Hopkins, R. O. & Angus, D. C. The Adult Respiratory Distress Syndrome Cognitive Outcomes Study: Long-Term Neuropsychological Function in Survivors of Acute Lung Injury. *Am J Respir Crit Care Med* **185**, 1307-1315 (2012). https://doi.org:10.1164/rccm.201111-2025OC

18 Needham, D. M., Davidson, J., Cohen, H., Hopkins, R. O., Weinert, C., Wunsch, H., Zawistowski, C., Bemis-Dougherty, A., Berney, S. C., Bienvenu, O. J., Brady, S. L., Brodsky, M. B., Denehy, L., Elliott, D., Flatley, C., Harabin, A. L., Jones, C., Louis, D., Meltzer, W., Muldoon, S. R., Palmer, J. B., Perme, C., Robinson, M., Schmidt, D. M., Scruth, E., Spill, G. R., Storey, C. P., Render, M., Votto, J. & Harvey, M. A. Improving Long-Term Outcomes After Discharge from Intensive Care Unit: Report from a Stakeholders' Conference. *Crit Care Med* **40**, 502-509 (2012). https://doi.org:10.1097/CCM.0b013e318232da75

19 Needham, D. M., Wozniak, A. W., Hough, C. L., Morris, P. E., Dinglas, V. D., Jackson, J. C., Mendez-Tellez, P. A., Shanholtz, C., Ely, E. W., Colantuoni, E., Hopkins, R. O. & National Institutes of Health NHLBI ARDS Network. Risk Factors for Physical Impairment After Acute Lung Injury in a National, Multicenter Study. *Am J Respir Crit Care Med* **189**, 1214-1224 (2014). https://doi.org:10.1164/rccm.201401-0158OC

20 Fletcher, S. N., Kennedy, D. D., Ghosh, I. R., Misra, V. P., Kiff, K., Coakley, J. H. & Hinds, C. J. Persistent Neuromuscular and Neurophysiologic Abnormalities in Long-Term Survivors of Prolonged Critical Illness. *Crit Care Med* **31**, 1012-1016 (2003). https://doi.org:10.1097/01.CCM.0000053651.38421.D9

21 Hermans, G., Van Mechelen, H., Clerckx, B., Vanhullebusch, T., Mesotten, D., Wilmer, A., Casaer, M. P., Meersseman, P., Debaveye, Y., Van Cromphaut, S., Wouters, P. J., Gosselink, R. & Van den Berghe, G. Acute Outcomes and 1-Year Mortality of Intensive Care Unit-Acquired Weakness. A Cohort Study and Propensity-Matched Analysis. *Am J Respir Crit Care Med* **190**, 410-420 (2014). https://doi.org:10.1164/rccm.201312-2257OC

22 Herridge, M. S., Cheung, A. M., Tansey, C. M., Matte-Martyn, A., Diaz-Granados, N., Al-Saidi, F., Cooper, A. B., Guest, C. B., Mazer, C. D., Mehta, S., Stewart, T. E., Barr, A., Cook, D., Slutsky, A. S. & Canadian Critical Care Trials Group. One-year Outcomes in Survivors of the Acute Respiratory Distress Syndrome. *N Engl J Med* **348**, 683-693 (2003). https://doi.org:10.1056/NEJMoa022450

23 Balczon, R., Morrow, K. A., Leavesley, S., Francis, C. M., Stevens, T. C., Agwaramgbo, E., Williams, C., Stevens, R. P., Langham, G., Voth, S., Cioffi, E. A., Weintraub, S. E. & Stevens, T. Cystatin C Regulates the Cytotoxicity of Infection-Induced Endothelial-Derived β-Amyloid. *FEBS Open Bio* **10**, 2464-2477 (2020). https://doi.org:10.1002/2211-5463.12997

24 Balczon, R., Morrow, K. A., Zhou, C., Edmonds, B., Alexeyev, M., Pittet, J. F., Wagener, B. M., Moser, S. A., Leavesley, S., Zha, X., Frank, D. W. & Stevens, T. *Pseudomonas aeruginosa* Infection Liberates Transmissible, Cytotoxic Prion Amyloids. *FASEB J* **31**, 2785-2796 (2017). https://doi.org:10.1096/fj.201601042RR

25 Balczon, R., Pittet, J. F., Wagener, B. M., Moser, S. A., Voth, S., Vorhees, C. V., Williams, M. T., Bridges, J. P., Alvarez, D. F., Koloteva, A., Xu, Y., Zha, X. M., Audia, J. P., Stevens, T. & Lin, M. T. Infection-induced Endothelial Amyloids Impair Memory. *FASEB J* **33**, 10300-10314 (2019). https://doi.org:10.1096/fj.201900322R

26 Lin, M. T., Balczon, R., Morrow, K. A., Wagener, B. M., Pittet, J.F. & Stevens, T. *Pseudomonas aeruginosa*-Induced Pulmonary Endothelial Amyloid Proteins Impair Long-Term Plasticity. *FASEB J* **31**, 861.3 (2017). https://doi.org:10.1096/fasebj.31.1_supplement.861.3

27 Lin, M. T., Balczon, R., Pittet, J. F., Wagener, B. M., Moser, S. A., Morrow, K. A., Voth, S., Francis, C. M., Leavesley, S., Bell, J., Alvarez, D. F. & Stevens, T. Nosocomial Pneumonia Elicits an Endothelial Proteinopathy: Evidence for a Source of Neurotoxic Amyloids in Critically Ill Patients. *Am J Respir Crit Care Med* **198**, 1575-1578 (2018). https://doi.org:10.1164/rccm.201801-0060LE

28 Morrow, K. A., Ochoa, C. D., Balczon, R., Zhou, C., Cauthen, L., Alexeyev, M., Schmalzer, K. M., Frank, D. W. & Stevens, T. *Pseudomonas aeruginosa* Exoenzymes U and Y Induce a Transmissible Endothelial Proteinopathy. *Am J Physiol Lung Cell Mol Physiol* **310**, L337-L353 (2016). https://doi.org:10.1152/ajplung.00103.2015

29 Morrow, K. A., Seifert, R., Kaever, V., Britain, A. L., Sayner, S. L., Ochoa, C. D., Cioffi, E. A., Frank, D. W., Rich, T. C. & Stevens, T. Heterogeneity of Pulmonary Endothelial Cyclic Nucleotide Response to *Pseudomonas aeruginosa* ExoY Infection. *Am J Physiol Lung Cell Mol Physiol* **309**, L1199-1207 (2015). https://doi.org:10.1152/ajplung.00165.2015

30 Morrow, K. A., Stevens, T. C., Agwaramgbo, E., Langham, G., Francis, M., Balczon, R. & Stevens, T. Studies On The Physical Properties of the *Pseudomonas aeruginosa*-Induced Endothelial Prion Amyloid Cytotoxin(s). *FASEB J* **31**, 1074.1 (2017). https://doi.org:10.1096/fasebj.31.1_supplement.1074.1

31 Scott, A. M., Jager, A. C., Gwin, M., Voth, S., Balczon, R., Stevens, T. & Lin, M. T. Pneumonia-Induced Endothelial Amyloids Reduce Dendritic Spine Density in Brain Neurons. *Sci Rep* **10**, 9327 (2020). https://doi.org:10.1038/s41598-020-66321-1

32 Voth, S., Gwin, M., Francis, C. M., Balczon, R., Frank, D. W., Pittet, J. F., Wagener, B. M., Moser, S. A., Alexeyev, M., Housley, N., Audia, J. P., Piechocki, S., Madera, K., Simmons, A., Crawford, M. & Stevens, T. Virulent *Pseudomonas aeruginosa* Infection Converts Antimicrobial Amyloids into Cytotoxic Prions. *FASEB J* **34**, 9156-9179 (2020). https://doi.org:10.1096/fj.202000051rrr

33 Wagener, B. M., Anjum, N., Christiaans, S. C., Banks, M. E., Parker, J. C., Threet, A. T., Walker, R. R., Isbell, K. D., Moser, S. A., Stevens, T., Alexeyev, M. F., Audia, J. P., Richter, W., Hardy, K. S., Saleh, L. A., Morgan, C. & Pittet, J.F. Exoenzyme Y Contributes to End-Organ Dysfunction Caused by *Pseudomonas aeruginosa* Pneumonia in Critically Ill Patients: An Exploratory Study. *Toxins* **12**, 369 (2020). https://doi.org:10.3390/toxins12060369

34 Soscia, S. J., Kirby, J. E., Washicosky, K. J., Tucker, S. M., Ingelsson, M., Hyman, B., Burton, M. A., Goldstein, L. E., Duong, S., Tanzi, R. E. & Moir, R. D. The Alzheimer's Disease-Associated Amyloid β-Protein is an Antimicrobial Peptide. *PLoS One* **5**, e9505 (2010). https://doi.org:10.1371/journal.pone.0009505

35 Kumar, D. K. V., Choi, S. H., Washicosky, K. J., Eimer, W. A., Tucker, S., Ghofrani, J., Lefkowitz, A., McColl, G., Goldstein, L. E., Tanzi, R. E. & Moir, R. D. Amyloid-β Peptide Protects Against Microbial Infection in Mouse and Worm Models of Alzheimer's Disease. *Sci Transl Med* **8**, 340ra72 (2016). https://doi.org:10.1126/scitranslmed.aaf1059

36 De Strooper, B. Aph-1, Pen-2, and Nicastrin with Presenilin Generate an Active γ-Secretase Complex. *Neuron* **38**, 9-12 (2003). https://doi.org:10.1016/S0896-6273(03)00205-8

37 Zhang, Y.W., Thompson, R., Zhang, H. & Xu, H. APP Processing in Alzheimer's Disease. *Mol Brain* **4**, 3 (2011). https://doi.org:10.1186/1756-6606-4-3

38 He, G., Luo, W., Li, P., Remmers, C., Netzer, W.J., Hendrick, J., Bettayeb, K., Flajolet, M., Gorelick, F., Wennogle, L. P. & Greengard, P. Gamma-Secretase Activating Protein is a Therapeutic Target for Alzheimer's Disease. *Nature* **467**, 95-98 (2010). https://doi.org:10.1038/nature09325

39 Wong, E., Liao, G. P., Chang, J. C., Xu, P., Li, Y. M. & Greengard, P. GSAP Modulates γ-Secretase Specificity by Inducing Conformational Change in PS1. *Proc Natl Acad Sci U S A* **116**, 6385-6390 (2019). https://doi.org:10.1073/pnas.1820160116

CHAPTER II

BACKGROUND

2.1 Introduction

Pneumonia is defined as lung inflammation caused by viral, bacterial, or fungal infection in which the air sacs or alveoli fill with pus and may become solid[1-4]. Symptoms of pneumonia include cough that may produce phlegm, fatigue, fever, dyspnea, nausea, chest pain when breathing or coughing, and occasionally, even changes in mental status. Pneumonia that is caused by bacteria or viruses can be treated with antibiotics or antiviral medications, respectively[4,5]. There are three main types of pneumonia: community-acquired pneumonia that occurs outside of the hospital or healthcare setting, nosocomial or hospital-acquired pneumonia (HAP) that occurs when a person is in a hospital setting, and healthcare-associated pneumonia that occurs in places like nursing homes or dialysis centers[5]. Other types of pneumonia include aspiration pneumonia that occurs if a patient inhales food, drink, saliva, or vomit into their lungs, and pneumonia that is passed from person-to-person[5].

HAP is the second most common nosocomial infection in the United States. A nosocomial infection is defined as an infection acquired in the hospital by a patient who was admitted for a reason other than that infection[6]. HAP is associated with both increased length of stay and cost-of-care with costs estimated to be greater than $40,000

per patient[7]. Further, the costs of HAP are not only defined by the monetary impact. The affected often suffer significant sequela with poor health outcomes. There are many different factors that contribute to the historically high cost of HAP, including age, prior health history, and mechanical ventilation. Patients in the intensive care unit (ICU) that contract HAP suffer increased incidences of morbidity and mortality, including cognitive impairment[8] and secondary end-organ damage post-discharge. HAP occurs in 5 to 15 patients per 1,000 hospital admissions[9], accounts for 25% of all ICU infections[9], and more than 50% of all prescribed antibiotics[10]. Contracting HAP increases patients' length of stay to 7-9 days compared to the normal 4.5 days[10]. It is estimated that the attributable mortality of HAP is between 33% and 50%[7]. Furthermore, survivors often have a higher rate of healthcare utilization[11]. Cardiovascular and neurocognitive dysfunction are major concerns in the first year post-release from the ICU, although not all patients are affected[8]. **The understanding of the grave impact of HAP on the outcomes of the critically ill has evolved to include neurocognitive decline.**

2.2 Early Descriptions of Pneumonia

The term "pneumonia" was used as far back as the Hippocratic era when Hippocrates described "peripneumonia" as an illness causing violent fever, dyspnea, a sense of weight in the chest, sharp pain around the clavicle that worsens with breathing, delirium, and a cough that produces white and frothy sputum[12]. While Hippocrates used the term "peripneumonia," it seems that he was not describing what we now know as pneumonia; it is more likely that he was describing pleurisy. It was not until the 1700s that De Konilfeld made the distinction between pneumonia and pleurisy[13]. The study of

pneumonia was advanced when Leopold Auenbrugger introduced percussion of the human thorax as a way to detect diseases within the chest[14-17]. As a musician and composer, it makes sense that he would be interested in the differentiation of chest sounds. Watching his father tap the sides of barrels to determine how much fluid was present, he wondered if the same thing could be done in humans to differentiate disease[13-15]. In his 1761 paper, "*Inventum novum ex percussion thoracis humani ut signo abstrusos interni pectoris morbos detegendi,*" he describes in detail healthy and diseased chest sounds in a variety of sizes of people[13-15]. Auenbrugger's technique went widely unnoticed until 1808 when Corvisart published a volume that analyzed Auenbrugger's method and added many additions to it. Corvisart's publication gave percussion its place as a widely used technique.

After the introduction of percussion, Corvisart's pupil, Rene Laennec built on the method and developed the first stethoscope[16]. His idea for the stethoscope came from observing children with their ears placed to hollow pieces of wood[18]. Describing the source of his inspiration, Laennec related that, "*I recalled a well-known acoustic phenomenon: if you place your ear against one end of a wood beam the scratch of a pin at the other end is distinctly audible*[17,18]*."* He spent years testing different materials for his stethoscope and listening to the chest sounds of people with pneumonia[17]. In his 1819 treatise, he describes the use of his stethoscope to make the diagnosis of pneumonia and sharply differentiates it from pleurisy, for the first time[17]. His invention of the stethoscope and identification of different diseases helped move the field forward and paved the way for future discovery and innovation.

2.3 Connection Between Bacteria and Infection

The next breakthrough in the study of pneumonia came in the late 19th century with the work of Joseph Lister, Louis Pasteur, and Edwin Klebs. Lister, a surgeon in England, became fascinated with the high mortality rate of surgical patients in hospitals. By his own calculations, the mortality rate was 45 percent, and he was curious to find out why. Around this same time, Louis Pasteur published his work on airborne bacteria. Learning of this, Lister thought that it could be bacteria from the air getting into the wounds and causing the deadly infections. Lister began to protect open fractures with carbolic acid, greatly decreasing the number of post-surgical mortalities. He later extended this practice to all fields of surgery and called the technique the antiseptic principle[19,20]. None of this was happening in a vacuum. Klebs' findings strongly supported Lister's theory. As a physician through the Franco-Prussian war, he dealt regularly with wound infections[21]. Curious, he put tissue from a gunshot wound on a slide and viewed it under the microscope. He noticed rod-shaped bacteria that increased in number when pus and fever were present. Boldly, Klebs asserted that the presence of bacteria was the cause of infection. He noted that bacteria were found in every instance of inflamed wounds. In his 1875 paper, "*Contributions to the Knowledge of the Pathogenic Schistomycetes"* Klebs observed bacteria in the airways of a person who had died from pneumonia[19,22]. This was the first time someone related bacterial infection to pneumonia. Klebs' work was instrumental in paving the way for bacteriology and inspiring people like Robert Koch. Following Klebs, Carl Friedlander and Albert Fraenkel identified two common bacterial causes of pneumonia[23-25]. They both isolated the bacteria from patients' sputum with Friedlander isolating *Streptococcus pneumoniae* and Fraenkel isolating what

Christian Gram would later call *Klebsiella pneumoniae*. It was Friedlander's work that introduced the Gram stain and Christian Gram who adapted the procedure to the one that is still used today to differentiate between two different types of bacteria based on their distinctive cell wall characteristics. At the time it provided evidence that two different types of bacteria could cause pneumonia whereas today it provides a diagnostic basis for appropriate antibiotic treatment.

2.4 Antibiotics and Hospital Acquired Infections

While the end of the 19th century saw major triumphs in asepsis and hospital reform, pneumonia became recognized as a major cause of death towards the end of the 1800s. In 1900, it was the leading cause of death in the United States[26,27]. The increased morbidity and mortality associated with pneumonia piqued the interest of many scientists. Doctors began noting that pneumonia seemed to preferentially affect children and the elderly[28,29]. They also started noticing that infections spread rapidly in the hospital setting[30], which, in part, led to the development and eventual implementation of antibiotics in the 1940s. Antibiotics are substances produced by or derived from a microorganism that can inhibit or kill other microorganisms.

With the invention of antibiotics, the number of deaths caused by pneumonia began to decrease dramatically. The drop in pneumonia-related deaths led to a drop in research related to treating or preventing pneumonia. However, with the increase in use and development of antibiotics, bacteria began developing antibiotic resistance quickly[31-33]. A pandemic of staphylococcal infections among newborns in hospitals between 1946-1966 grabbed the public's attention and highlighted the need to prevent hospital-acquired

infections[34,35]. Newer antibiotics were developed, to result in bacteria subsequently developing resistance. Nationwide programs were established to develop epidemiologic research, hospital surveillance, and education in methods to prevent and control the spread of disease[34]. Throughout the 1950s, Gram-negative bacterial infections began increasing and, by 1960, had overtaken *S. aureus* as the most prevalent cause of hospital-acquired infections[36-38]. In the 1980s *P. aeruginosa* infections gradually increased in incidence as a hospital-acquired pathogen and from 1975 to 2003, the incidence of HAP due to *P. aeruginosa* increased from 9.6% to 18.1% [39,40].

2.5 Hospital-Acquired Pneumonia

HAP is defined as a new onset pneumonia that is present 48 hours or more after a hospital admission[7]. HAP is commonly caused by Gram-negative or Gram-positive bacteria with *Pseudomonas aeruginosa* being the most commonly isolated Gram-negative bacteria at 24%[41]. *P. aeruginosa* is also one of the ESKAPE pathogens that pose a major global health risk due to their antibiotic resistance **(Fig. 1)**[42,43]. Risk factors for HAP include age, the status of the immune system, location in the hospital (e.g. intensive care unit (ICU) or regular ward), mechanical ventilation, prior intravenous antibiotic treatment, and length of stay[44,45]. Of these, HAP occurs frequently in patients in the ICU. Paradoxically, ICUs use specially trained staff, ventilator support, and a large array of powerful drugs, particularly antibiotics, to counter infection[46,47]. Even so, some of these instruments increase the risk of a patient contracting HAP. Mechanical ventilation increases the risk of contracting HAP by 3-to 21-fold[48-51]. *P. aeruginosa* is responsible for 25% of all ICU infections, including a prevalence of approximately 30% in ventilator-

associated pneumonia (VAP)[9,10,52,53]. The mortality in ventilated patients that contract HAP caused by *P. aeruginosa* is around 34 to 68% compared to 25% of ICU patients that are not ventilated[53-55]. Pulmonary infections (HAP/VAP) are a major cause of acute respiratory distress syndrome (ARDS), and ARDS is a common cause of respiratory failure of patients in the ICU as well as a major cause of death[56-60]. Aside from the increase in mortality, the patients that do survive and recover face a different set of problems post-discharge.

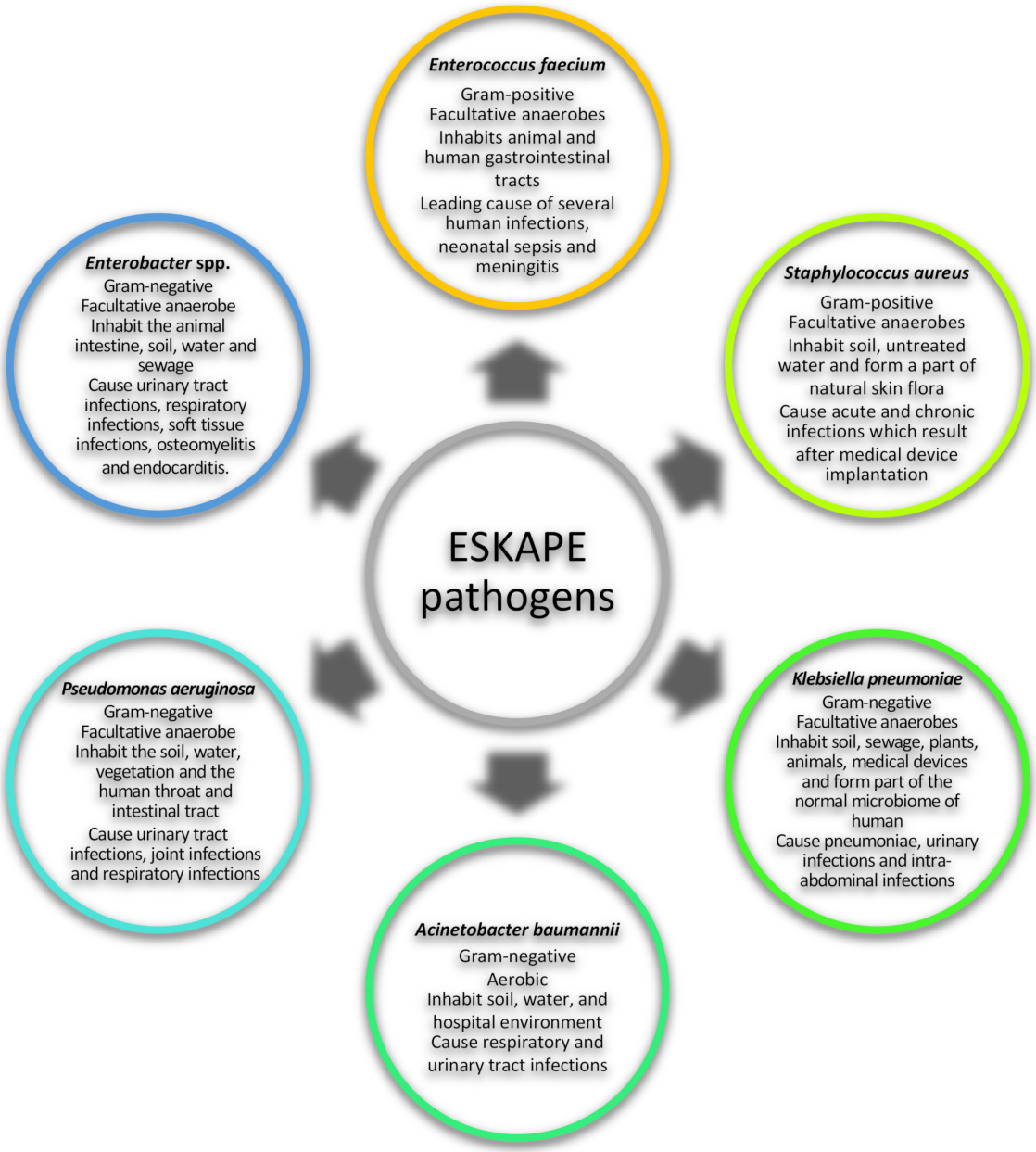

Figure 1. Image depicting the ESKAPE pathogens. These include *Enterococcus faecium, Staphylococcus aureus, Klebsiella pneumoniae, Acinetobacter baumannii, Pseudomonas aeruginosa* and *Enterobacter spp*[42].

2.6 Increases in Morbidity of ICU Patients Post-Discharge

While advancement of clinical care in the intensive care unit has led to a significant increase in survival after critical illness, this has led scientists and physicians to discover different types of disabilities that occur in the survivors. It was not until the late 1900s and early 2000s that people began to look hard at the relationship between the causative factors of HAP and the outcomes of those patients post-discharge[61-64]. Many ICU survivors and their families report a wide range of impairments in their health status that lasts for months to years after discharge from the ICU[8,65-67]. In 2012 the term post-intensive care syndrome (PICS) was coined to describe the sequela of impairments survivors of critical illness face[66,68]. Categories of post-ICU morbidities include new or worsened impairments in physical, cognitive, and mental health[8,66,67,69-74]. To address this problem, physicians and scientists began looking at mechanisms that could be causing the large increase in morbidity.

2.7 Mechanisms of *P. aeruginosa* Virulence and Pathogenicity

As mentioned earlier, *P. aeruginosa* is a common cause of pneumonia in ICU patients. *P. aeruginosa* exerts its toxic effects by producing pathogenic toxins, including exoenzymes, which are secreted into the cytosol of target cells via the type 3 secretion system (T3SS) to cause injury **(Fig. 2)** [58,75-79]. *P. aeruginosa* intoxicates the host cells with four known exoenzymes including ExoY, ExoU, ExoT, and ExoS[78,79]. For the purpose of my dissertation, I solely focused on the effects ExoY by using an *P. aeruginosa* mutant only expressing the exoenzyme Y ($ExoY^+$). Many of the previous studies from our lab have utilized $ExoY^+$ and determined that it is the exoenzyme Y, and not the others that is

responsible for the increase in cytosolic cAMP leading to hyperphosphorylation of tau, microtubule breakdown causing cell rounding and intracellular gap formation that leads to pulmonary edema, and production of cytotoxic Aβ. ExoY was the last of the 4 exoenzymes to be discovered[78]. It is found in about 90% of clinical isolates[80,81]. ExoY functions as a soluble purine and pyrimidine cyclase, meaning it coverts nucleoside triphosphates into cyclic nucleotides (cAMP, cGMP, cUMP, and cCMP)[82-86]. cAMP plays an essential role in cellular functions, including control of cell shape. Once inside the host cell, ExoY interacts with its co-factor f-actin, stimulating its enzymatic activity thereby increasing the cytosolic pool of cNMPs leading to tau hyperphosphorylation, dissociation of tau from microtubules, and finally cell rounding that causes interendothelial gap formation[82-88]. This exoenzyme intoxication leads to the lung injury that is associated with poor outcomes in *P. aeruginosa*-induced pneumonia[58]. In addition, it has recently been shown that ExoY intoxication is sufficient to elicit the production and release of amyloid proteins, including beta amyloid, from pulmonary microvascular endothelial cells (PMVECs) during *P. aeruginosa* infection[87,89-95]. The release of these amyloid species following infection causes endothelial cell cytotoxicity and hinders vascular repair[93,94,83,85]. These infection-induced endothelial amyloid proteins are resistant to proteases, nucleases, and heat, and they are self-propagating. Amyloids are associated with and cause Alzheimer's disease, which is a form of amyloidosis[96]. According to the amyloid cascade hypothesis, the accumulation of Aβ in the brain is the cause of Alzheimer's disease, although this hypothesis is not uniformly accepted. A current hypothesis is that tau and Aβ are produced during HAP, and are disseminated through the

vasculature where they access the brain and other organs, causing neurocognitive dysfunction and end-organ damage seen in survivors of ICU-HAP.

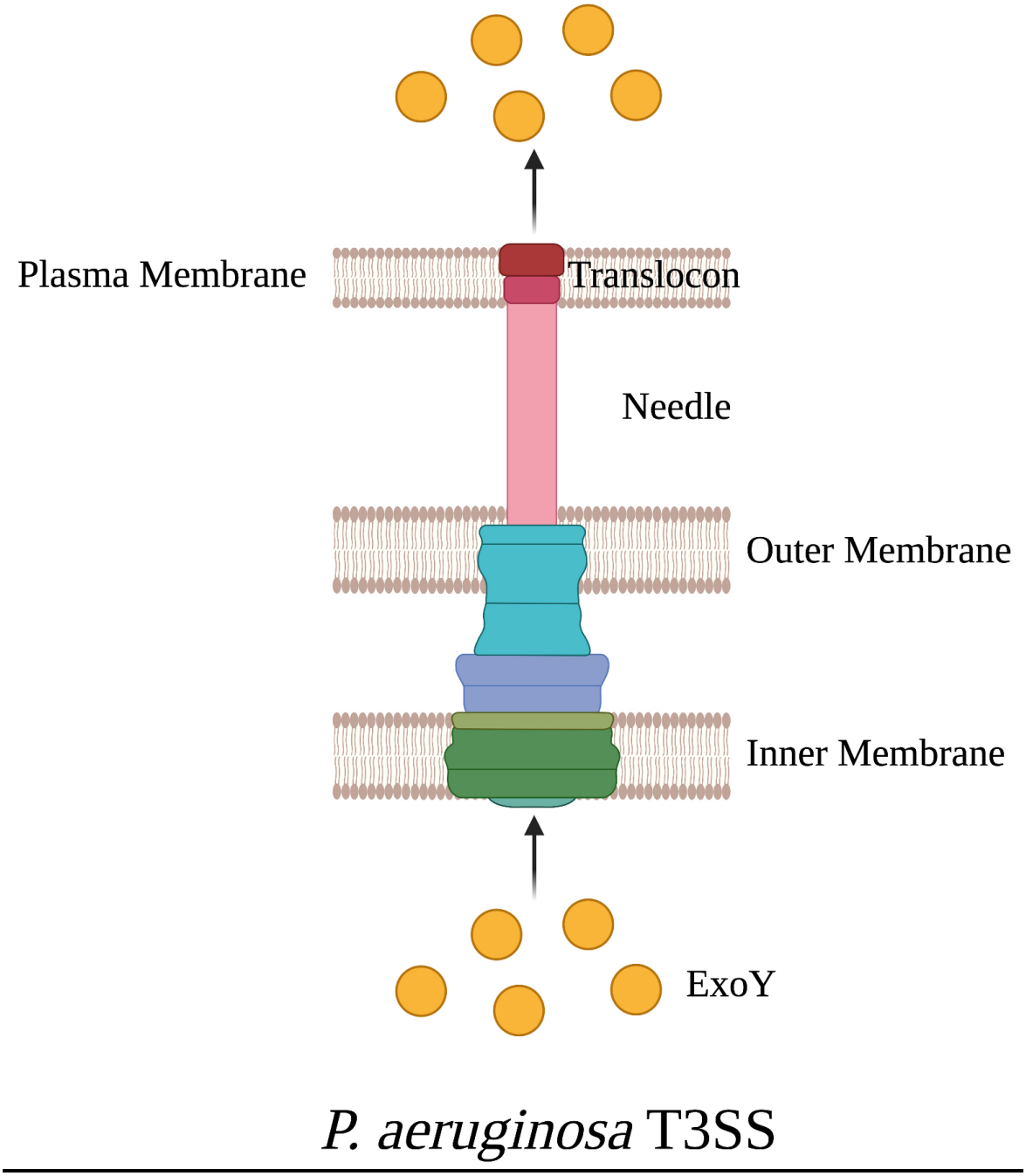

Created with BioRender.com

Figure 2. Schematic illustrating the T3SS of *P. aeruginosa*. ExoY is transported from the bacteria through the T3SS and into the cytoplasm of the host cell.

2.8 Cytotoxic Tau Production and Infectious Proteinopathy

Work done in the lab in 2016 by Dr. Morrow revealed that infection with ExoY competent *P. aeruginosa* induces the release of a high molecular weight cytotoxic tau[87]. When this tau protein was isolated with antibodies and transferred to naïve endothelial cells, it led to the intracellular accumulation of tau aggregates and was sufficient to cause injury, including cell gap formation and increased lung permeability[87]. A few years later this work was expanded on. Pulmonary infection with ExoY-competent *P. aeruginosa* caused the production and release of high molecular weight tau that then disseminated through the circulation to the brain, where it indirectly or directly impaired learning and memory in mice[97]. Learning and memory was measured via hippocampal long-term potentiation experiments. Increased tau immunoreactivity was seen in the plasma, heart, and brain tissues. In a follow-up study our lab found that tau variants were present in extracorporeal membrane oxygenation oxygenators of ICU patients with pneumonia, indicating that tau species are produced by humans during pneumonia and circulate in the blood[97].

2.9 Cytotoxic Beta-Amyloid Production and Infectious Proteinopathy

Aβ is a peptide that has up to 43 amino acids and is derived from amyloid precursor protein (APP) through consecutive cleavages by β- and γ-secretases; it has both physiologic and pathologic roles[98-101]. APP is a type-1 single pass transmembrane protein that contains a large extracellular domain. It is synthesized in the endoplasmic reticulum and transported through the Golgi apparatus to the trans-Golgi network (TGN) and is expressed in many tissue types, including the heart, lung, and brain[102-106]. APP can be

transported via the TGN to the cell surface where it can be processed or reinternalized and processed through the endosomal/lysosomal pathway[107-110]. There are multiple isoforms of APP with the most studied being APP_{695}, APP_{751}, and APP_{770}[102,103,111]. Cleavage of APP can be divided into an amyloidogenic or non-amyloidogenic pathway[112,113]. In the prevalent non-amyloidogenic pathway, APP is first cleaved by α-secretase (within the domain that would become Aβ) between Lys16 and Leu17 leading to the production of APPsα (soluble N-terminal fragment) and C83 (membrane-bound C-terminal fragment), with C83 being further cleaved by γ-secretase generating the p3 peptide (soluble extracellular) preventing the formation of functional Aβ **(Fig. 3)**[100,114-116]. In the amyloidogenic pathway, β-secretase (BACE1 or β-site APP cleaving enzyme 1) is the first to cleave APP generating APPsβ (soluble N-terminal fragment) and C99 (membrane-bound C-terminal fragment). C99 is further cleaved by γ-secretase within the membrane, releasing a cytoplasmic AICD (amyloid intracellular domain) and Aβ peptides[100,112,114]. γ-secretase is able to cleave C99 at different sites leading to Aβ species of various sizes up to 43 amino acids in length **(Fig. 3)**[117,118]. γ-secretase cleavage of C99 is the limiting step in the production of Aβ, thus making it a good target for inhibiting Aβ synthesis. γ-secretase is a high molecular weight multiprotein complex composed of four essential subunits: presenilin (PS1 or PS2), nicastrin (NCT), anterior pharynx defective-1 (APH1), and presenilin enhancer 2 (PEN2)[119-121]. PS1 acts as the catalytic subunit of the complex[122-124] while NCT functions as the scaffolding protein[125,126]. APH1 is needed to ensure proper subcellular transport of the PS1/NCT to the cell surface,[127] and PEN2 is involved in the processing of stabilized PS1/PS2 and in stabilizing the complex[128-132]. Along with these four essential components of the γ-secretase complex, GSAP is the

most recently discovered, yet non-essential subunit. While γ-secretase is an attractive target for limiting production of Aβ, deletion of γ-secretase is not an option as γ-secretase has numerous targets aside from APP, including NOTCH, which if not functioning properly, causes detrimental effects to the cells/animals.

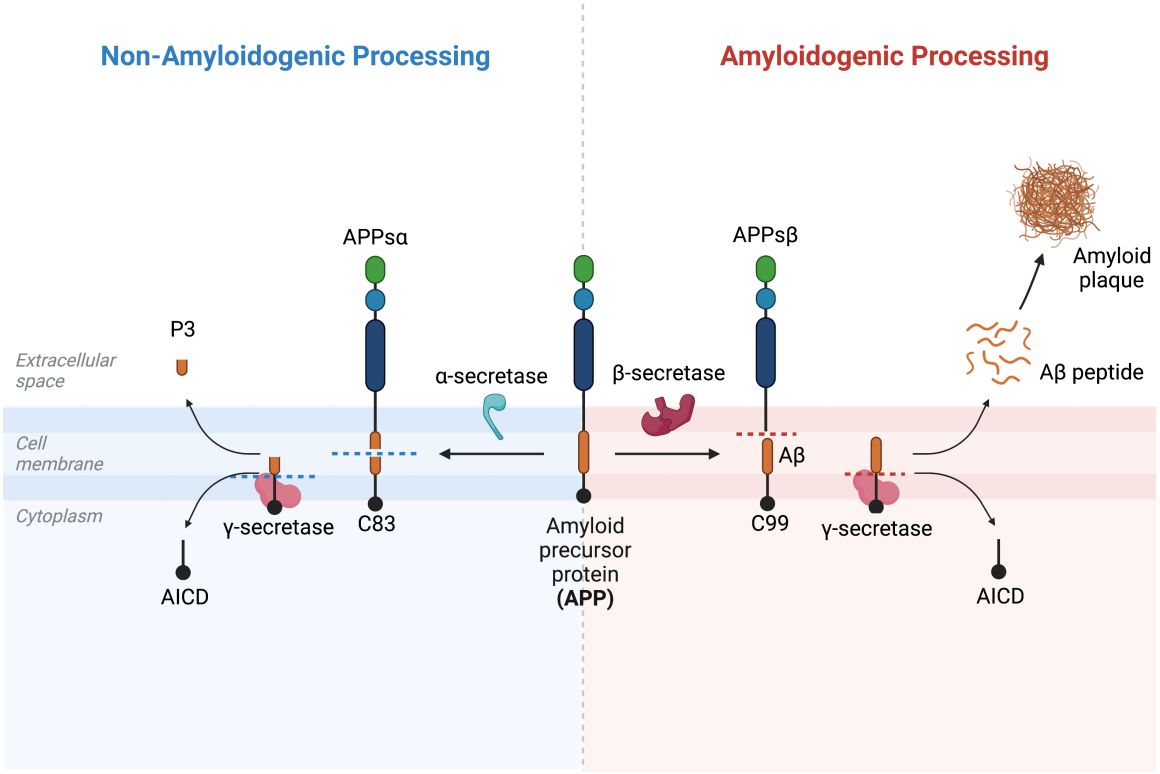

Created with BioRender.com

Figure 3. Schematic of the amyloidogenic and non-amyloidogenic processing of APP. The left blue section details the non-amyloidogenic processing in which APP is first cleaved by α-secretase through what would become the Aβ peptide inhibiting its production instead producing an APPsα and a C83 fragment. The C83 fragment goes on to be cleaved by γ-secretase leading to a P3 fragment and an AICD fragment. The right red section details the amyloidogenic processing of APP in which APP if first cleaved by β-secretase to produce an APPsβ fragment and a C99 fragment. The C99 fragment which contains a functional Aβ segment is next cleaved by γ-secretase producing an Aβ peptide and an AICD peptide.

2.10 GSAP

GSAP was discovered in 2010 by the Nobel Prize winning scientist Paul Greengard, while looking for the target of a cancer drug that happened to also lower Aβ without impacting NOTCH[133,134]. Gleevec, also known as imatinib, was shown to decrease the amount of Aβ species by inhibiting the cleavage of C99 by γ-secretase[133]. Using a photoactivatable derivative of imatinib they determined that it was not binding to any of the four known components of γ-secretase, rather it interacted with a 16-kDa protein that co-precipitated with PS1. Using polyacrylamide gel electrophoresis, they were able to separate the PS1 and the unknown fragment, which they excised and analyzed via tandem mass spectrophotometry and found that it corresponded to an uncharacterized protein called the pigeon homolog protein or PION. They characterized PION as GSAP[134]. The full open reading frame of human GSAP encodes a protein that is 854 amino acids in length and has a weight of about 98-kDa. Using pulse chase analysis they determined that GSAP is produced as a 98-kDa holoprotein that is later processed into the 16-kDa C-terminal fragment[134]. A few years later it was discovered that 5-Lipoxygenase acts as an endogenous modulator of GSAP by activating caspase-3, which goes on to cleave the 98-kDa GSAP into the 16-kDa form[135,136]. This 16-kDa GSAP interacts with Fe65 and PS1 in the mitochondria-associated membrane, where it binds to APP and regulates APP trafficking[137]. Along with regulating APP trafficking, the GSAP complex regulates a multitude of other cellular functions, including protein phosphorylation, lipid metabolism, and mitochondrial function **(Fig. 4)**[137]. GSAP can regulate γ-secretase specificity via altering the conformation of the active site of PS1. In the presence of GSAP the γ-secretase complex is in its native confirmation, allowing for

normal processing of APP and other substrates, but when GSAP is not present the γ-secretase activity for APP is reduced leading to a reduction in Aβ production **(Fig. 5)**[138,139]. The ability of GSAP to regulate γ-secretase activity and specificity and directly reduce Aβ production makes it an ideal target for Alzheimer's disease and other types of dementia[134,137,139-143].

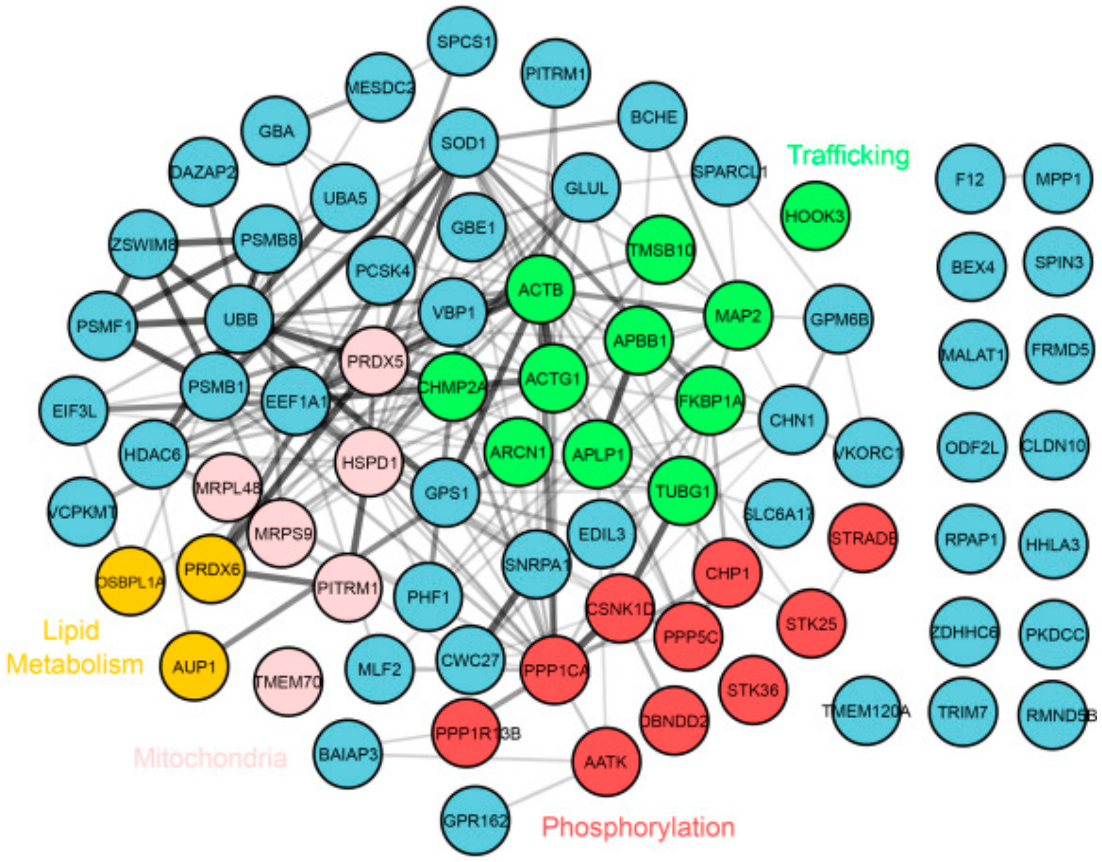

Figure 4. STRING application of GSAP-binding proteins generated with Cytoscape. Using yeast two-hybrid screening of a human cDNA library with the 16-kDa portion of the GSAP protein as bait, 80 proteins were identified that can directly bind GSAP and are involved in mitochondrial function, lipid metabolism, protein phosphorylate and trafficking[137].

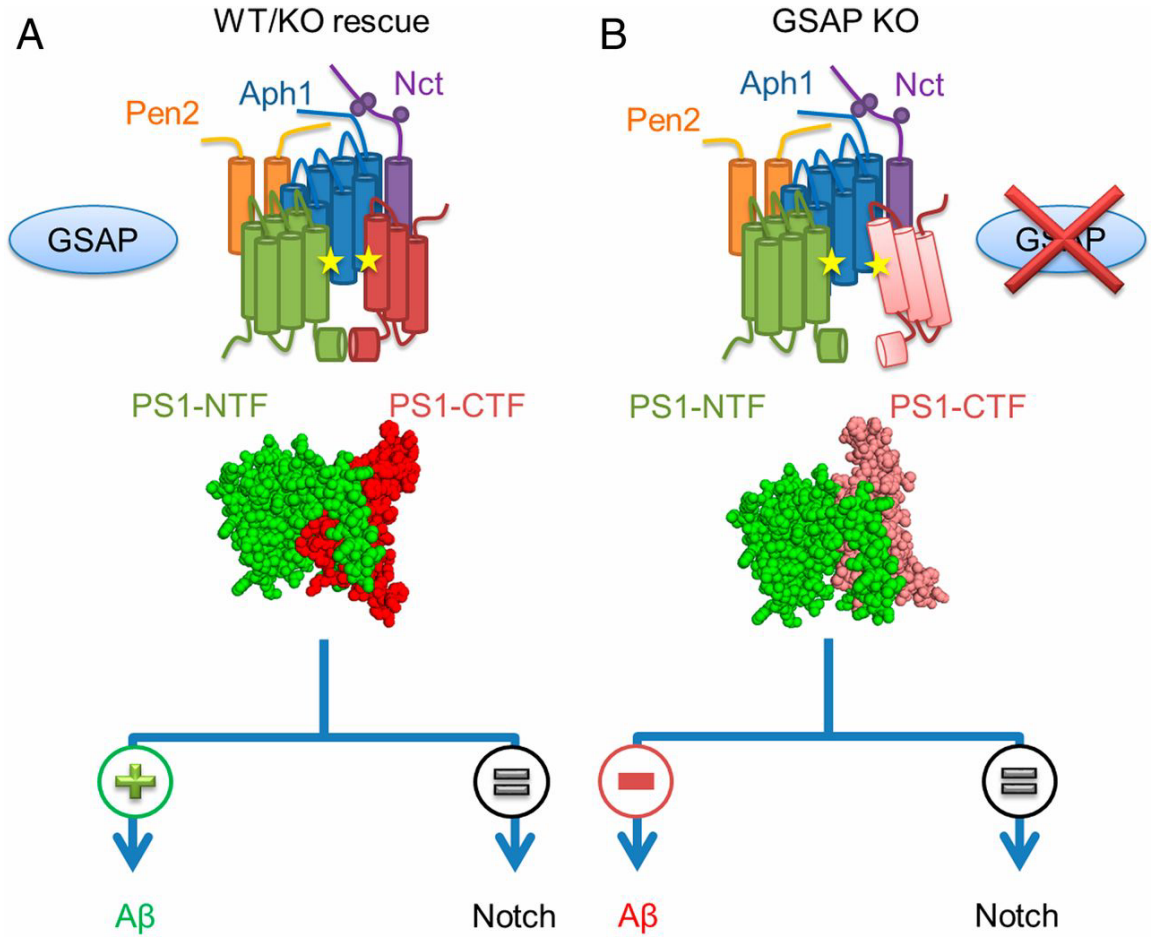

Figure 5. Proposed model of GSAP modulation of γ-secretase activity. (*A* and *B*) γ-Secretase complex presented as transmembrane rods containing PS1-NTF (green), PS1-CTF (red), Nct (purple), Aph1 (blue), and Pen2 (orange) in the presence (*A*) of GSAP (blue sphere) in WT or in GSAP rescue with induced PS1 conformation, which leads to γ-secretase activity for both APP and Notch. When GSAP is absent (*B*) PS1 adopts a different conformation, which leads to a decrease in APP processing and a reduction in Aβ secretion, but not in Notch processing[139].

2.11 Pulmonary Dysfunction Seen in Survivors of ICU-HAP

Pneumonia is a leading cause of ARDS as well as sepsis. Many patients that contract HAP, recover, and are discharged never get back to their baseline. Many longitudinal studies have been done on survivors of HAP and show that these patients suffer from a wide range of morbidities[60]. Pulmonary function was the original outcome doctors looked at in survivors of ARDS[144-146]. These early reports showed that some survivors of ARDS had obstructive or restrictive ventilatory insufficiencies that lasted weeks to months after illness but that most patients were able to recover to near normal ranges of pulmonary function between 6 and 12 months after illness[144-146]. While their spirometry results indicated pulmonary function was back to normal, patients consistently demonstrated significant exercise limitations and poor physical quality of life[74,147,148]. Even with improved pulmonary function, mechanisms responsible for the persistent disability and decreased quality of life are undetermined.

2.12 Myocardial Dysfunction Seen in Survivors of ICU-HAP

Cardiovascular disease, including myocardial infarction and stroke, is the leading cause of death worldwide[149]. Infections like pneumonia can cause demand ischemia, instability in atherosclerotic plaques, and procoagulant changes in the blood, and these factors alone or in combination are able to increase the short-term risk of cardiovascular events by 2-to 8-fold within the first 30 days after a respiratory infection[150-152]. While the short-term risk of cardiovascular disease is well established, the long-term risk is less well understood. Recently, studies assessing the long term impact of pneumonia on cardiovascular disease show that up to 35% of patients experience a cardiovascular event

within 10 years after pneumonia hospitalization[153]. While the mechanisms underlying cardiovascular complications after pneumonia are not fully understood, many believe it is a combination of things[153-155]: pneumonia causes a state of hypoxemia and consolidation that impacts normal homeostasis of ventilation and perfusion[154]; pneumonia is a pro-inflammatory disease with patients having high levels of circulating chemokines and cytokines that aid in getting rid of the infection but when uncontrolled can lead to tissue damage and malfunction[156,157]; the presence of certain bacterial toxins and cellular byproducts are able to generate a procoagulant state[158-160]; increase in the sympathetic nervous system which is a normal response to infection but can lead to an increase in heart rate and vascular resistance and a decrease in cardiac output and coronary perfusion of the heart[151].

2.13 Neurocognitive Dysfunction Seen in Survivors of ICU-HAP

Cognitive impairment is seen in one-third of ICU survivors[8]. Patients in the ICU with neurocognitive dysfunction, whether it is caused by ventilator-associated pneumonia or ventilator-induced lung injury, present with symptoms such as depression, anxiety, agitation, short-term memory loss, long-term memory loss, and delirium, an acute form of brain dysfunction[8,161]. These symptoms, especially delirium, can be seen while the patient is in the ICU but in some people, symptoms do not surface until the person has been discharged. For many, delirium is gone once the patient is back home, but other symptoms of neurocognitive dysfunction emerge and worsen over time. As for specific parts of the brain that are affected, one theory is that mechanical ventilation triggers hippocampal apoptosis which could provide an explanation for neurological changes in

ventilated patients[162]. Both long- and short-term cognition is affected as well as processing deficits. It is unknown which patient will develop what type of neurocognitive dysfunction, but there has been a link between severity of delirium during ICU stay and cognitive impairment reported at the time of discharge[163]. Treatments for ICU-related cognitive impairment focus on prevention, including choice of sedatives, early mobilization, and cognitive training, in which a patient practices tasks targeting different brain regions[164].

2.14 Conclusion

Pneumonia, with a definition that has evolved, is a disease of the lung that causes inflammation in which the air sacs or alveoli fill with pus or fluid. It can be acquired via healthcare or hospital settings or through the community. Hospital-acquired pneumonia is a major concern due to its association with increased length of stay, cost of care, and morbidity and mortality. HAP frequently occurs in the ICU where incidences of neurocognitive dysfunction are seen. During *P. aeruginosa*-induced pneumonia, cells and animals produce and secrete amyloid species that have been shown to cause significantly impaired learning and memory in animal models in ex-vivo hippocampal long-term potentiation experiments. Conventionally, the main focus of the ICU was to decrease short-term mortality. While this is extremely important for obvious reasons, this goal fails to address the issue of what it actually means to be a survivor of the ICU. Optimum long-term outcomes of these ICU patients need to be a top priority. By knowing more about these outcomes and what is causing them, it will be possible to make better ICU care decisions that will improve the patients' quality of life post-discharge. It is plausible that

the neurocognitive dysfunction seen in HAP patients post-discharge is from these endothelial-derived amyloids. There is work currently being done to better understand this mechanism of action with the hopes of developing prophylactic therapies to improve patient outcomes post-discharge.

2.15 References

1 Pneumonia. Definition. O*xford English Dictionary* (2023). https://www.oed.com/view/Entry/146345?redirectedFrom=Pneumonia&

2 Pneumonia - Symptoms and Causes*. Mayo Clinic* (2020). https://www.mayoclinic.org/diseases-conditions/pneumonia/symptoms-causes/syc-20354204

3 Pneumonia. *National Heart, Lung, and Blood Institute* (2022). https://www.nhlbi.nih.gov/health-topics/pneumonia

4 Pneumonia. *World Health Organization* (2022). http://www.who.int/mediacentre/factsheets/fs331/en/

5 Pneumonia - Types of Pneumonia-Types. *National Heart, Lung, and Blood Institute*. https://www.nhlbi.nih.gov/node/3496

6 Girard, R., Perraud, M., Prüss, A., Savey, A., Tikhomirov, E., Thuriaux, M., Vanhems, P. *Prevention of Hosptial-Acquired Infections. A Practical Guide.* 2nd edition. (eds G. Cucel, J. Fabry & L. Nicolle, L) (World Health Organization, 2002) https://apps.who.int/iris/bitstream/handle/10665/67350/WHO_CDS_CSR_EPH_2002.12.pdf

7 American Thoracic Society & Infectious Diseases Society of America. Guidelines for the Management of Adults with Hospital-Acquired, Ventilator-Associated, and Healthcare-Associated Pneumonia. *Am J Respir Crit Care Med* **171**, 388-416 (2005). https://doi.org:10.1164/rccm.200405-644ST

8 Pandharipande, P. P., Girard, T. D., Jackson, J. C., Morandi, A., Thompson, J. L., Pun, B. T., Brummel, N. E., Hughes, C. G., Vasilevskis, E. E., Shintani, A. K., Moons, K. G., Geevarghese, S. K., Canonico, A., Hopkins, R. O., Bernard, G. R., Dittus, R. S., Ely, E. W. & BRAIN-ICU Study Investigators. Long-Term Cognitive Impairment after Critical Illness. *N Engl J Med* **369**, 1306-1316 (2013). https://doi.org:10.1056/NEJMoa1301372

9 Williams, D. B., Raghunathan, A., Spain, D. A. & Brundage, S. I. Nosocomial Pneumonia in *Current Therapy of Trauma and Surgical Critical Care* (eds Juan A. Asensio & Donald D. Trunkey) 682-688 (Mosby, 2008).

10 Kalanuria, A. A., Zai, W. & Mirski, M. Ventilator-Associated Pneumonia in the ICU. *Crit Care* **18**, 208 (2014). https://doi.org:10.1186/cc13775

11 Lancaster, J. W., Lawrence, K. R., Fong, J. J., Doron, S. I., Garpestad, E., Nasraway, S. A. & Devlin, J. W. Impact of an Institution-Specific Hospital-Acquired Pneumonia Protocol on the Appropriateness of Antibiotic Therapy and Patient Outcomes. *Pharmacotherapy* **28**, 852-862 (2008). https://doi.org:10.1592/phco.28.7.852

12 Hippocrates, G. *The Works Of Hippocrates and Galen*. http://archive.org/details/TheWorksOfHippocratesAndGalen

13 Taussig, L. M. & Landau, L. I. *Pediatric Respiratory Medicine*. (Elsevier Health Sciences, 2008).

14 Auenbrugger, L. *Inventum Novum ex Percussione Thoracis Humani ut Signo Abstrusos Interni Pectoris Morbos Detegendi*. (Vindobonae : Typis Joannis Thomae Trattner, Caes. Reg. Majest. aulae typographi, 1761).

15 Smith, J. J. The Inventum Novum of Joseph Leopold Auenbrugger. *Bull N Y Acad Med* **38**, 691-701 (1962).

16 Cummins, S. L. Auenbrugger and Laennec: The Discoverers of Percussion and Auscultation. *Proc R Soc Med* **38**, 409-412 (1945). http://doi.org:10.1177/003591574503800802

17 Lenneac, R.T.H. *Treatise on the Diseases of the Chest in Which They are Described According to Their Anatomical Characters, and Their Diagnosis Established on a New Principle by Means of Acoustick Instruments.* (Philadelphia : James Webster, 1823). https://collections.nlm.nih.gov/ext/mhl/65340230R/PDF/65340230R.pdf

18 Roguin, A. Rene Theophile Hyacinthe Laënnec (1781–1826): The Man Behind the Stethoscope. *Clin Med Res* **4**, 230-235 (2006). https://doi.org:10.3121/cmr.4.3.230

19 Ackerknecht, E. H. *A Short History of Medicine*. (Baltimore : Johns Hopkins University Press, 2016).

20 Lister, J. *The Collected Papers of Joseph Baron Lister*. (Oxford : The Clarendon Press, 1909).

21 Stürchler, D. Klebsiella and Klebs the Person Behind the Name. *Travel Med Infect Dis* **14**, 654 (2016). https://doi.org:10.1016/j.tmaid.2016.11.003

22 Klebs, E. Beiträge zur Kenntniss der Pathogenen Schistomyceten. *Archiv für experimentelle Pathologie und Pharmakologie* **4**, 207-247 (1875). https://doi.org:10.1007/BF01830956

23 Fraenkel, A. Weitere Beiträge zur Lehre von den Micrococcus der Genuinen Fibrinosen Pneumonie. *Zeitscrift für Klinische Medicin* **11**, 437-458 (1886).

24 Fraenkel, A. Über die Genuine Pneumonie. *Verhandlungen des Congresses für innere Medicin* **3**, 17-31 (1884).

25 Friedlaender, C. Ueber die Schizomyceten bei der Acuten Fibrösen Pneumonie. *Archiv für pathologische Anatomie und Physiologie und für klinische Medicin* **87**, 319-324 (1882). https://doi.org:10.1007/BF01880516

26 Achievements in Public Health, 1900-1999: Control of Infectious Diseases. *Centers for Disease Control*. (2001) https://www.cdc.gov/mmwr/preview/mmwrhtml/mm4829a1.htm

27 Leading Causes of Death, 1900-1998. *Centers for Disease Control.* (2015) https://www.cdc.gov/nchs/data/dvs/lead1900_98.pdf

28 Dunlop, G. H. Some Considerations Regarding Pneumonia in Children: Drawn from an Analysis of 500 Cases. *Br Med J* **2**, 367-372 (1908). https://doi.org:10.1136/bmj.2.2485.367

29 Townsend, C. W. & Coolidge, A. The Mortality of Acute Lobar Pneumonia: From a Study of All the Cases of this Disease Treated at the Massachusetts General Hospital, from the First Case, in 1822, up to the Present Day. *Trans Am Climatol Assoc Meet* **6**, 22-49 (1889).

30 Barber, M. Hospital Infection Yesterday and Today. *J Clin Pathol* **14**, 2-10 (1961). https://doi.org:10.1136/jcp.14.1.2

31 Lowbury, E. J., Lilly, H. A., Kidson, A., Ayliffe, G. A. & Jones, R. J. Sensitivity of *Pseudomonas aeruginosa* to Antibiotics: Emergence of Strains Highly Resistant to Carbenicillin. *Lancet* **2**, 448-452 (1969). https://doi.org:10.1016/S0140-6736(69)90163-9

32 Kobayashi, F., Yamaguchi, M. & Mitsuhashi, S. Drug Resistance to Aminoglycosidic Antibiotics in *Pseudomonas aeruginosa* and its lability. *Jpn J Microbiol* **16**, 425-431 (1972). https://doi.org:10.1111/j.1348-0421.1972.tb00677.x

33 Tillett, W. S., Cambier, M. J. & Harris, W. H. Sulfonamide-fast Pneumococci. A Clinical Report of two Cases of Pneumonia Together with Experimental Studies on the Effectiveness of Penicillin and Tyrothricin Against Sulfonamide-Resistant Strains. *J Clin Invest* **22**, 249-255 (1943). https://doi.org:10.1172/JCI101390

34 Wise, R. I., Ossman, E. A. & Littlefield, D. R. Personal Reflections on Nosocomial Staphylococcal Infections and the Development of Hospital Surveillance. *Rev Infect Dis* **11**, 1005-1019 (1989). https://doi.org:10.1093/clinids/11.6.1005

35 Control of Health-Care--Associated Infections, 1961--2011. *Centers for Disease Control.* https://www.cdc.gov/mmwr/preview/mmwrhtml/su6004a10.htm

36 Forder, A. A. A Brief History of Infection Control - Past and Present. *S Afr Med J* **97**, 1161-1164 (2007).

37 Selwyn, S., Maccabe, A. F. & Gould, J. C. Hospital Infection in Perspective: The Importance of the Gram-Negative Bacilli. *Scott Med J* **9**, 409-417 (1964). https://doi.org:10.1177/003693306400901001

38 Tinne, J. E., Gordon, A. M., Bain, W. H. & Mackey, W. A. Cross-Infection by *Pseudomonas aeruginosa* as a Hazard of Intensive Surgery. *Br Med J* **4**, 313-315 (1967). https://doi.org:10.1136/bmj.4.5575.313

39 Fujitani, S., Sun, H.Y., Yu, V. L. & Weingarten, J. A. Pneumonia Due to *Pseudomonas aeruginosa*: Part I: Epidemiology, Clinical Diagnosis, and Source. *Chest* **139**, 909-919 (2011). https://doi.org:10.1378/chest.10-0166

40 Gaynes, R., Edwards, J. R. & National Nosocomial Infections Surveillance System. Overview of Nosocomial Infections Caused by Gram-Negative Bacilli. *Clin Infect Dis* **41**, 848-854 (2005). https://doi.org:10.1086/432803

41 Cilloniz, C., Martin-Loeches, I., Garcia-Vidal, C., San Jose, A. & Torres, A. Microbial Etiology of Pneumonia: Epidemiology, Diagnosis and Resistance Patterns. *Int J Mol Sci* **17**, 2120 (2016). https://doi.org:10.3390/ijms17122120

42 Motiwala, T., Mthethwa, Q., Achilonu, I. & Khoza, T. ESKAPE Pathogens: Looking at Clp ATPases as Potential Drug Targets. *Antibiotics (Basel)* **11**, 1218 (2022). https://doi.org:10.3390/antibiotics11091218

43 Rice, L. B. Federal Funding for the Study of Antimicrobial Resistance in Nosocomial Pathogens: No ESKAPE. *J Infect Dis* **197**, 1079-1081 (2008). https://doi.org:10.1086/533452

44 Guidelines for Preventing Health-Care--Associated Pneumonia, 2003. *Centers for Disease Control.* https://www.cdc.gov/mmwr/preview/mmwrhtml/rr5303a1.htm

45 Lynch, J. P., 3rd. Hospital-Acquired Pneumonia: Risk Factors, Microbiology, and Treatment. *Chest* **119**, 373S-384S (2001). https://doi.org:10.1378/chest.119.2_suppl.373s

46 Dandagi, G. L. Nosocomial Pneumonia in Critically Ill Patients. *Lung India* **27**, 149-153 (2010). https://doi.org:10.4103/0970-2113.68321

47 ICU (Intensive Care Unit). *California Pacific Medical Center*. https://www.sutterhealth.org/cpmc/services/emergency/intensive-unit

48 Cross, A. S. & Roup, B. Role of Respiratory Assistance Devices in Endemic Nosocomial Pneumonia. *Am J Med* **70**, 681-685 (1981). https://doi.org:10.1016/0002-9343(81)90596-9

49 Hanson, L. C., Weber, D. J. & Rutala, W. A. Risk Factors for Nosocomial Pneumonia in the Elderly. *Am J Med* **92**, 161-166 (1992). https://doi.org:10.1016/0002-9343(92)90107-m

50 Langer, M., Mosconi, P., Cigada, M. & Mandelli, M. Long-Term Respiratory Support and Risk of Pneumonia in Critically Ill Patients. Intensive Care Unit Group of Infection Control. *Am Rev Respir Dis* **140**, 302-305 (1989). https://doi.org:10.1164/ajrccm/140.2.302

51 Chevret, S., Hemmer, M., Carlet, J. & Langer, M. Incidence and Risk Factors of Pneumonia Acquired in Intensive Care Units. Results from a Multicenter Prospective Study on 996 Patients. European Cooperative Group on Nosocomial Pneumonia. *Intensive Care Med* **19**, 256-264 (1993). https://doi.org:10.1007/BF01690545

52 Ramírez-Estrada, S., Borgatta, B. & Rello, J. *Pseudomonas aeruginosa* Ventilator-Associated Pneumonia Management. *Infect Drug Resist* **9**, 7-18 (2016). https://doi.org:10.2147/IDR.S50669

53 Chung, D. R., Song, J. H., Kim, S. H., Thamlikitkul, V., Huang, S. G., Wang, H., So, T. M., Yasin, R. M., Hsueh, P. R., Carlos, C. C., Hsu, L. Y., Buntaran, L., Lalitha, M. K., Kim, M. J., Choi, J. Y., Kim, S. I., Ko, K. S., Kang, C. I., Peck, K. R. & Asian Network for Surveillance of Resistant Pathogens Study Group. High Prevalence of Multidrug-Resistant Nonfermenters in Hospital-Acquired Pneumonia in Asia. *Am J Respir Crit Care Med* **184**, 1409-1417 (2011). https://doi.org:10.1164/rccm.201102-0349OC

54 Fagon, J. Y., Chastre, J., Hance, A. J., Montravers, P., Novara, A. & Gibert, C. Nosocomial Pneumonia in Ventilated Patients: A Cohort Study Evaluating Attributable Mortality and Hospital Stay. *Am J Med* **94**, 281-288 (1993). https://doi.org:10.1016/0002-9343(93)90060-3

55 El Solh, A. A., Akinnusi, M. E., Wiener-Kronish, J. P., Lynch, S. V., Pineda, L. A. & Szarpa, K. Persistent Infection with *Pseudomonas aeruginosa* in Ventilator-Associated Pneumonia. *Am J Respir Crit Care Med* **178**, 513-519 (2008). https://doi.org:10.1164/rccm.200802-239OC

56 Ashbaugh, D. G., Bigelow, D. B., Petty, T. L. & Levine, B. E. Acute Respiratory Distress in Adults. *Lancet* **2**, 319-323 (1967). https://doi.org:10.1016/s0140-6736(67)90168-7

57 Bellani, G., Laffey, J. G., Pham, T., Fan, E., Brochard, L., Esteban, A., Gattinoni, L., van Haren, F., Larsson, A., McAuley, D. F., Ranieri, M., Rubenfeld, G., Thompson, B. T., Wrigge, H., Slutsky, A. S., Pesenti, A., LUNG SAFE Investigators, & ESICM Trials Group. Epidemiology, Patterns of Care, and Mortality for Patients with Acute Respiratory Distress Syndrome in Intensive Care Units in 50 Countries. *JAMA* **315**, 788-800 (2016). https://doi.org:10.1001/jama.2016.0291

58 Sawa, T. The Molecular Mechanism of Acute Lung Injury Caused by *Pseudomonas aeruginosa*: From Bacterial Pathogenesis to Host Response. *J Intensive Care* **2**, 10 (2014). https://doi.org:10.1186/2052-0492-2-10

59 ARDS Definition Task Force., Ranieri, V. M., Rubenfeld, G. D., Thompson, B. T., Ferguson, N. D., Caldwell, E., Fan, E., Camporota, L. & Slutsky, A. S. Acute Respiratory Distress Syndrome: The Berlin Definition. *JAMA* **307**, 2526-2533 (2012). https://doi.org:10.1001/jama.2012.5669

60 Herridge, M. S., Cheung, A. M., Tansey, C. M., Matte-Martyn, A., Diaz-Granados, N., Al-Saidi, F., Cooper, A. B., Guest, C. B., Mazer, C. D., Mehta, S., Stewart, T. E., Barr, A., Cook, D., Slutsky, A. S. & Canadian Critical Care Trials Group. One-Year Outcomes in Survivors Of the Acute Respiratory Distress Syndrome. *N Engl J Med* **348**, 683-693 (2003). https://doi.org:10.1056/NEJMoa022450

61 Harris, A., Torres-Viera, C., Venkataraman, L., DeGirolami, P., Samore, M. & Carmeli, Y. Epidemiology and Clinical Outcomes of Patients with Multiresistant *Pseudomonas aeruginosa*. *Clin Infect Dis* **28**, 1128-1133 (1999). https://doi.org:10.1086/514760

62 Kepple, S. R. Study Quantifies Impact of Resistant *Pseudomonas* on Outcomes. *Am J Health Syst Pharm* **56**, 1392 (1999). https://doi.org:10.1093/ajhp/56.14.1392a

63 Cao, B., Wang, H., Sun, H., Zhu, Y. & Chen, M. Risk Factors and Clinical Outcomes of Nosocomial Multi-Drug Resistant *Pseudomonas aeruginosa* Infections. *J Hosp Infect* **57**, 112-118 (2004). https://doi.org:10.1016/j.jhin.2004.03.021

64 Nielsen, S. L., Røder, B., Magnussen, P., Engquist, A. & Frimodt-Møller, N. Nosocomial Pneumonia in an Intensive Care Unit in a Danish University Hospital: Incidence, Mortality and Etiology. *Scand J Infect Dis* **24**, 65-70 (1992). https://doi.org:10.3109/00365549209048402

65 Desai, S., Law, T., Bienvenu, J. & Needham, D. Psychiatric Long-Term Complications of Intensive Care Unit Survivors. *Crit Care Med* **39**, 2790 (2011). https://doi.org:10.1097/CCM.0b013e318236e2db

66 Needham, D. M., Davidson, J., Cohen, H., Hopkins, R. O., Weinert, C., Wunsch, H., Zawistowski, C., Bemis-Dougherty, A., Berney, S. C., Bienvenu, O. J., Brady, S. L., Brodsky, M. B., Denehy, L., Elliott, D., Flatley, C., Harabin, A. L., Jones, C., Louis, D., Meltzer, W., Muldoon, S. R., Palmer, J. B., Perme, C., Robinson, M., Schmidt, D. M., Scruth, E., Spill, G. R., Storey, C. P., Render, M., Votto, J. & Harvey, M. A. Improving Long-Term Outcomes After Discharge from Intensive Care Unit: Report From a Stakeholders' Conference. *Crit Care Med* **40**, 502-509 (2012). https://doi.org:10.1097/CCM.0b013e318232da75

67 Needham, D. M., Wozniak, A. W., Hough, C. L., Morris, P. E., Dinglas, V. D., Jackson, J. C., Mendez-Tellez, P. A., Shanholtz, C., Ely, E. W., Colantuoni, E., Hopkins, R. O. & National Institutes of Health, Health NHLBI ARDS Network. Risk Factors for Physical Impairment After Acute Lung Injury in a National, Multicenter Study. *Am J Respir Crit Care Med* **189**, 1214-1224 (2014). https://doi.org:10.1164/rccm.201401-0158OC

68 Angus, D. C., Carlet, J. & 2002 Brussels Roundtable Participants. Surviving Intensive Care: A Report from the 2002 Brussels Roundtable. *Intensive Care Med* **29**, 368-377 (2003). https://doi.org:10.1007/s00134-002-1624-8

69 Hopkins, R. O. & Jackson, J. C. Assessing Neurocognitive Outcomes After Critical Illness: Are Delirium and Long-Term Cognitive Impairments Related? *Curr Opin Crit Care* **12**, 388-394 (2006). https://doi.org:10.1097/01.ccx.0000244115.24000.f5

70 Hopkins, R. O., Weaver, L. K., Collingridge, D., Parkinson, R. B., Chan, K. J. & Orme, J. F., Jr. Two-Year Cognitive, Emotional, and Quality-Of-Life Outcomes in Acute Respiratory Distress Syndrome. *Am J Respir Crit Care Med* **171**, 340-347 (2005). https://doi.org:10.1164/rccm.200406-763OC

71 Hopkins, R. O., Weaver, L. K., Pope, D., Orme, J. F., Bigler, E. D. & Larson-Lorh, V. Neuropsychological Sequelae and Impaired Health Status in Survivors of Severe Acute Respiratory Distress Syndrome. *Am J Respir Crit Care Med* **160**, 50-56 (1999). https://doi.org:10.1164/ajrccm.160.1.9708059

72 Jackson, J. C., Pandharipande, P. P., Girard, T. D., Brummel, N. E., Thompson, J. L., Hughes, C. G., Pun, B. T., Vasilevskis, E. E., Morandi, A., Shintani, A. K., Hopkins, R. O., Bernard, G. R., Dittus, R. S., Ely, E. W., & Bringing to Light the Risk Factors and Incidence of Neuropsychological dysfunction in ICU survivors (BRAIN-ICU) study investigators. Depression, Post-Traumatic Stress Disorder, and Functional Disability in Survivors of Critical Illness in the Brain-ICU Study: A Longitudinal Cohort Study. *Lancet Respir Med* **2**, 369-379 (2014). https://doi.org:10.1016/S2213-2600(14)70051-7

73 Mikkelsen, M. E., Christie, J. D., Lanken, P. N., Biester, R. C., Thompson, B. T., Bellamy, S. L., Localio, A. R., Demissie, E., Hopkins, R. O. & Angus, D. C. The Adult Respiratory Distress Syndrome Cognitive Outcomes Study: Long-Term Neuropsychological Function in Survivors of Acute Lung Injury. *Am J Respir Crit Care Med* **185**, 1307-1315 (2012). https://doi.org:10.1164/rccm.201111-2025OC

74 Weinert, C. R., Gross, C. R., Kangas, J. R., Bury, C. L. & Marinelli, W. A. Health-Related Quality of Life After Acute Lung Injury. *Am J Respir Crit Care Med* **156**, 1120-1128 (1997). https://doi.org:10.1164/ajrccm.156.4.9611047

75 Wiener-Kronish, J. P., Frank, D. & Sawa, T. Mechanisms of Lung Epitheliel Cell Injury by *Pseudomonas aeruginosa.* in *Molecular Biology of Acute Lung Injury Molecular and Cellular Biology of Critical Care Medicine* (eds Hector R. Wong & Thomas P. Shanley) 149-161 (Boston, MA : Springer 2001).

76 Kudoh, I., Wiener-Kronish, J. P., Hashimoto, S., Pittet, J. F. & Frank, D. Exoproduct Secretions of *Pseudomonas aeruginosa* Strains Influence Severity of Alveolar Epithelial Injury. *Am J Physiol* **267**, L551-556 (1994). https://doi.org:10.1152/ajplung.1994.267.5.L551

77 Vallis, A. J., Finck-Barbançon, V., Yahr, T. L. & Frank, D. W. Biological Effects of *Pseudomonas aeruginosa* Type III-Secreted Proteins on Cho Cells. *Infect Immun* **67**, 2040-2044 (1999). https://doi.org:10.1128/IAI.67.4.2040-2044.1999

78 Yahr, T. L., Vallis, A. J., Hancock, M. K., Barbieri, J. T. & Frank, D. W. ExoY, an Adenylate Cyclase Secreted by the *Pseudomonas aeruginosa* Type III System. *Proc Natl Acad Sci U S A* **95**, 13899-13904 (1998). https://doi.org:10.1073/pnas.95.23.13899

79 Roy-Burman, A., Savel, R. H., Racine, S., Swanson, B. L., Revadigar, N. S., Fujimoto, J., Sawa, T., Frank, D. W. & Wiener-Kronish, J. P. Type III Protein Secretion is Associated with Death in Lower Respiratory and Systemic *Pseudomonas aeruginosa* Infections. *J Infect Dis* **183**, 1767-1774 (2001). https://doi.org:10.1086/320737

80 Feltman, H., Schulert, G., Khan, S., Jain, M., Peterson, L. & Hauser, A. R. Prevalence of Type III Secretion Genes in Clinical and Environmental Isolates of *Pseudomonas aeruginosa*. *Microbiology* **147**, 2659-2669 (2001). https://doi.org:10.1099/00221287-147-10-2659

81 Winsor, G. L., Griffiths, E. J., Lo, R., Dhillon, B. K., Shay, J. A. & Brinkman, F. S. Enhanced Annotations and Features for Comparing Thousands of *Pseudomonas* Genomes in the Pseudomonas Genome Database. *Nucleic Acids Res* **44**, D646-653 (2016). https://doi.org:10.1093/nar/gkv1227

82 Stevens, T. C., Ochoa, C. D., Morrow, K. A., Robson, M. J., Prasain, N., Zhou, C., Alvarez, D. F., Frank, D. W., Balczon, R. & Stevens, T. The *Pseudomonas aeruginosa* Exoenzyme Y Impairs Endothelial Cell Proliferation and Vascular Repair Following Lung Injury. *Am J Physiol Lung Cell Mol Physiol* **306**, L915-L924 (2014). https://doi.org:10.1152/ajplung.00135.2013

83 Ochoa, C. D., Alexeyev, M., Pastukh, V., Balczon, R. & Stevens, T. *Pseudomonas aeruginosa* Exotoxin Y is a Promiscuous Cyclase that Increases Endothelial Tau Phosphorylation and Permeability. *J Biol Chem* **287**, 25407-25418 (2012). https://doi.org:10.1074/jbc.M111.301440

84 Sayner, S. L., Frank, D. W., King, J., Chen, H., VandeWaa, J. & Stevens, T. Paradoxical cAMP-Induced Lung Endothelial Hyperpermeability Revealed by *Pseudomonas aeruginosa* ExoY. *Circ Res* **95**, 196-203 (2004). https://doi.org:10.1161/01.RES.0000134922.25721.d9

85 Balczon, R., Prasain, N., Ochoa, C., Prater, J., Zhu, B., Alexeyev, M., Sayner, S., Frank, D. W. & Stevens, T. *Pseudomonas aeruginosa* Exotoxin Y-Mediated Tau Hyperphosphorylation Impairs Microtubule Assembly in Pulmonary Microvascular Endothelial Cells. *PLoS One* **8**, e74343 (2013). https://doi.org:10.1371/journal.pone.0074343

86 Morrow, K. A., Seifert, R., Kaever, V., Britain, A. L., Sayner, S. L., Ochoa, C. D., Cioffi, E. A., Frank, D. W., Rich, T. C. & Stevens, T. Heterogeneity of Pulmonary Endothelial Cyclic Nucleotide Response to *Pseudomonas aeruginosa* ExoY Infection. *Am J Physiol Lung Cell Mol Physiol* **309**, L1199-L1207 (2015). https://doi.org:10.1152/ajplung.00165.2015

87 Morrow, K. A., Ochoa, C. D., Balczon, R., Zhou, C., Cauthen, L., Alexeyev, M., Schmalzer, K. M., Frank, D. W. & Stevens, T. *Pseudomonas aeruginosa* Exoenzymes U and Y Induce a Transmissible Endothelial Proteinopathy. *Am J Physiol Lung Cell Mol Physiol* **310**, L337-L353 (2016). https://doi.org:10.1152/ajplung.00103.2015

88 Belyy, A., Raoux-Barbot, D., Saveanu, C., Namane, A., Ogryzko, V., Worpenberg, L., David, V., Henriot, V., Fellous, S., Merrifield, C., Assayag, E., Ladant, D., Renault, L. & Mechold, U. Actin Activates *Pseudomonas aeruginosa* ExoY Nucleotidyl Cyclase Toxin and ExoY-Like Effector Domains from MARTX Toxins. *Nat Commun* **7**, 13582 (2016). https://doi.org:10.1038/ncomms13582

89 Lin, M. T., Balczon, R., Pittet, J. F., Wagener, B. M., Moser, S. A., Morrow, K. A., Voth, S., Francis, C. M., Leavesley, S., Bell, J., Alvarez, D. F. & Stevens, T. Nosocomial Pneumonia Elicits an Endothelial Proteinopathy: Evidence for a Source of Neurotoxic Amyloids in Critically Ill Patients. *Am J Respir Crit Care Med* **198**, 1575-1578 (2018). https://doi.org:10.1164/rccm.201801-0060LE

90 Balczon, R., Pittet, J. F., Wagener, B. M., Moser, S. A., Voth, S., Vorhees, C. V., Williams, M. T., Bridges, J. P., Alvarez, D. F., Koloteva, A., Xu, Y., Zha, X. M., Audia, J. P., Stevens, T. & Lin, M. T. Infection-Induced Endothelial Amyloids Impair Memory. *FASEB J* **33**, 10300-10314 (2019). https://doi.org:10.1096/fj.201900322R

91 Voth, S., Gwin, M., Francis, C. M., Balczon, R., Frank, D. W., Pittet, J. F., Wagener, B. M., Moser, S. A., Alexeyev, M., Housley, N., Audia, J. P., Piechocki, S., Madera, K., Simmons, A., Crawford, M. & Stevens, T. Virulent *Pseudomonas aeruginosa* Infection Converts Antimicrobial Amyloids into Cytotoxic Prions. *FASEB J* **34**, 9156-9179 (2020). https://doi.org:10.1096/fj.202000051rrr

92 Scott, A. M., Jager, A. C., Gwin, M., Voth, S., Balczon, R., Stevens, T. & Lin, M. T. Pneumonia-Induced Endothelial Amyloids Reduce Dendritic Spine Density in Brain Neurons. *Sci Rep* **10**, 9327 (2020). https://doi.org:10.1038/s41598-020-66321-1

93 Balczon, R., Morrow, K. A., Zhou, C., Edmonds, B., Alexeyev, M., Pittet, J. F., Wagener, B. M., Moser, S. A., Leavesley, S., Zha, X., Frank, D. W. & Stevens, T. *Pseudomonas aeruginosa* Infection Liberates Transmissible, Cytotoxic Prion Amyloids. *FASEB J* **31**, 2785-2796 (2017). https://doi.org:10.1096/fj.201601042RR

94 Morrow, K. A., Stevens, T. C., Agwaramgbo, E., Langham, G., Francis, M., Balczon, R. & Stevens, T. Studies on the Physical Properties of the *Pseudomonas aeruginosa*-Induced Endothelial Prion Amyloid Cytotoxin(s). *FASEB J* **31**, 1074.1 (2017). https://doi.org:10.1096/fasebj.31.1_supplement.1074.1

95 Lin, M. T., Balczon, R., Morrow, K. A., Wagener, B. M., Pittet, J.F. & Stevens, T. *Pseudomonas aeruginosa*-Induced Pulmonary Endothelial Amyloid Proteins Impair Long-Term Plasticity. *FASEB J* **31**, 861.3 (2017). https://doi.org:10.1096/fasebj.31.1_supplement.861.3

96 Prasansuklab, A. & Tencomnao, T. Amyloidosis in Alzheimer's Disease: The Toxicity of Amyloid Beta (Aβ), Mechanisms of its Accumulation and Implications of Medicinal Plants for Therapy. *J Evid Based Complementary Altern Med* **2013**, 413808 (2013). https://doi.org:10.1155/2013/413808

97 Balczon, R., Lin, M. T., Lee, J. Y., Abbasi, A., Renema, P., Voth, S. B., Zhou, C., Koloteva, A., Michael Francis, C., Sodha, N. R., Pittet, J. F., Wagener, B. M., Bell, J., Choi, C. S., Ventetuolo, C. E. & Stevens, T. Pneumonia Initiates a Tauopathy. *FASEB J* **35**, e21807 (2021). https://doi.org:10.1096/fj.202100718R

98 Kamenetz, F., Tomita, T., Hsieh, H., Seabrook, G., Borchelt, D., Iwatsubo, T., Sisodia, S. & Malinow, R. APP Processing and Synaptic Function. *Neuron* **37**, 925-937 (2003). https://doi.org:10.1016/S0896-6273(03)00124-7

99 Glenner, G. G. & Wong, C. W. Alzheimer's Disease: Initial Report of the Purification and Characterization of a Novel Cerebrovascular Amyloid Protein. *Biochem Biophys Res Commun* **120**, 885-890 (1984). https://doi.org:10.1016/S0006-291X(84)80190-4

100 Vassar, R., Bennett, B. D., Babu-Khan, S., Kahn, S., Mendiaz, E. A., Denis, P., Teplow, D. B., Ross, S., Amarante, P., Loeloff, R., Luo, Y., Fisher, S., Fuller, J., Edenson, S., Lile, J., Jarosinski, M. A., Biere, A. L., Curran, E., Burgess, T., Louis, J. C., Collins, F., Treanor, J., Rogers, G. & Citron, M. β-Secretase Cleavage of Alzheimer's Amyloid Precursor Protein by the Transmembrane Aspartic Protease BACE. *Science* **286**, 735-741 (1999). https://doi.org:10.1126/science.286.5440.735

101 Morley, J. E., Farr, S. A., Banks, W. A., Johnson, S. N., Yamada, K. A. & Xu, L. A Physiological Role for Amyloid-β Protein: Enhancement of Learning and Memory. *J Alzheimers Dis* **19**, 441-449 (2010). https://doi.org:10.3233/JAD-2010-1230

102 Bayer, T. A., Cappai, R., Masters, C. L., Beyreuther, K. & Multhaup, G. It All Sticks Together-The APP--Related Family of Proteins and Alzheimer's Disease. *Mol Psychiatry* **4**, 524-528 (1999). https://doi.org:10.1038/sj.mp.4000552

103 Agca, C., Fritz, J. J., Walker, L. C., Levey, A. I., Chan, A. W., Lah, J. J. & Agca, Y. Development of Transgenic Rats Producing Human β-Amyloid Precursor Protein as a Model for Alzheimer's Disease: Transgene and Endogenous APP Genes are Regulated Tissue-Specifically. *BMC Neurosci* **9**, 28 (2008). https://doi.org:10.1186/1471-2202-9-28

104 Xu, H., Sweeney, D., Wang, R., Thinakaran, G., Lo, A. C., Sisodia, S. S., Greengard, P. & Gandy, S. Generation of Alzheimer β-Amyloid Protein in the Trans-Golgi Network in the Apparent Absence of Vesicle Formation. *Proc Natl Acad Sci U S A* **94**, 3748-3752 (1997). https://doi.org:10.1073/pnas.94.8.3748

105 Hartmann, T., Bieger, S. C., Bruhl, B., Tienari, P. J., Ida, N., Allsop, D., Roberts, G. W., Masters, C. L., Dotti, C. G., Unsicker, K. & Beyreuther, K. Distinct Sites of Intracellular Production for Alzheimer's Disease Aβ40/42 Amyloid Peptides. *Nat Med* **3**, 1016-1020 (1997). https://doi.org:10.1038/nm0997-1016

106 Greenfield, J. P., Tsai, J., Gouras, G. K., Hai, B., Thinakaran, G., Checler, F., Sisodia, S. S., Greengard, P. & Xu, H. Endoplasmic Reticulum and Trans-Golgi Network Generate Distinct Populations of Alzheimer β-Amyloid Peptides. *Proc Natl Acad Sci U S A* **96**, 742-747 (1999). https://doi.org:10.1073/pnas.96.2.742

107 Nordstedt, C., Caporaso, G. L., Thyberg, J., Gandy, S. E. & Greengard, P. Identification of the Alzheimer β/A4 Amyloid Precursor Protein in Clathrin-Coated Vesicles Purified from Pc12 Cells. *J Biol Chem* **268**, 608-612 (1993). http://doi.org:10.1016/S0021-9258(18)54194-6

108 Caporaso, G. L., Takei, K., Gandy, S. E., Matteoli, M., Mundigl, O., Greengard, P. & De Camilli, P. Morphologic and Biochemical Analysis of the Intracellular Trafficking of the Alzheimer β/A4 Amyloid Precursor Protein. *J Neurosci* **14**, 3122-3138 (1994). https://doi.org:10.1523/JNEUROSCI.14-05-03122.1994

109 Haass, C., Hung, A. Y., Schlossmacher, M. G., Teplow, D. B. & Selkoe, D. J. β-Amyloid Peptide and a 3-kDa Fragment are Derived by Distinct Cellular Mechanisms. *J Biol Chem* **268**, 3021-3024 (1993). http://doi.org:10.1016/S0021-9258(18)53650-4

110 Haass, C., Hung, A. Y., Schlossmacher, M. G., Oltersdorf, T., Teplow, D. B. & Selkoe, D. J. Normal Cellular Processing of the β-Amyloid Precursor Protein Results in the Secretion of the Amyloid β Peptide and Related Molecules. *Ann N Y Acad Sci* **695**, 109-116 (1993). https://doi.org:10.1111/j.1749-6632.1993.tb23037.x

111 Nalivaeva, N. N. & Turner, A. J. The Amyloid Precursor Protein: A Biochemical Enigma in Brain Development, Function and Disease. *FEBS Lett* **587**, 2046-2054 (2013). https://doi.org:10.1016/j.febslet.2013.05.010

112 Kojro, E. & Fahrenholz, F. The Non-Amyloidogenic Pathway: Structure and Function of α-Secretases in *Alzheimer's disease: Cellular and Molecular Aspects of Amyloid β* (eds J. Robin Harris & Falk Fahrenholz) 105-127 (New York : Springer, 2005).

113 Ehehalt, R., Keller, P., Haass, C., Thiele, C. & Simons, K. Amyloidogenic Processing of the Alzheimer β-Amyloid Precursor Protein Depends on Lipid Rafts. *J Cell Biol* **160**, 113-123 (2003). https://doi.org:10.1083/jcb.200207113

114 Anderson, J. P., Esch, F. S., Keim, P. S., Sambamurti, K., Lieberburg, I. & Robakis, N. K. Exact Cleavage Site of Alzheimer Amyloid Precursor in Neuronal PC-12 Cells. *Neurosci Lett* **128**, 126-128 (1991). https://doi.org:10.1016/0304-3940(91)90775-o

115 Sisodia, S. S. Secretion of the β-Amyloid Precursor Protein. *Ann N Y Acad Sci* **674**, 53-57 (1992). https://doi.org:10.1111/j.1749-6632.1992.tb27476.x

116 Wilson, C. A., Doms, R. W. & Lee, V. M. Intracellular APP Processing and Aβ Production in Alzheimer Disease. *J Neuropathol Exp Neurol* **58**, 787-794 (1999). https://doi.org:10.1097/00005072-199908000-00001

117 Kakuda, N., Funamoto, S., Yagishita, S., Takami, M., Osawa, S., Dohmae, N. & Ihara, Y. Equimolar Production of Amyloid β-Protein and Amyloid Precursor Protein Intracellular Domain from β-Carboxyl-Terminal Fragment by γ-Secretase. *J Biol Chem* **281**, 14776-14786 (2006). https://doi.org:10.1074/jbc.M513453200

118 Selkoe, D. J. & Wolfe, M. S. Presenilin: Running with Scissors in the Membrane. *Cell* **131**, 215-221 (2007). https://doi.org:10.1016/j.cell.2007.10.012

119 De Strooper, B. APH-1, Pen-2, and Nicastrin with Presenilin Generate an Active γ-Secretase Complex. *Neuron* **38**, 9-12 (2003). https://doi.org:10.1016/S0896-6273(03)00205-8

120 Kimberly, W. T., LaVoie, M. J., Ostaszewski, B. L., Ye, W., Wolfe, M. S. & Selkoe, D. J. γ-Secretase is a Membrane Protein Complex Comprised of Presenilin, Nicastrin, APH-1, and Pen-2. *Proc Natl Acad Sci U S A* **100**, 6382-6387 (2003). https://doi.org:10.1073/pnas.1037392100

121 Iwatsubo, T. The γ-Secretase Complex: Machinery for Intramembrane Proteolysis. *Curr Opin Neurobiol* **14**, 379-383 (2004). https://doi.org:10.1016/j.conb.2004.05.010

122 De Strooper, B., Saftig, P., Craessaerts, K., Vanderstichele, H., Guhde, G., Annaert, W., Von Figura, K. & Van Leuven, F. Deficiency of Presenilin-1 Inhibits the Normal Cleavage of Amyloid Precursor Protein. *Nature* **391**, 387-390 (1998). https://doi.org:10.1038/34910

123 De Strooper, B., Annaert, W., Cupers, P., Saftig, P., Craessaerts, K., Mumm, J. S., Schroeter, E. H., Schrijvers, V., Wolfe, M. S., Ray, W. J., Goate, A. & Kopan, R. A Presenilin-1-Dependent γ-Secretase-Like Protease Mediates Release of Notch Intracellular Domain. *Nature* **398**, 518-522 (1999). https://doi.org:10.1038/19083

124 Wolfe, M. S., Xia, W., Ostaszewski, B. L., Diehl, T. S., Kimberly, W. T. & Selkoe, D. J. Two Transmembrane Aspartates in Presenilin-1 Required for Presenilin Endoproteolysis and γ-Secretase Activity. *Nature* **398**, 513-517 (1999). https://doi.org:10.1038/19077

125 Shah, S., Lee, S. F., Tabuchi, K., Hao, Y. H., Yu, C., LaPlant, Q., Ball, H., Dann, C. E. 3rd, Sudhof, T. & Yu, G. Nicastrin Functions as a γ-Secretase-Substrate Receptor. *Cell* **122**, 435-447 (2005). https://doi.org:10.1016/j.cell.2005.05.022

126 Dries, D. R., Shah, S., Han, Y. H., Yu, C., Yu, S., Shearman, M. S. & Yu, G. Glu-333 of Nicastrin Directly Participates in γ-Secretase Activity. *J Biol Chem* **284**, 29714-29724 (2009). https://doi.org:10.1074/jbc.M109.038737

127 Goutte, C., Tsunozaki, M., Hale, V. A. & Priess, J. R. APH-1 is a Multipass Membrane Protein Essential for the Notch Signaling Pathway in Caenorhabditis Elegans Embryos. *Proc Natl Acad Sci U S A* **99**, 775-779 (2002). https://doi.org:10.1073/pnas.022523499

128 Steiner, H., Winkler, E., Edbauer, D., Prokop, S., Basset, G., Yamasaki, A., Kostka, M. & Haass, C. PEN-2 is an Integral Component of the γ-Secretase Complex Required for Coordinated Expression of Presenilin and Nicastrin. *J Biol Chem* **277**, 39062-39065 (2002). https://doi.org:10.1074/jbc.C200469200

129 Prokop, S., Haass, C. & Steiner, H. Length and Overall Sequence of the PEN-2 C-Terminal Domain Determines its Function in the Stabilization of Presenilin Fragments. *J Neurochem* **94**, 57-62 (2005). https://doi.org:10.1111/j.1471-4159.2005.03165.x

130 Kaether, C., Scheuermann, J., Fassler, M., Zilow, S., Shirotani, K., Valkova, C., Novak, B., Kacmar, S., Steiner, H. & Haass, C. Endoplasmic Reticulum Retention of the γ-Secretase Complex Component PEN2 by Rer1. *EMBO Rep* **8**, 743-748 (2007). https://doi.org:10.1038/sj.embor.7401027

131 Prokop, S., Shirotani, K., Edbauer, D., Haass, C. & Steiner, H. Requirement of PEN-2 for Stabilization of the Presenilin N-/C-Terminal Fragment Heterodimer within the γ-Secretase Complex. *J Biol Chem* **279**, 23255-23261 (2004). https://doi.org:10.1074/jbc.M401789200

132 Holmes, O., Paturi, S., Selkoe, D. J. & Wolfe, M. S. PEN-2 is Essential for γ-Secretase Complex Stability and Trafficking but Partially Dispensable for Endoproteolysis. *Biochemistry* **53**, 4393-4406 (2014). https://doi.org:10.1021/bi500489j

133 Wong, G. T., Manfra, D., Poulet, F. M., Zhang, Q., Josien, H., Bara, T., Engstrom, L., Pinzon-Ortiz, M., Fine, J. S., Lee, H. J., Zhang, L., Higgins, G. A. & Parker, E. M. Chronic Treatment with the γ-Secretase Inhibitor Ly-411,575 Inhibits β-Amyloid Peptide Production and Alters Lymphopoiesis and Intestinal Cell Differentiation. *J Biol Chem* **279**, 12876-12882 (2004). https://doi.org:10.1074/jbc.M311652200

134 He, G., Luo, W., Li, P., Remmers, C., Netzer, W. J., Hendrick, J., Bettayeb, K., Flajolet, M., Gorelick, F., Wennogle, L. P. & Greengard, P. γ-Secretase Activating Protein, a Therapeutic Target for Alzheimer's Disease. *Nature* **467**, 95-98 (2010). https://doi.org:10.1038/nature09325

135 Chu, J., Li, J. G., Hoffman, N. E., Stough, A. M., Madesh, M. & Praticò, D. Regulation of γ-Secretase Activating Protein by the 5lipoxygenase: in Vitro and in Vivo Evidence. *Sci Rep* **5**, 11086 (2015). https://doi.org:10.1038/srep11086

136 Chu, J., Li, J. G., Joshi, Y. B., Giannopoulos, P. F., Hoffman, N. E., Madesh, M. & Praticò, D. γ Secretase Activating Protein is a Substrate for Caspase-3: Implications for Alzheimer's Disease. *Biol Psychiatry* **77**, 720-728 (2015). https://doi.org:10.1016/j.biopsych.2014.06.003

137 Xu, P., Chang, J. C., Zhou, X., Wang, W., Bamkole, M., Wong, E., Bettayeb, K., Jiang, L. L., Huang, T., Luo, W., Xu, H., Nairn, A. C., Flajolet, M., Ip, N. Y., Li, Y. M. & Greengard, P. Gsap Regulates Lipid Homeostasis and Mitochondrial Function Associated with Alzheimer's Disease. *J Exp Med* **218**, e20202446 (2021). https://doi.org:10.1084/jem.20202446

138 Jin, C., Wang, J., Wang, Y., Jia, B., Guo, X., Yang, G., Xu, P., Greengard, P., Zhou, R. & Shi, Y. Modulation of Amyloid Precursor Protein Cleavage by γ-Secretase Activating Protein Through Phase Separation. *Proc Natl Acad Sci U S A* **119**, e2122292119 (2022). https://doi.org:10.1073/pnas.2122292119

139 Wong, E., Liao, G. P., Chang, J. C., Xu, P., Li, Y. M. & Greengard, P. GSAP Modulates γ-Secretase Specificity by Inducing Conformational Change in PS1. *Proc Natl Acad Sci U S A* **116**, 6385-6390 (2019). https://doi.org:10.1073/pnas.1820160116

140 Zhu, M., Tao, Y., He, Q., Gao, H., Song, F., Sun, Y. M., Li, H. L., Wu, Z. Y. & Saffen, D. Common GSAP Promoter Variant Contributes to Alzheimer's Disease Liability. *Neurobiol Aging* **35**, 2656.e1-2656.e7 (2014). https://doi.org:10.1016/j.neurobiolaging.2014.05.018

141 Satoh, J., Tabunoki, H., Ishida, T., Saito, Y. & Arima, K. Immunohistochemical Characterization of γ-Secretase Activating Protein Expression in Alzheimer's Disease Brains. *Neuropathol Appl Neurobiol* **38**, 132-141 (2012). https://doi.org:10.1111/j.1365-2990.2011.01206.x

142 Chu, J., Lauretti, E., Craige, C. P. & Pratico, D. Pharmacological Modulation of GSAP Reduces Amyloid-β Levels and Tau Phosphorylation in a Mouse Model of Alzheimer's Disease with Plaques and Tangles. *J Alzheimers Dis* **41**, 729-737 (2014). https://doi.org:10.3233/JAD-140105

143 Hussain, I., Fabrègue, J., Anderes, L., Ousson, S., Borlat, F., Eligert, V., Berger, S., Dimitrov, M., Alattia, J. R., Fraering, P. C. & Beher, D. The Role of γ-Secretase Activating Protein (GSAP) and Imatinib in the Regulation of γ-Secretase Activity and Amyloid-β Generation. *J Biol Chem* **288**, 2521-2531 (2013). https://doi.org:10.1074/jbc.M112.370924

144 Downs, J. B. & Olsen, G. N. Pulmonary Function Following Adult Respiratory Distress Syndrome. *Chest* **65**, 92-93 (1974). https://doi.org:10.1378/chest.65.1.92

145 Petty, T. L., Pierson, D. J., Dick, N. P., Hudson, L. D. & Walker, S. H. Follow-up Evaluation or a Prevalence Study for Chronic Bronchitis and Chronic Airway Obstruction. *Am Rev Respir Dis* **114**, 881-890 (1976). https://doi.org:10.1164/arrd.1976.114.5.881

146 Simpson, D. L., Goodman, M., Spector, S. L. & Petty, T. L. Long-Term Follow-up and Bronchial Reactivity Testing in Survivors of the Adult Respiratory Distress Syndrome. *Am Rev Respir Dis* **117**, 449-454 (1978). https://doi.org:10.1164/arrd.1978.117.3.449

147 Davidson, T. A., Caldwell, E. S., Curtis, J. R., Hudson, L. D. & Steinberg, K. P. Reduced Quality of Life in Survivors of Acute Respiratory Distress Syndrome Compared with Critically Ill Control Patients. *JAMA* **281**, 354-360 (1999). https://doi.org:10.1001/jama.281.4.354

148 Eisner, M. D. & Matthay, M. A. Health-Related Quality of Life After Acute Lung Injury. *Crit Care Med* **27**, 2825-2826 (1999). https://doi.org:10.1097/00003246-199912000-00037

149 World Health Organization. *WHO methods and data sources for country-level causes of death 2000-2019* <https://cdn.who.int/media/docs/default-source/gho-documents/global-health-estimates/ghe2019_cod_methods.pdf?sfvrsn=37bcfacc_5> (2020).

150 Corrales-Medina, V. F., Madjid, M. & Musher, D. M. Role of Acute Infection in Triggering Acute Coronary Syndromes. *Lancet Infect Dis* **10**, 83-92 (2010). https://doi.org:10.1016/S1473-3099(09)70331-7

151 Corrales-Medina, V. F., Musher, D. M., Shachkina, S. & Chirinos, J. A. Acute Pneumonia and the Cardiovascular System. *Lancet* **381**, 496-505 (2013). https://doi.org:10.1016/S0140-6736(12)61266-5

152 Reyes, L. F., Restrepo, M. I., Hinojosa, C. A., Soni, N. J., Anzueto, A., Babu, B. L., Gonzalez-Juarbe, N., Rodriguez, A. H., Jimenez, A., Chalmers, J. D., Aliberti, S., Sibila, O., Winter, V. T., Coalson, J. J., Giavedoni, L. D., Dela Cruz, C. S., Waterer, G. W., Witzenrath, M., Suttorp, N., Dube, P. H. & Orihuela, C. J. Severe Pneumococcal Pneumonia Causes Acute Cardiac Toxicity and Subsequent Cardiac Remodeling. *Am J Respir Crit Care Med* **196**, 609-620 (2017). https://doi.org:10.1164/rccm.201701-0104OC

153 Corrales-Medina, V. F., Alvarez, K. N., Weissfeld, L. A., Angus, D. C., Chirinos, J. A., Chang, C. C., Newman, A., Loehr, L., Folsom, A. R., Elkind, M. S., Lyles, M. F., Kronmal, R. A. & Yende, S. Association Between Hospitalization for Pneumonia and Subsequent Risk of Cardiovascular Disease. *JAMA* **313**, 264-274 (2015). https://doi.org:10.1001/jama.2014.18229

154 Corrales-Medina, V. F., Suh, K. N., Rose, G., Chirinos, J. A., Doucette, S., Cameron, D. W. & Fergusson, D. A. Cardiac Complications in Patients with Community-Acquired Pneumonia: A Systematic Review and Meta-Analysis of Observational Studies. *PLoS Med* **8**, e1001048 (2011). https://doi.org:10.1371/journal.pmed.1001048

155 Rae, N., Finch, S. & Chalmers, J. D. Cardiovascular Disease as a Complication of Community-Acquired Pneumonia. *Curr Opin Pulm Med* **22**, 212-218 (2016). https://doi.org:10.1097/MCP.0000000000000261

156 Moore, T. A. & Standiford, T. J. The Role of Cytokines in Bacterial Pneumonia: An Inflammatory Balancing Act. *Proc Assoc Am Physicians* **110**, 297-305 (1998).

157 Kellum, J. A., Kong, L., Fink, M. P., Weissfeld, L. A., Yealy, D. M., Pinsky, M. R., Fine, J., Krichevsky, A., Delude, R. L., Angus, D. C. & GenIMS Investigators. Understanding the Inflammatory Cytokine Response in Pneumonia and Sepsis: Results of the Genetic and Inflammatory Markers of Sepsis (GenIMS) Study. *Arch Intern Med* **167**, 1655-1663 (2007). https://doi.org:10.1001/archinte.167.15.1655

158 Cangemi, R., Pignatelli, P., Carnevale, R., Bartimoccia, S., Nocella, C., Falcone, M., Taliani, G., Violi, F. & SIXTUS Study Group. Low-Grade Endotoxemia, Gut Permeability and Platelet Activation in Community-Acquired Pneumonia. *J Infect* **73**, 107-114 (2016). https://doi.org:10.1016/j.jinf.2016.05.013

159 Plotkowski, M. C., Feliciano, L. F., Machado, G. B., Cunha, L. G. Jr., Freitas, C., Saliba, A. M. & de Assis, M. C. ExoU-Induced Procoagulant Activity in *Pseudomonas aeruginosa*-Infected Airway Cells. *Eur Respir J* **32**, 1591-1598 (2008). https://doi.org:10.1183/09031936.00086708

160 Beristain-Covarrubias, N., Perez-Toledo, M., Thomas, M. R., Henderson, I. R., Watson, S. P. & Cunningham, A. F. Understanding Infection-Induced Thrombosis: Lessons Learned from Animal Models. *Front Immunol* **10**, 2569 (2019). https://doi.org:10.3389/fimmu.2019.02569

161 de Azevedo, J. R., Montenegro, W. S., Rodrigues, D. P., de C. Souza, S. C., Araujo, V. F., de Paula, M. P., Prazeres, P. H., da Luz Leitão, A. & Mendonça, A. V. Long-Term Cognitive Outcomes Among Unselected Ventilated and Non-Ventilated ICU Patients. *J Intensive Care* **5**, 18 (2017). https://doi.org:10.1186/s40560-017-0213-4

162 González-López, A., López-Alonso, I., Aguirre, A., Amado-Rodríguez, L., Batalla-Solís, E., Astudillo, A., Tomás-Zapico, C., Fueyo, A., dos Santos, C. C., Talbot, K. & Albaiceta, G. M. Mechanical Ventilation Triggers Hippocampal Apoptosis by Vagal and Dopaminergic Pathways. *Am J Respir Crit Care Med* **188**, 693-702 (2013). https://doi.org:10.1164/rccm.201304-0691OC

163 Sakuramoto, H., Subrina, J., Unoki, T., Mizutani, T. & Komatsu, H. Severity of Delirium in the ICU is Associated with Short Term Cognitive Impairment. A Prospective Cohort Study. *Intensive Crit Care Nurs* **31**, 250-257 (2015). https://doi.org:10.1016/j.iccn.2015.01.001

164 Wergin, R. & Modrykamien, A. Cognitive Impairment in ICU Survivors: Assessment and Therapy. *Cleve Clin J Med* **79**, 705-712 (2012). https://doi.org:10.3949/ccjm.79a.12038

CHAPTER III

HYPOTHESIS AND SPECIFIC AIMS

Pseudomonas aeruginosa induces the production and release of amyloids, including beta amyloid, from pulmonary microvascular endothelial cells. Once released, these pathologic amyloid species disrupt the endothelial barrier, and they may propagate through the vasculature to promote secondary end-organ damage, including prolonged pulmonary dysfunction, cardiovascular complications, and neurocognitive decline.

Beta amyloid is a peptide derived from amyloid precursor protein through consecutive cleavages by β- and γ-secretases and has both physiologic and pathologic roles. In the production of beta amyloid, β-secretase first cleaves amyloid precursor protein, followed by γ-secretase. γ-secretase is a multiprotein complex consisting of presenilin 1, anterior pharynx defective 1, presenilin enhancer 2, and nicastrin.

γ-secretase activating protein (GSAP) is a newly discovered component of γ-secretase. GSAP modifies γ-secretase activity by causing a conformational change in the γ-secretase structure leading to its increased affinity for amyloid precursor protein versus other substrates. Studies from our lab show GSAP activity is required for infection-induced production of cytotoxic beta amyloid[1]. GSAP was deleted in endothelial cells using CRISPR-Cas9. In the absence of GSAP, endothelial cells were protected from the

primary infection, and the infection-elicited beta amyloid species were not cytotoxic, but rather had antimicrobial properties. These data suggest the presence of a functional GSAP is essential for bacteria to induce a cytotoxic response. To assess the role of GSAP in the end-organ damage seen in survivors of hospital acquired pneumonia, I studied a first-in-kind GSAP knockout rat, testing the hypothesis that **infection acts through GSAP to promote end-organ dysfunction**.

Specific aims test the related hypotheses that GSAP expression:

AIM 1: Contributes to pulmonary alveolar-capillary barrier dysfunction during *P. aeruginosa* induced bacterial pneumonia,

AIM 2: Contributes to susceptibility to myocardial infarction during *P. aeruginosa* induced bacterial pneumonia and,

AIM 3: Contributes to neurocognitive dysfunction during *P. aeruginosa* induced bacterial pneumonia.

1 Gwin, M. S., Voth, S. B., Paudel, S. S., Onanyan, N., Darby, A., Francis, C. M. & Stevens, T. in *C47. CRITICAL CARE: INSIGHTS FROM ANIMAL, EXPERIMENTAL, AND TRANSLATIONAL MODELS IN ARDS AND SEPSIS* A5275-A5275.

CHAPTER VI

GAMMA SECRETASE ACTIVATING PROTEIN PROMOTES END-ORGAN DYSFUNCTION FOLLOWING BACTERIAL PNEUMONIA

4.1 Introduction

Gamma secretase activating protein is a recently described subunit of the gamma (γ)- secretase complex[1]. GSAP is expressed as a 98-kD holoprotein, and the holoprotein is cleaved by caspase-3 or other enzymes to generate a 16-kD product [2,3]. The 16-kD GSAP interacts with the adaptor protein Fe65 and presenilin-1, which are components of the γ-secretase enzyme complex, in the mitochondria-associated membrane, where it also binds to amyloid precursor protein [4,5]. GSAP thus localizes the γ-secretase enzyme complex with amyloid precursor protein important to produce Aβ variants, including $A\beta_{40}$ and $A\beta_{42}$ [4,6,7]. GSAP deletion in cells and mice attenuates the production of both $A\beta_{40}$ and $A\beta_{42}$. Cognitive function is improved in GSAP knockout animal models of Alzheimer's disease, consistent with the amyloid hypothesis of neurodegeneration [1,2,4,6,8]. While GSAP is best known for its influence on Aβ production, recent studies also reveal GSAP contributes to subcellular signal transduction and protein trafficking in excitatory

neurons [5]. Yet, the function(s) of GSAP outside of the brain have not been addressed, and thus, its physiological relevance remains incompletely understood.

GSAP is ubiquitously expressed, including in the lungs and heart [9], and Aβ has diverse physiological functions within and outside the brain [10]. For example, Aβ plays a pivotal role in the host's response to infection. It can have antimicrobial properties [11-15] and it can also be pathogenic to the host [16-18]. Aβ is increased in the bronchoalveolar lavage fluid, blood, and/or cerebrospinal fluid during infection [16-18], and infection is potentially an adverse effect of Aβ-lowering medical therapy [19]. Aβ contributes to the pathogenesis of ischemic heart disease [20], it can activate platelets [21], and it can injure the lung [22,23]. While these studies suggest a central role for Aβ in the innate immune response, mechanisms contributing to the increase in Aβ during infection are unresolved.

Pneumonia is a common cause of acute respiratory failure, and it substantially increases the risk of morbidity and mortality during, and in the aftermath, of infection [24]. Cardiovascular disease and neurocognitive dysfunction, including dementia, impairments in learning and memory, depression, anxiety, and post-traumatic stress disorder, are prevalent among survivors of critical illness [25-27]. Approximately one-third of patients who survive their critical illness exhibit cognitive impairment, similar to patients with mild Alzheimer's disease [25]. The mechanism(s) of this incident cognitive impairment is unknown, however, we found cytotoxic forms of Aβ in the airways, blood, and cerebrospinal fluid of intensive care unit patients and animal subjects with nosocomial pneumonia [16-18,28]. Based on these studies, and the role that GSAP plays in regulating Aβ production, we sought to determine whether GSAP contributes to the host-pathogen

response during infection, mediating end-organ dysfunction that is a consequence of pneumonia.

4.2 Results

4.2.1 GSAP Contributes to the Lung's Innate Immune Response in Pneumonia.

We generated a first-in-kind GSAP knockout rat using CRISPR-Cas9 gene editing (**Fig. 6A**). A 5-nucleotide deletion was generated in exon 16 and was confirmed by genomic sequencing. The deletion resulted in a frameshift and premature termination of protein synthesis. Breeding of rats heterozygous for the GSAP allele over 27 pairings resulted in 626 progenies. Three hundred and fifteen of these pups were male and 311 were female, distributed among wild type (28%), knockout (25%), and heterozygote (46%) genotypes according to the expected Mendelian distribution. Body weights (**Fig. 2**), organ sizes (**Table 1**), complete blood cell counts (**Table 2**), and electrolytes (**Fig. 7** and **Fig. 8**) were not significantly different among wild type and GSAP knockout littermates under baseline conditions.

To examine whether GSAP contributes to the innate immune response following infection, *Pseudomonas aeruginosa* (PA103Δ*exoU*:*exoT*::Tc/pUCP-*exoY*; ExoY^{+}) was introduced by intratracheal inoculation into wild type and GSAP knockout rats (10^8 CFU; ~LD_{50}). Fifty percent of wild type rats survived 48 hours post-infection, whereas 65% of the knockout rats survived to this time point (**Fig. 6B**). Both the wild type and knockout rats lost ~25 g body weight (10-15%) 48 hours post-infection (**Fig. 6C**), and hematocrit and hemoglobin were increased, consistent with volume depletion (**Fig. 9**). Whereas

circulating $A\beta_{40}$ and $A\beta_{42}$ concentrations were similar among the rats at baseline, infection increased $A\beta_{42}$ (~2-fold) in the wild type but not in the knockout rats (**Fig. 6D**). Nonetheless, the $A\beta_{42/40}$ ratio increased in the plasma of both wild type and knockout rats, post-infection, suggesting that GSAP is not a principal determinant of the circulating amyloid pool. Cardiopulmonary ultrasonography revealed a hyperdynamic circulatory state (**Fig. 6E**). Hyperechoic vertical B lines characteristic of lung edema and consolidation were apparent in both groups, and gross morphological assessment showed a heterogenous pattern of lung injury (**Fig. 6F**). The cardiopulmonary response to infection was therefore generally similar among wild type and GSAP knockout rats.

Complete blood cell counts with differential revealed no difference in circulating platelets, red blood cells, or total white blood cell counts among genotypes under basal conditions. The percent of circulating neutrophils and monocytes was increased, and the percent of circulating lymphocytes was decreased, following infection (**Fig. 9**). Neutrophilia and monocytosis were prominent after infection whereas total lymphocyte counts were unchanged (**Fig. 9A**). Two anti-inflammatory cytokines, IL-10 and GM-CSF trended toward higher values in GSAP knockout rats at baseline and were significantly reduced following infection. Two pro-inflammatory cytokines, MCP-1 and IL-6 were increased in wild type rats following infection (**Fig. 9B**). Bicarbonate was elevated and lactate trended toward lower values in GSAP knockout rats at baseline, which lowered the anion gap, yet after infection, anion gap fell within the normal range in both wild type and knockout rats (**Fig. 9C**). Infection increased lactate and impaired oxygenation; it was

notable that oxygenation was better in the knockout rats, indicating improved alveolar-capillary barrier integrity (**Fig. 9C** and **Fig. 10**).

To assess whether GSAP contributes to the recruitment of neutrophils and monocytes to the airways, BALF was analyzed by flow cytometry. The heart and lungs were isolated *en bloc* and BALF was collected *ex vivo* using 25 cm H_2O pressure to fill the lung with ~10 mL of PBS. Three successive washes yielded ~30 mL of BALF. Similar numbers of cells were recovered in the BALF of wild type and GSAP knockout rats at baseline and following infection, yet 10-fold more cells were recovered following infection (**Fig. 11A**). Cells recovered in the BALF were labeled with fluorophore-conjugated antibodies directed against CD68 (monocytes, macrophages), CD45 (hematopoietic cells), CD11b,c (monocytes, macrophage, granulocytes), RP1 (neutrophils), CD43 (leukocytes), and His48 (granulocytes). The gating strategy to identify alveolar macrophages and neutrophils is shown in **Fig. 12**. Analysis of the flow cytometry results revealed cells in the BALF at baseline were CD11b,c positive, CD45 positive, and CD68 high, consistent with the presence of alveolar macrophages (**Fig. 11B**). After infection, a new CD11b,c positive, CD45 positive, and CD68 low cell population was resolved (**Fig. 11B**). To assess whether these cells were neutrophils, we selected the CD68 low cell population and gated for RP1. RP1 positive cells were identified in the BALF from both wild type and GSAP knockout rats, yet two distinct neutrophil populations were seen in the knockout rats, as illustrated by the bimodal peak (**Fig. 11C**). To better resolve the nature of these neutrophils, the CD45 positive, His48 positive, and CD68 low cells were sorted for histological assessment. Neutrophils retrieved from the BALF of the knockout rats appeared immature, suggesting GSAP

contributes to the neutrophil phenotype that is recruited to the airway following bacterial infection (**Fig. 11D**).

To assess the pattern of acute lung injury, lungs were formalin-fixed at 25 cm H_2O airway pressure, serially sectioned in hilar regions with consolidation, and H&E stained. Histology revealed a pathological pattern consistent with pneumonia, including prominent leukocyte recruitment to the alveoli, a heterogeneous pattern of inflammation, alveolar consolidation and atelectasis, and perivascular fluid cuffing (**Fig. 11E**). Lungs from both wild type and GSAP knockout rats exhibited a similar decrease in static lung compliance, illustrating the restrictive physiology seen in acute lung injury (data not shown). Yet, widespread fluid accumulation was not observed in GSAP knockout rats following infection, consistent with relatively preserved oxygenation in the knockout rats. These results reveal a central role for GSAP in the lung's innate immune response to bacterial pneumonia and disruption of the alveolar-capillary barrier.

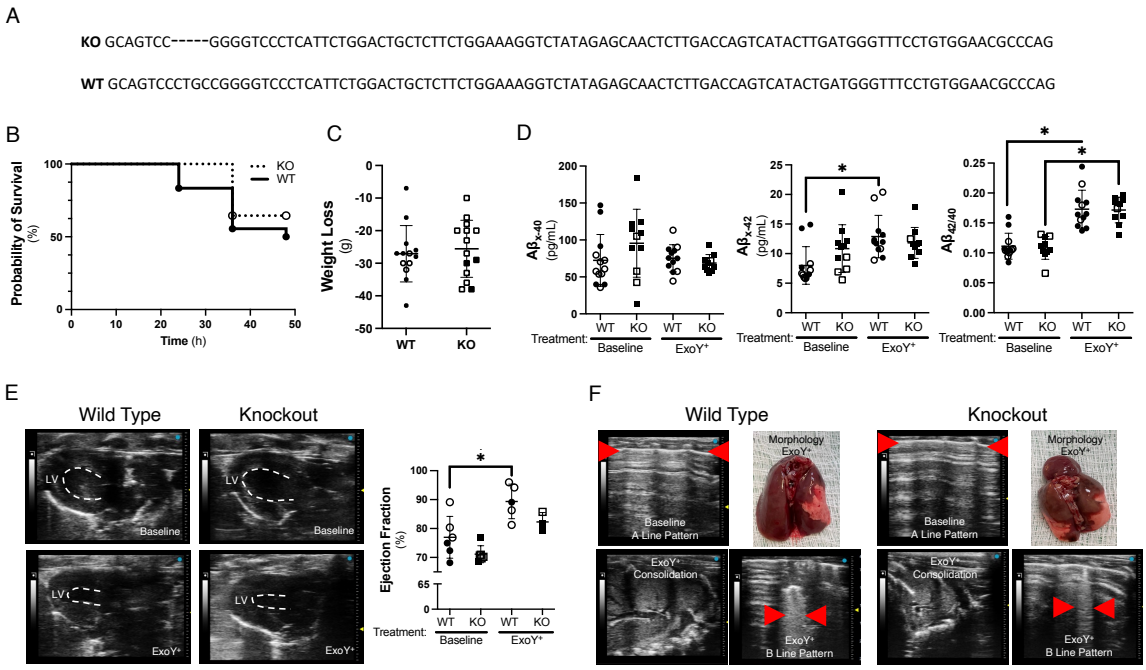

Figure 6. Wild type and GSAP knockout rats exhibit similar infection-induced hemodynamic responses. *(A)* Schematic showing the 5 bp deletion in exon 16 of the GSAP gene produced using CRISPR/Cas9 technology. *(B)* Wild type (WT; $N = 18$) and knockout (KO; $N = 31$) rats were infected with ExoY$^+$ and survival was recorded. Eighty three percent of wild type rats survived 24 h post infection, while 55% and 50% of the rats survived to 36 and 48 h post-infection, respectively. One hundred percent of the knockout rats survived 24 h post-infection, while 65% of the rats survived to 48 h post-infection (P = ns between WT and KO rats). *(C)* Wild type ($N = 13$) and knockout ($N = 14$) rats were weighed before infection and 48 h post-infection. Rats lost ~25 g body weight 48 h post-infection. There was no significant difference in weight loss between the two groups (two-tailed Welch's t-test, P = ns). *(D)* $A\beta_{x\text{-}40}$ ($A\beta_{40}$) was measured in rats at baseline and 48 h following infection. There was no difference in the baseline circulating $A\beta_{40}$ concentrations (P = ns; N = 4-6). $A\beta_{x\text{-}42}$ ($A\beta_{42}$) was measured in rats at baseline and 48 h following infection. There was no difference in the baseline circulating $A\beta_{42}$ concentrations (P = ns), yet the $A\beta_{42}$ concentration was increased in wild type but not in the knockout rats 48 h post-infection ($P = 0.0069$; N = 4-6). The $A\beta_{42/40}$ ratio was not different among the animal genotypes, but it was increased in both wild type and knockout rats following infection. *(E)* Cardiac ultrasound was assessed at baseline and 48 h post-infection. Ejection fraction was significantly increased post-infection in WT ($P = 0.0365$; N = 5-6) rats. *(F)* Pulmonary ultrasonography revealed consolidation and B lines (red arrowheads) in both the wild type and knockout rats, post-infection. Lung morphology showed a heterogeneous pattern of lung injury indicative of bi-lobar pneumonia. Summary data are reported as mean ± standard deviation. Open symbols reflect female subjects and closed symbols indicate male subjects. Statistics were done using two-way ANOVA with a Tukey's multiple comparisons test unless otherwise stated.

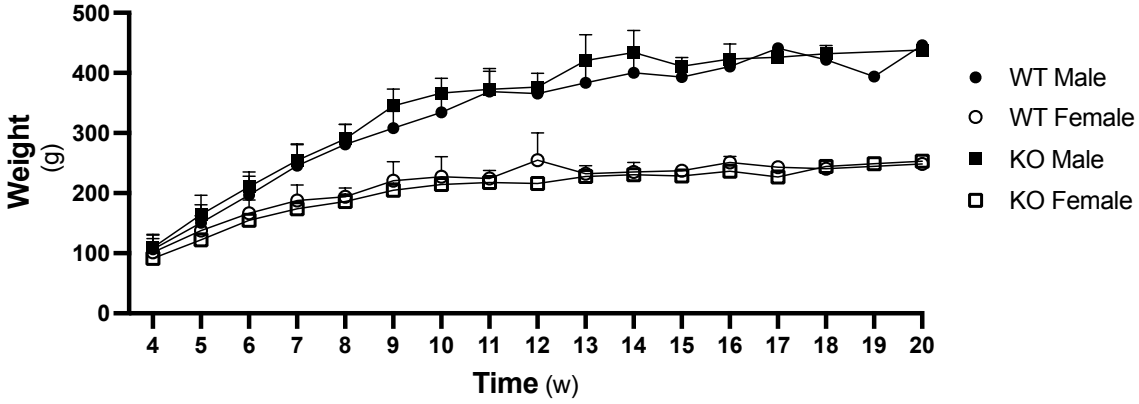

Figure 7. GSAP does not impact growth rates. WT and KO rat weights were assessed over a 20-week time course. Growth rates were not different among WT and KO male and female rats (P = ns), as assessed Sidak's multiple comparison test (N per time point = 2-83). Error bars indicate mean $\pm$ standard deviation.

Table 1. GSAP does not impact organ size. Rats were sacrificed at 3-4 months of age. Organs were harvested and weighed and then dried for 7 days to allow for calculation of wet to dry ratios. Organ weights and ratios were compared between groups using a Student's T-test (*P* = ns across all organs), *N* = 5-8 per group.

Organs	**Wild type**		**Knockout**	
Wet Weight	**Male**	**Female**	**Male**	**Female**
	Mean(g) ± SD	Mean(g) ± SD	Mean(g) ± SD	Mean(g) ± SD
Kidney	2.32 ± 0.130	1.63 ± 0.229	2.25 ± 0.095	1.63 ± 0.247
Liver	14.31 ± 1.311	8.06 ± 0.285	13.88 ± 0.843	8.72 ± 0.787
Lung	1.19 ± 0.059	1.03 ± 0.036	1.13 ± 0.007	1.08 ± 0.186
Spleen	0.66 ± 0.040	0.48 ± 0.070	0.62 ± 0.055	0.58 ± 0.198
Thymus	0.48 ± 0.137	0.23 ± 0.026	0.60 ± 0.131	0.34 ± 0.160
RV	0.15 ± 0.015	0.10 ± 0.021	0.18 ± 0.014	0.22 ± 0.207
LV	0.67 ± 0.101	0.51 ± 0.046	0.62 ± 0.028	0.59 ± 0.195
	Wild type		**Knockout**	
Wet:Dry Ratio	**Male**	**Female**	**Male**	**Female**
	Mean(g) ± SD	Mean(g) ± SD	Mean(g) ± SD	Mean(g) ± SD
Kidney	3.64g ± 0.183	3.85 ± 0.320	3.56 ± 0.108	4.08 ± 0.440
Liver	2.76 ± 0.105	2.88 ± 0.100	2.73 ± 0.104	2.89 ± 0.099
Lung	3.91 ± 0.159	3.91 ± 0.096	3.88 ± 0.028	4.45 ± 1.000
Spleen	3.80 ± 0.368	3.61 ± 0.176	3.83 ± 0.312	4.04 ± 1.052
Thymus	3.55 ± 0.582	3.25 ± 0.545	3.86 ± 0.373	4.15 ± 2.162
RV	3.87 ± 1.206	3.84 ± 1.630	3.71 ± 0.764	4.32 ± 3.603
LV	5.243 ± 3.013	3.56 ± 0.263	3.55 ± 0.021	4.24 ± 1.738

Table 2. GSAP does not alter complete blood counts. Arterial blood was collected from rats prior to their sacrificed at 3-4 months of age for a complete blood count. Complete blood counts were compared between groups using a Student's T-test (P = ns across all groups), N = 5-8 per group.

Variable	Wild type		Knockout	
	Male	**Female**	**Male**	**Female**
	Mean ± SD	Mean ± SD	Mean ± SD	Mean ± SD
WBC (10^6/4)	5.06 ± 0.85	2.96 ± 0.51	4.30 ± 2.18	3.57 ± 0.58
RBC (10^6/4)	8.13 ± 0.71	8.13 ± 0.62	7.62 ± 0.81	8.16 ± 0.81
Hemoglobin (g/dL)	14.7 ± 1.04	14.53 ± 0.85	14.33 ± 0.85	14.68 ± 0.76
Hematocrit (%)	47.77 ± 7.47	44.90 ± 2.25	45.40 ± 4.33	45.78 ± 2.75
MCV (fL)	57.93 ± 3.86	55.47 ± 1.44	59.73 ± 3.81	59.28 ± 2.61
RDW-SD (fL)	24.98 ± 4.59	23.07 ± 1.46	25.28 ± 2.24	22.75 ± 0.93
RDW-CV (%)	15.45 ± 3.05	15.17 ± 1.91	13.98 ± 1.15	15.13 ± 2.49
Platelets (10^3/4)	742.5 ± 71.08	735.67 ± 59.77	1005.25 ± 240.24	709.75 ± 82.42

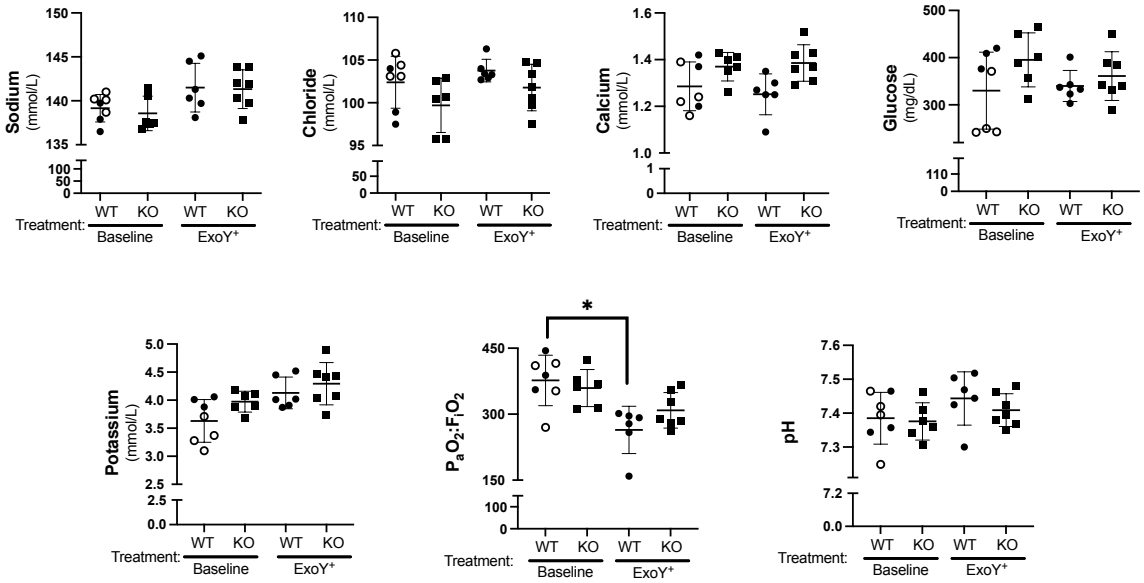

Figure 8. GSAP contributes to the arterial hypoxemia that develops following bacterial pneumonia. Blood was collected from the abdominal aorta of uninfected controls and rats 48 hours post-infection for electrolyte and arterial blood gas analysis. No differences were in the sodium, chloride, glucose, and pH values between groups (P = ns determined by two-way ANOVA with Tukey's multiple comparisons test; N = 6-7). Calcium and potassium were unchanged in both WT and KO animals after infection. (P = ns; N = 6-7). The partial pressure of oxygen in the arterial blood compared to the fraction of inspired oxygen, the P_aO_2 to F_iO_2 ratio, was significantly decreased in the WT infected rats compared to their uninfected counterparts (P = 0.0029; N = 6-7). Error bars indicate mean $\pm$ standard deviation. Open symbols reflect female subjects and closed symbols indicate male subjects. All statistics were determined by two-way ANOVA with Tukey's multiple comparisons test unless stated otherwise.

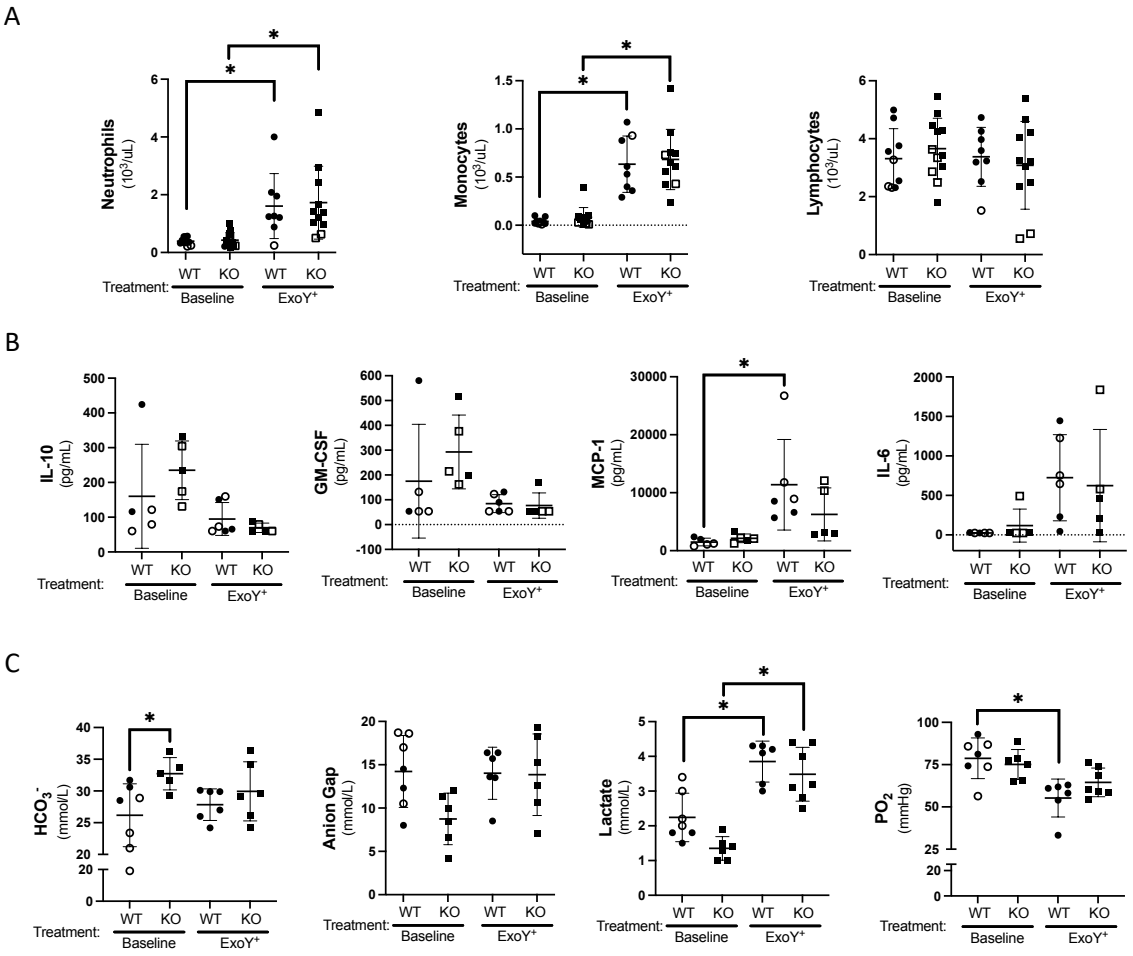

Figure 9. GSAP contributes to innate immunity and alveolar-capillary barrier integrity. Blood was collected from the abdominal aorta of control and ExoY^{+}-infected WT and KO rats and a complete blood count with differential, a cytokine immunoassay in plasma, and an electrolyte panel were analyzed. *(A)* WT and KO rats exhibited neutrophilia (WT, P = 0.037 and KO, P = 0.0025) and monocytosis (WT, $P < 0.0001$ and KO, $P < 0.0001$) (WT, N = 8-10 and KO, N = 11-12), whereas lymphocyte count remained unchanged (P = ns), after infection. *(B)* The pro-inflammatory cytokine MCP-1 was increased following infection in the WT rats (P = 0.0096; N = 5-6). *(C)* KO rats had an increase in the bicarbonate concentration when compared to the WT controls at baseline (P = 0.0411 using; N = 5-7). After infection, lactate was increased in both WT (P = 0.0006) and KO rats ($P < 0.0001$), while only WT rats exhibited a significant decrease in arterial oxygenation (P_aO_2, P = 0.0029; N = 5-7). All statistics were determined by two-way ANOVA with Tukey's multiple comparisons test. Summary data are reported as mean $\pm$ standard deviation. Open symbols reflect female subjects and closed symbols indicate male subjects.

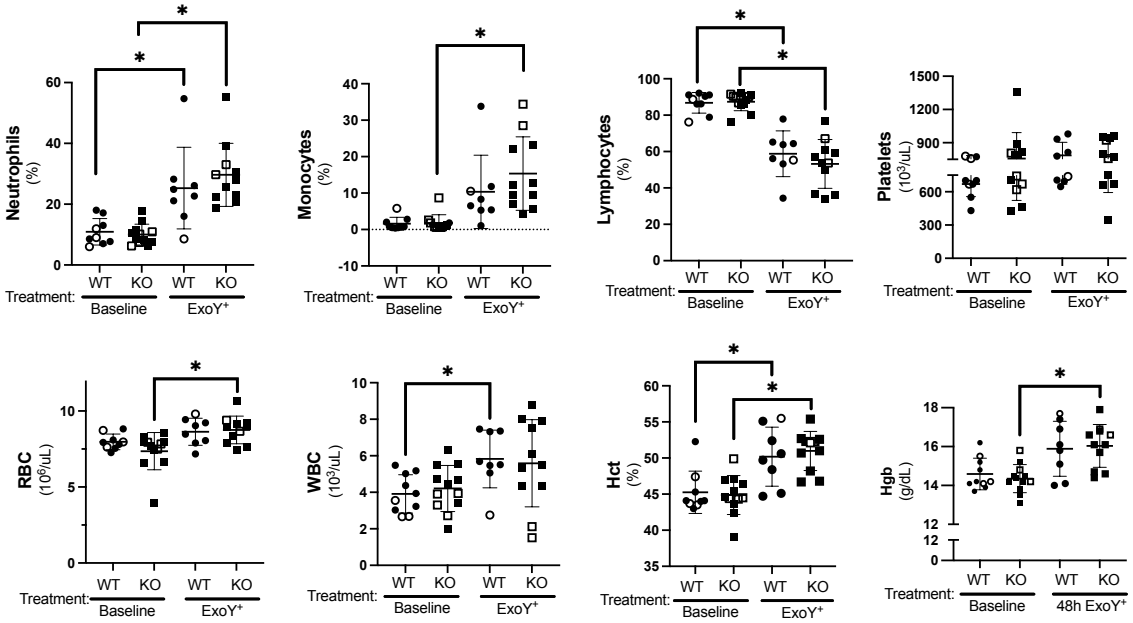

Figure 10. GSAP does not contribute to the infection-elicited neutrophilia, monocytosis, and dehydration observed following infection. Blood was collected from the abdominal aorta of uninfected controls and rats 48 hours post-infection for a complete blood count with differential. The percentages of neutrophils (WT: $P = 0.0014$; KO: $P < 0.0001$) and monocytes (WT: P = ns; KO: $P = 0.0006$) in the circulation increased, whereas the percentage of lymphocytes (WT: $P < 0.0001$; KO: $P < 0.0001$) decreased, following infection in both the WT and KO rats, respectively (N = 8-12). Red blood cell (RBC) count was increased in the KO animals post-infection ($P = 0.0078$; N = 8-12), while the white blood cell (WBC) count was increased only in the WT animals post-infection ($N = 0.0380$; N = 8-12). Hematocrit (Hct) was increased in both WT (Hct: $P = 0.03$) and KO (Hct: $P = 0.0007$) rats after infection, consistent with dehydration while hemoglobin (Hgb) was only increased in the KO ($P = 0.0046$;) after infections (N = 8-12). Error bars indicate mean $\pm$ standard deviation. Open symbols reflect female subjects and closed symbols indicate male subjects. Statistics were determined by two-way ANOVA with Tukey's multiple comparisons test.

Figure 11. Infection evokes neutrophil recruitment to the airways, revealing immature neutrophil populations in GSAP knockout rats. *(A)* BALF was collected from WT and KO control and infected rats and analyzed using flow cytometry. Both the WT and KO infected rats had a higher number of cells in their BALF 48 h post-infection, indicating GSAP does not interfere with neutrophil recruitment. WT ($P < 0.0001$ using two-way ANOVA with Tukey's multiple comparisons test; $N = 5$-7) and KO ($P < 0.0001$ using one-way ANOVA with Tukey's multiple comparisons test; $N = 5$-6). *(B)* Cells retrieved from the BALF were labeled with antibodies targeting macrophages (i.e., CD68-pan macrophage and CD11b,c-monocytes, granulocytes, macrophages, dendritic, natural killer cells), hematopoietic cells (i.e., CD45), and neutrophils (i.e., RP-1). CD45 and CD11b,c double positive cells were selected and then screened for CD68. Cells retrieved from uninfected rats displayed a CD68 high population, consistent with alveolar macrophages. Cells retrieved from the BALF following infection exhibited a new left shifted distinct population that was CD68 low. *(C)* To assess whether the CD68 low cell population was neutrophils, we examined RP-1. The CD45 and CD11b,c double positive, CD68low cells were positive for RP-1, indicating they are neutrophils. Whereas a single population was identified from the wild type rats, two distinct populations of RP-1 positive cells were resolved in the knockout rats. *(D)* The CD45 positive, His48 positive, and CD68low cells were selected and cytospun onto glass slides to examine morphology. Cells from WT rats exhibited the expected polylobar nuclear morphology, consistent with mature neutrophils. In contrast, cells from KO rats possessed a mixed population, with both immature (i.e., hyposegmented) and mature (polysegmented) neutrophils. Black arrows highlight mature neutrophils and red and yellow arrowheads identify immature neutrophils at differing stages of nuclear segmentation. **Fig 11 cont.** *(E)* H & E staining of lung slices after $ExoY^+$ infection shows inflammatory cell recruitment to the distal airways with consolidation and perivascular cuffing, consistent with pneumonia in both WT and KO rats. Summary data are reported as mean $\pm$ standard deviation. Open symbols reflect female subjects and closed symbols indicate male subjects.

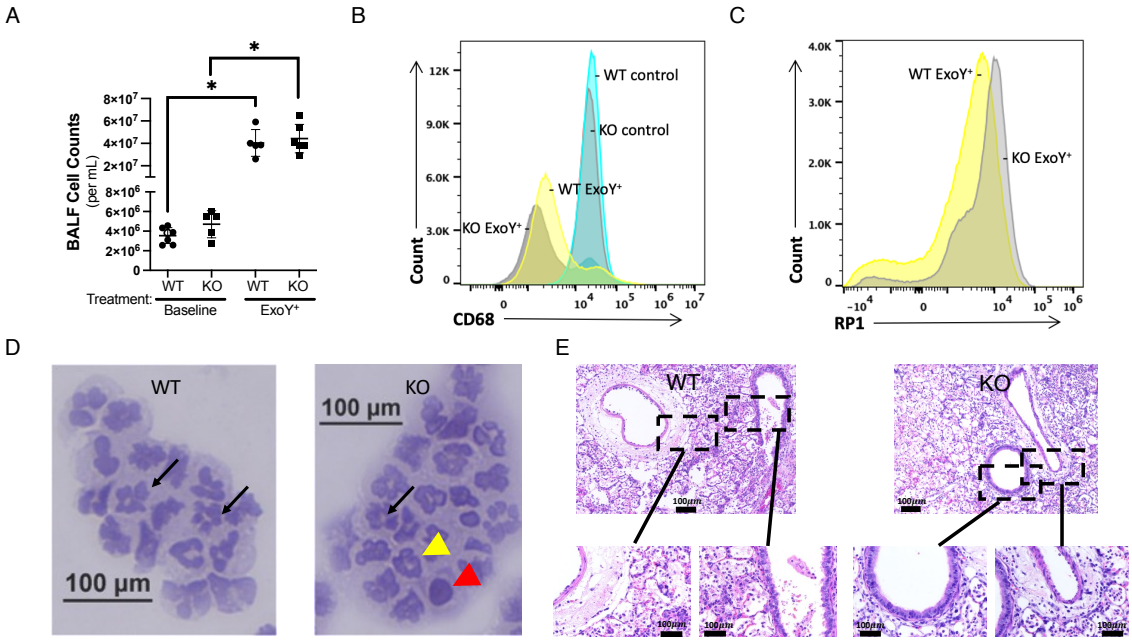
A
B
C
BALF Cell Counts (per mL)
Treatment:
WT
KO
WT
KO
Baseline
ExoY+
WT control
KO control
WT ExoY+
KO ExoY+
Count
CD68
WT ExoY+
KO ExoY+
RP1
D
E
WT
KO
100 µm
100 µm

Figure 11.

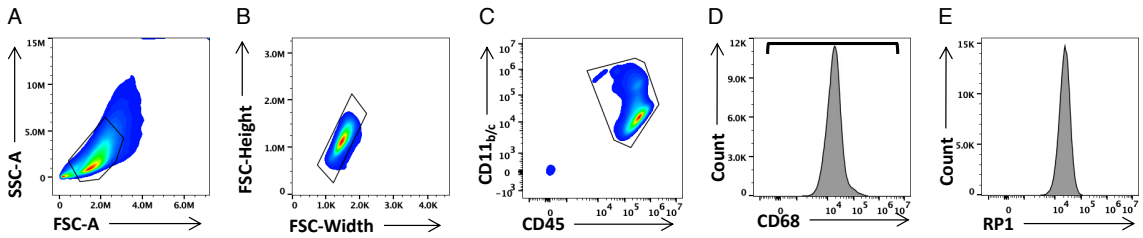

Figure 12. Neutrophils in the bronchoalveolar lavage fluid were identified by a CD45 and CD11b,c double positive, CD68 low, RP1 positive gating strategy. (*A*) Leukocyte cell populations were selected based on their forward and side-scatter area. (*B*) Single cells were selected using forward scatter width and height. From the single cell populations, the CD45 and CD11b,c double positive cells (*C*) were further selected based on their high or low CD68 immunoreactivity (*D*; uninfected control is shown). (*E*; uninfected control is shown) CD68 low cell populations were gated for RP1 populations to identify neutrophils.

4.2.2 GSAP Contributes to Disruption of the Alveolar-Capillary Barrier and Susceptibility to Myocardial Infarction During Infection

Results from blood oxygenation and lung histological analyses suggested that GSAP knockout rats exhibit improved alveolar-capillary barrier integrity during infection. To directly test this idea, bacteria was added directly to an isolated perfused lung and the filtration coefficient was measured to evaluate vascular permeability. After an initial isogravimetric period and baseline filtration coefficient measurement, *P. aeruginosa* was introduced into the trachea and the filtration coefficient was measured 4-hours later (**Fig. 13A**). Baseline filtration coefficient was not different in the lungs from wild type and GSAP knockout rats. Whereas *P. aeruginosa* induced an increase in filtration coefficient in the wild type lungs, this increase in permeability was not present in lungs from the GSAP knockout rats. Thus, GSAP contributes to disruption of the alveolar-capillary barrier during infection, even in the absence of a substantial neutrophil recruitment to the airways.

Susceptibility to cardiovascular disease, including myocardial infarction, stroke, and fatal coronary heart disease, is increased following pneumonia [29], although the mechanism(s) for this observation is unknown. We examined whether GSAP contributes to the severity of myocardial ischemia reperfusion injury at baseline and following infection. The left anterior descending coronary artery was ligated for 30 minutes, followed by 2 hours of reperfusion. Heart rate and blood pressure were not different between wild type and knockout rats throughout the experiment, although both hemodynamic parameters gradually decreased over the 2.5-hour time course (**Fig. 14**). Quantification of infarcts revealed no differences between the ischemic zones in the

hearts of wild type and GSAP knockout rats (**Fig. 13B** and **Fig. 14**). Thus, GSAP does not influence susceptibility to myocardial ischemia and reperfusion injury in uninfected rats.

In wild type rats, pneumonia increased the infarcted myocardial region size by ~30% compared to uninfected controls (**Fig. 13B** and **Fig. 14**). However, pneumonia did not increase infarct size in hearts from the knockout rats. No post-infection differences in heart rate and blood pressure were seen in wild type and GSAP knockout rats (**Fig. 14**). Thus, infection reveals a novel GSAP-dependent mechanism of myocardial injury during ischemia and reperfusion.

Figure 13. GSAP contributes to disruption of the alveolar-capillary barrier and susceptibility to myocardial ischemia-reperfusion injury following infection. *(A)* $ExoY^+$ was introduced into the trachea of the isolated perfused lung and filtration coefficient *(*K_f) measured 4 hours later. Infection increased K_f in the lungs from WT rats *(*$P = 0.0003$; $N =$ 10-11) but did not increase K_f in the lungs from KO rats ($P =$ ns). Kf in lungs from KO rats was significantly reduced when compared to WT rats post-infection ($P = 0.02$; $N =$ 10-11). Top left panel represents summary data, means $\pm$ standard deviation, and the bottom left panel shows representative lungs before (baseline) and after infection ($ExoY^+$). Red arrowheads highlight edematous lung regions. *(B)* Control and 48-hour infected rats were assessed for myocardial susceptibility to 30 minutes of regional myocardial ischemia followed by 2 hours of reperfusion. In uninfected rats, both WT and KO rats exhibited ~45% infarction of the ischemic (risk) area and were not different from each other ($P =$ ns between groups). Following infection, the percent of the risk area that infarcted was increased by ~30% in WT rats ($P = 0.0370$). The percent of infarcted tissue between the infected WT and KO animals was significant ($P = 0.0028$; $N =$ 5-6). Infarct size in the infected KO rats was not different from that in the uninfected KO rats ($P =$ ns). A representative slice of the ischemic zone from a tetrazolium-stained heart from each of the 4 groups is shown below the summary data. The amount of infarct on each slice as determined by the Image J software is outlined. A black 1 cm scale line appears in each panel. Each slice was from a heart with an infarct size closest to the mean for each group. See the supplement for more details on the infarct sizing. Summary data are reported as mean $\pm$ standard deviation. Open symbols reflect female subjects and closed symbols indicate male subjects. Statistics were determined by two-way ANOVA with Tukey's multiple comparisons test.

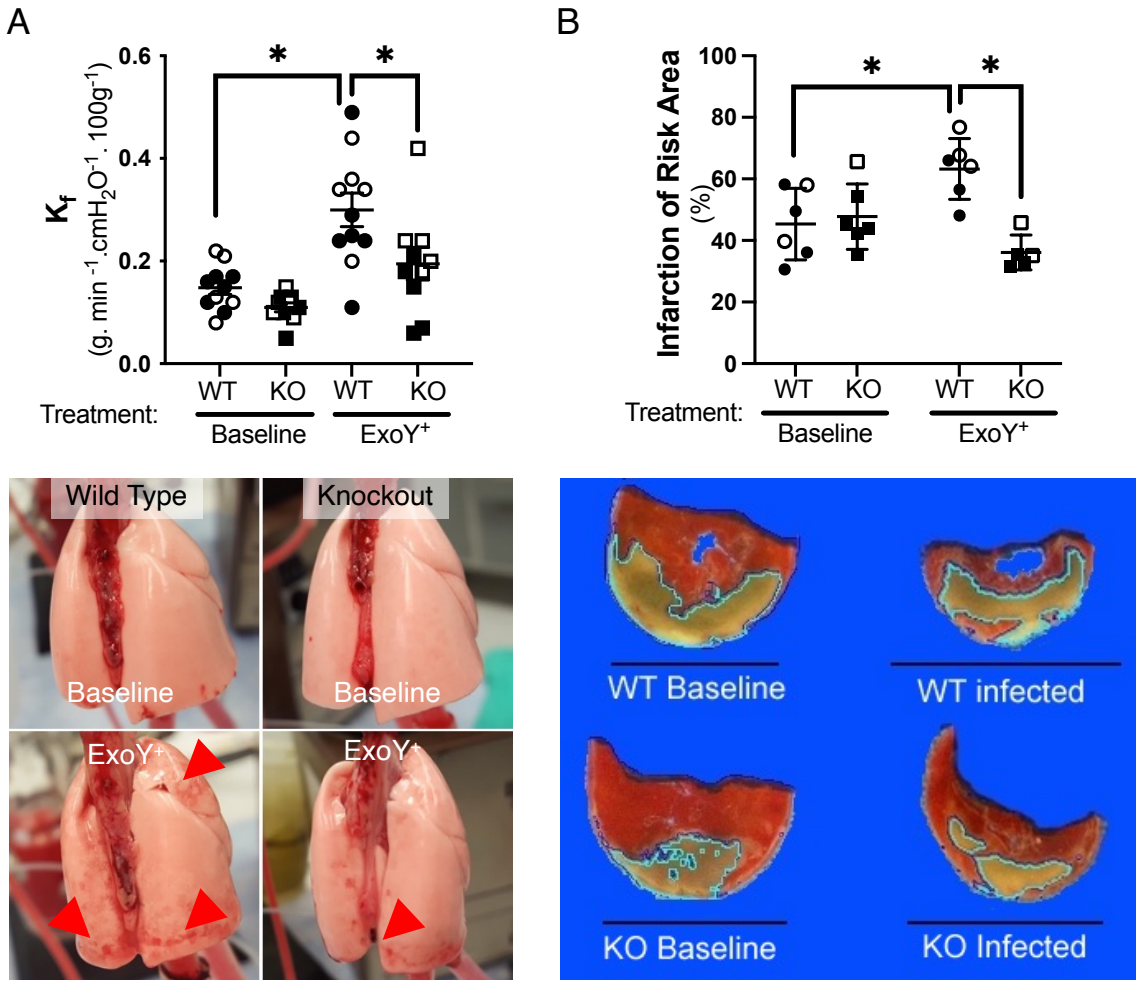
A
B
K_f
(g. min $^{-1}$.cmH$_2$O^{-1}. 100g^{-1})
0.6
0.4
0.2
0.0
*
*
WT
KO
WT
KO
Treatment:
Baseline
ExoY$^+$
Infarction of Risk Area
(%)
100
80
60
40
20
0
Wild Type
Knockout
Baseline
Baseline
ExoY$^+$
ExoY$^+$
WT Baseline
WT infected
KO Baseline
KO Infected

Figure 13.

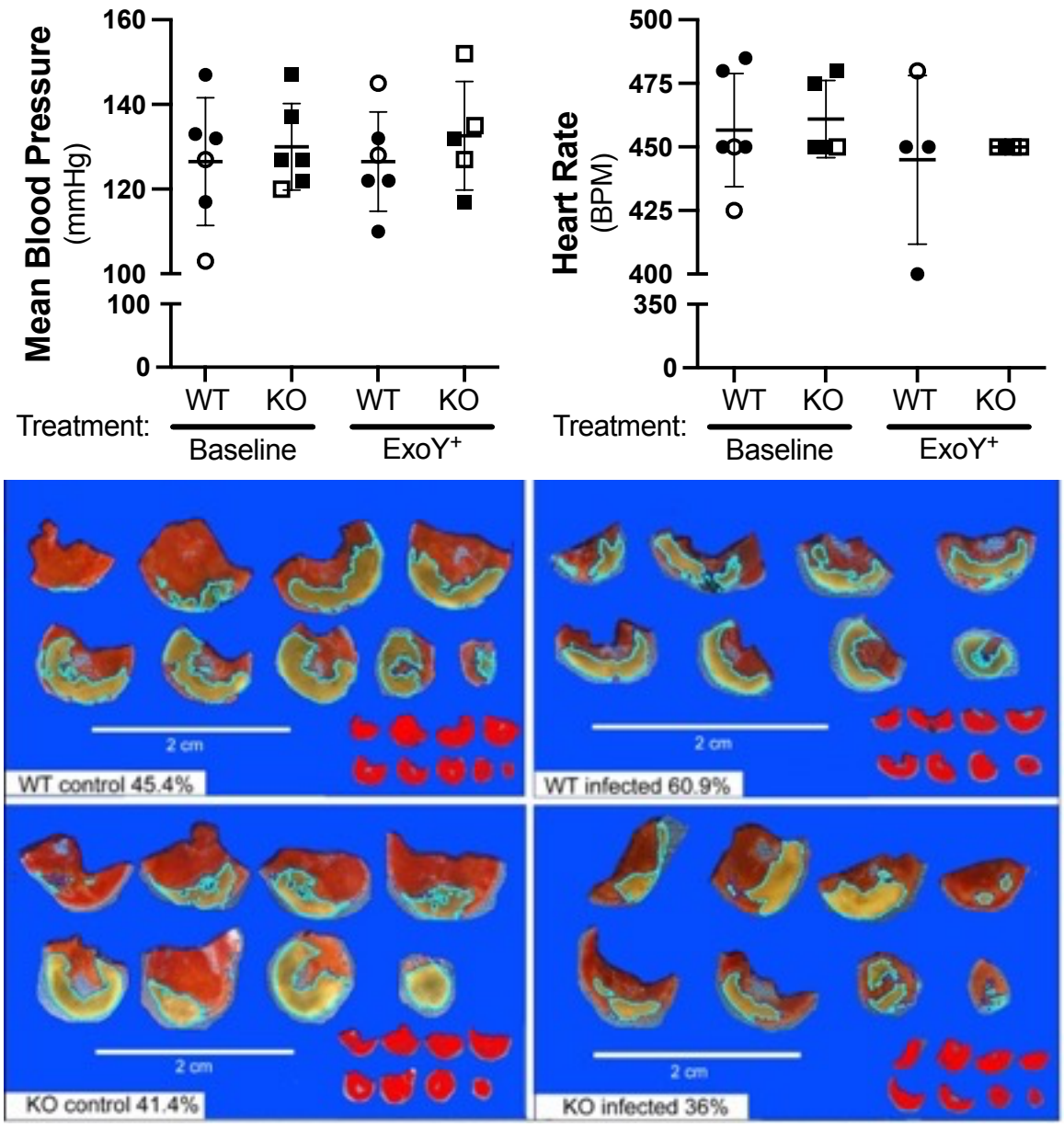

Figure 14. GSAP does not impact mean blood pressure or heart rate. Heart rate (beats per minute, BPM) and mean blood pressure were measured throughout the length of the ischemia and reperfusion experiment. No differences were seen between any of the groups (P = ns determined by two-way ANOVA with Tukey's multiple comparisons; N = 4-6). Error bars indicate mean ± standard deviation. Open symbols reflect female subjects and closed symbols indicate male subjects. A representative example of multiple heart slices from a tetrazolium-stained heart in each of the 4 groups is shown.

4.2.3 GSAP Limits Synaptic Strengthening and Suppresses Hyperexcitability of CA1 Neurons

Neurocognitive dysfunction is common during and in the aftermath of pneumonia [30]. Thus, we examined the impact of pneumonia on long-term potentiation (LTP) at the Schaffer collateral synapses in hippocampi isolated from wild type and GSAP knockout rats (**Fig. 15A**). When compared to controls, hippocampi obtained from the knockout rats exhibited a reduced synaptic response immediately after induction of LTP (at 5 min, E-LTP; WT: 118 ± 4.3% versus KO: 97.9 ± 3.2%, $P = 0.0005$). However, LTP in the GSAP knockout hippocampi was potentiated with time, surpassing the LTP seen in the control animal hippocampi 30 minutes post-theta burst stimulation. The late LTP (at 60 min, L-LTP) trended higher in the knockout rats than it was in the control rats (WT: 165 ± 8.7% versus KO: 195 ± 12.4%; $P = 0.1159$). The shift in synaptic strengthening from E-LTP to L-LTP appeared to differ. We assessed the amount of potentiation from E-LTP to L-LTP by examining their ratio. Results illustrate that GSAP knockout hippocampi had significantly higher L-LTP to E-LTP ratio than did the control hippocampi. Thus, the GSAP knockout hippocampi exhibited greater synaptic strengthening.

LTP was then measured 48 hours after lung infection. Consistent with our prior studies [17,18,22], hippocampal E-LTP and L-LTP was abolished in the hippocampi of controls (**Fig. 15**). LTP was also reduced in the hippocampi of GSAP knockout rats, however, the L-LTP was not abolished; the L-LTP response remained elevated when compared to the controls. Whereas infection decreased both E-LTP and L-LTP in GSAP knockout hippocampi, the magnitude of the decrease in both measurements was lower in the knockout hippocampi than it was in the wild type hippocampi (L-LTP, 148 ± 10.0%

versus 110 ± 6.3%, $P = 0.019$). The ratio of synaptic strengthening from L-LTP to E-LTP remained higher in the GSAP knockout rats with infection and did not differ from uninfected rats; the degree of synaptic potentiation was genotype-dependent and infection-independent. It is therefore likely that GSAP is not the principal mechanism linking infection to impaired LTP.

To further explore the mechanisms by which GSAP regulates neuronal information processing, we quantified the input-output relationship from the field presynaptic fiber volley and postsynaptic response, respectively (**Fig. 15B**). Presynaptic fiber volley, indicative of depolarization-mediated axonal recruitment, was reduced in the knockout rats, suggesting that GSAP contributes to CA3 axonal depolarization and action potential firing induced by fast Na^+ channels. However, for any given presynaptic depolarization, the excitatory postsynaptic response was higher in GSAP knockout rats (**Fig. 15B**), both at baseline and after lung infection, suggesting that GSAP governs coupling between presynaptic-to-postsynaptic (or input-output) neurotransmission. GSAP could increase presynaptic neurotransmission by modulating neurotransmitter release probability and it could decrease postsynaptic neurotransmission by reducing the neurotransmitter receptor density and/or signaling (i.e., NMDA and/or AMPA receptors), spine density, and/or the number of postsynaptic neurons recruited [17].

To investigate presynaptic neurotransmitter release probability, we recorded the paired-pulse ratio at 25, 50, 100, and 400 ms interstimulus intervals (**Fig. 15C**). Under baseline conditions, the paired-pulse ratio was lower throughout and significantly reduced at 50 ms in GSAP knockout versus the control hippocampi, indicating an increased neurotransmitter release probability in the knockout rats. Thus, whereas GSAP

knockout hippocampi displayed a decrease in the presynaptic fiber volley (**Fig. 15B**), they possessed a potentiated neurotransmitter release probability and postsynaptic response with each stimulation. Lung infection reduced the paired-pulse ratio in control but not in GSAP knockout hippocampi. Thus, GSAP optimizes the efficiency of coupling between CA3 depolarization and neurotransmitter release at presynaptic boutons and postsynaptic densities, modulating the neurotransmitter release and receptor response, respectively.

We noted that the GSAP knockout CA1 neurons were hyperexcitable following Schaffer collateral stimulation under baseline conditions, and further, that both the wild type and GSAP knockout neurons were hyperexcitable following infection (**Fig. 15B**). We surveyed excitability quantifying population spikes from the dendritic field excitatory postsynaptic potential recordings (**Fig. 15D**). The time-to-population spike was calculated from the peak of the fiber volley to the groove between the two subsequent field potential peaks (i.e., the first peak indicates excitatory postsynaptic response, and the second peak denotes population spike or postsynaptic cell firing). The time-to-population spike was significantly faster in GSAP knockout than it was in control hippocampi under basal conditions (WT: 7.9 ± 0.30 ms versus KO: 6.59 ± 0.32 ms, P = 0.0067), suggesting that the GSAP knockout postsynaptic neurons are hyperexcitable and more likely to fire action potentials. Lung infection increased the occurrence of population spikes in hippocampal slices prepared from both the control and GSAP knockout rats (WT: from 57 to 71% versus KO: from 63 to 80%) and shortened the time-to-population spike in both control and knockout rats. Thus, GSAP dampens CA1 neuron

excitability under basal conditions, and lung infection leads to hyperexcitability in both the wild type and knockout CA1.

Figure 15. GSAP knockout rats exhibit elevated long-term potentiation, neurotransmitter release probability, and excitability. *(A)* Left panel: Summary plot of long-term potentiation. Field excitatory postsynaptic potential (fEPSP) slopes were normalized to those before the theta-burst stimulation (TBS; delivered at time 0) and plotted against time (mean ± standard error of the mean). The bottom traces show averages of five representative traces obtained from time points 'a' (-3-0 min; black), 'b' (5-8 min; blue), and 'c' (57-60 min; red) for uninfected baseline wild type and GSAP knockout rats (WT, $N = 30$ slice recordings; KO, $N = 29$ slice recordings) and ExoY$^+$ infected rats (WT, $N =$ 40 recordings; KO, $N = 25$ recordings). Vertical and horizontal scale bars represent 0.1 mV and 5 ms, respectively. Middle panels: Early LTP (E-LTP; 5-8 min post TBS) responses were plotted and compared. The response from uninfected WT was significantly different from other groups ($F(3, 120) = 20.57$; $P < 0.0001$). The late LTP (L-LTP; 57-60 min post TBS) plot shows that ExoY$^+$ infection significantly reduced responses in both WT ($P =$ 0.0024) and KO rats ($P = 0.0179$). Right panel: Ratio of the L-LTP versus E-LTP plot shows that the amount of synaptic potentiation was higher in GSAP KO rats (WT versus KO: before ExoY$^+$: $P = 0.0002$). Within the same genotype, there was no difference before and after infection ($P =$ ns). *(B)* Left panel: Representative elicited fEPSP traces in response to increasing stimulus intensity (0 – 100 μA with 10 μA increments). The red traces were elicited with 100 μA and highlight the appearance of population spike in WT only after ExoY$^+$ infection and in KO with and without infection. From left to right, the first downward peak denotes presynaptic fiber volley elicited by Schaffer collateral electrical stimulation, and the next larger downward peak denotes the postsynaptic response; the third downward response indicates the population spike. Vertical and horizontal scale bars represent 0.3 mV and 5 ms, respectively. Middle panels: Presynaptic fiber volley amplitudes were plotted against stimulus intensities, and the obtained slopes (FV versus Stim) were compared across the four groups. Baseline (WT, $N = 30$ recordings; KO, $N =$ 30; $P = 0.0246$) and ExoY$^+$ infected (WT, $N = 38$; KO, $N = 25$; $P = 0.0410$). Right panels: Postsynaptic fEPSP slopes plotted against fiber volleys were line-fitted, and the slopes were compared. The postsynaptic responses were significantly different between WT and KO rats; baseline (WT versus KO; $P = 0.0027$) and ExoY$^+$ infected (WT versus KO; $P <$ 0.0001). *(C)* Left panel: Summary plot to study the presynaptic neurotransmitter release probability. A pair of stimuli were delivered to elicit fEPSPs. The paired-pulse ratios, determined from the amplitudes of second fEPSP over those of the first responses, were plotted against the inter-stimulus intervals (mean ± standard error of the mean). Uninfected WT showed significantly higher paired-pulse ratios at shorter stimulus intervals when compared with other groups: at 25 ms (**P* values of WT versus KO = 0.0196; versus WT ExoY$^+$ = 0.0072; versus KO ExoY$^+$ = 0.0037); Middle panel: Representative averages of five raw traces were overlayed, aligned, and normalized to the first fEPSP amplitude to show all evoked responses, and compared across the four groups. Vertical and horizontal scale bars represent 0.1 mV and 100 ms, respectively. *(D)* Population spike time was determined from the time between fiber volley peak (i.e., first downward peak in *B*) and the upward peak, between the postsynaptic response (second downward peak) and the population spike (third downward peak). When compared, the WT baseline was significantly different from the KO baseline (WT, $N = 17$ recordings; KO, $N = 19$; $P =$ 0.0067), and from the ExoY$^+$ infected WT (WT, $N =27$; KO, $N = 20$; $P = 0.0059$).

Unspecified summary data are reported as mean ± standard deviation. Open symbols reflect female subjects and closed symbols indicate male subjects. Statistics were determined using two-way ANOVA with Tukey's multiple comparisons test unless otherwise stated.

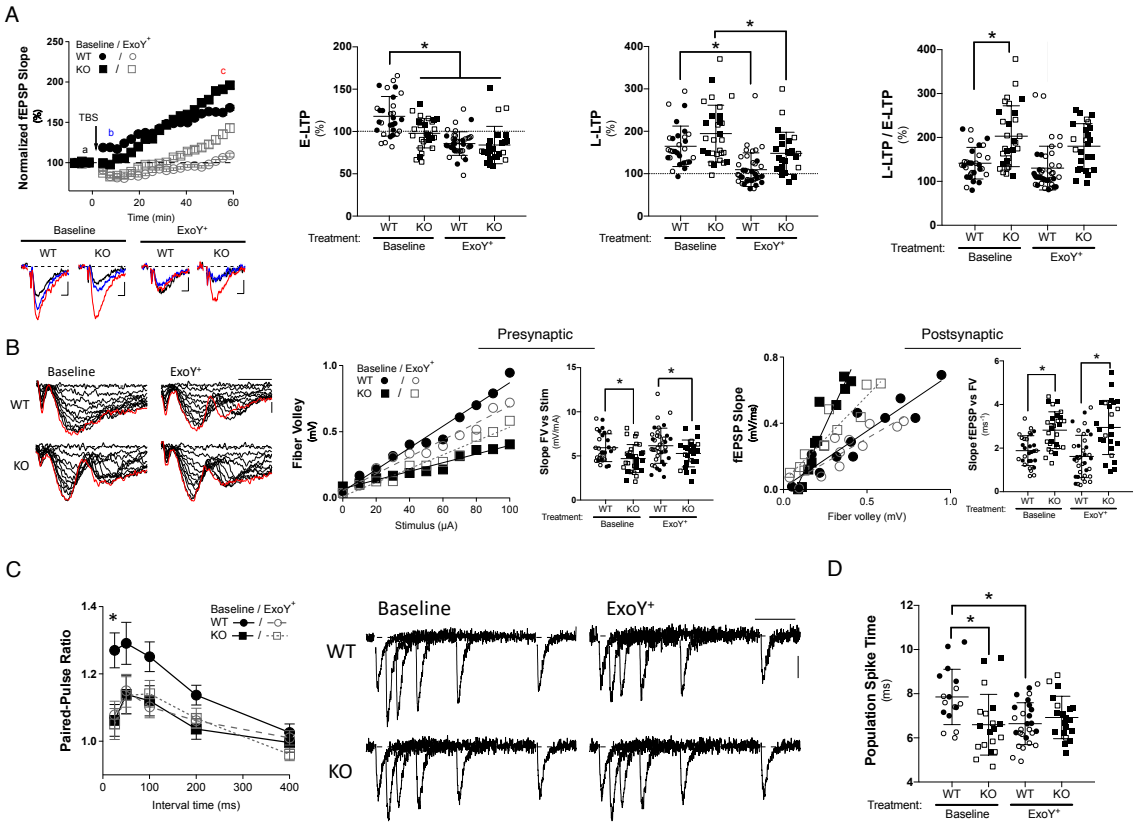
A
Normalized fEPSP Slope (%)
Baseline / ExoY+
WT
KO
TBS
a
b
c
Time (min)
Baseline
ExoY+
E-LTP (%)
L-LTP (%)
L-LTP / E-LTP (%)
Treatment:
B
Presynaptic
Postsynaptic
Fiber Volley (mV)
Stimulus (µA)
Slope FV vs Stim (mV/mA)
fEPSP Slope (mV/ms)
Fiber volley (mV)
Slope fEPSP vs FV (ms-1)
C
Paired-Pulse Ratio
Interval time (ms)
D
Population Spike Time (ms)

Figure 15.

4.3 Material and Methods

4.3.1 Ethical Use of Rats for Research

Rats were group-housed in microisolation caging with enrichment, according to the established guidelines for the care and use of laboratory rats. Rooms were on a 12:12-hour light-dark cycle, and the temperature was controlled. All animal procedures performed in this study were reviewed and approved by the University of South Alabama Institutional Animal Care and Use Committee.

4.3.2 Generation of GSAP Knockout Rats

GSAP knockout rats were generated at the Medical College of Wisconsin and shipped to the University of South Alabama for this study. Briefly, a single guide RNA targeting the sequence GTCCTTTGCAGTCCCTGCCG within exon 16 of GSAP (GenBank NM_001395028.2) was mixed with Cas9 (*S. pyogenes*) protein (QB3 MacroLab, UC Berkeley) and injected into the pronucleus of Sprague Dawley (Crl:SD, Charles River Laboratories) embryos. Among the offspring, a mutant founder was identified harboring a 5-bp deletion (rn72: chr4:13,849,488-13,849,492) mutation inducing a frame-shift in the GSAP coding sequence predicted to truncate the normal 846 amino acid GSAP protein (GenPept NP_001381957.1) after 382 amino acids. The founder was backcrossed to the parental Crl:SD strain to establish a breeding colony and was designated SD-*Gsap*^{em2Mcwi} (GSAP KO).

Once rats were received at the University of South Alabama, they underwent a 30-day quarantine, after which time, pathogen testing revealed they were all pathogen-free. Rats were bred in house. GSAP KO rats were genotyped using an equimolar mix of

primers rGSAP4delIntF (CGAGTCCTTTGCAGTCCG), rGSAP4delR (GAAGCACCAAGGGAGACTATG), rGSAP34F (AGGCTACTTTGTGGCTGTTTATTC) and rGSAPintR3 (GAGGGACCCCGGCAGGG). PCR conditions were: initial denaturation of 1 minute at 95° C followed by 35 cycles of 95° C for 10 seconds, 55.7° C for 20 seconds, and 72° C for 40 seconds, followed by a 5-minute hold at 7° C and an infinite hold at 10° C. With this strategy, the DNA of wild type rats produces an amplicon of 268 bp, the DNA of knockout rats produces an amplicon of 318 bp, and the DNA from heterozygous rats produces amplicons of both sizes.

4.3.3 *Pseudomonas aeruginosa*

ExoY is a *P. aeruginosa* type three secretion system effector. It is a promiscuous nucleotidyl cyclase that preferentially generates canonical (cGMP and cAMP) and non-canonical (cUMP and cCMP) cNMPs when injected into host cells, including the lung microvasculature [31-34]. The ExoY$^+$ (PA103Δ*exoU**exoT*::Tc/pUCP-*exoY*) mutant was generated by Dr. Dara Frank. The ExoY effector is expressed in ExoY$^+$ via a plasmid. Because of this, the bacteria are maintained in selection media consisting of Luria Broth (Miller's), glycerol, and carbenicillin (400 µg/mL) and kept in a -80° C freezer. The day before the planned experiment, bacteria were taken from previously frozen stocks, struck on Vogel-Bonner agar plates supplemented with 400 µg/mL of carbenicillin, and grown overnight at 37° C. The day of the experiment the bacteria are resuspended in PBS to an

optical density (OD_{540}) allowing for calculation of a final concentration of 10^7 – 10^8 bacteria (depending on the experiment conducted) in 250 µL of PBS.

4.3.4 Bacterial Culture and Intratracheal Inoculation

ExoY$^+$ bacteria were grown overnight on Vogel-Bonner medium containing 400 µg/mL of carbenicillin (SCBT CAS 4800-94-6) at 37° C. The morning of the inoculation the bacteria was resuspended in PBS until an OD_{540} of 0.500 (10^8 bacteria in 250 µL PBS) was reached, as determined by a spectrophotometer (ThermoFisher AquaMate UV/Vis). Rats were anesthetized using isoflurane gas (1-3%) and a surgical plane was achieved, as noted by the lack of toe and tail pinch reflex. The skin and muscle over the trachea were separated using a #11 scalpel and a 4-0 suture was placed to retract the muscle and allow for an unobstructed view of the trachea. Bacteria were thoroughly vortexed to ensure single cell suspension and collected into a 1 mL tuberculin syringe. The surgical table was adjusted to an ~70^o angle, the needle was inserted into the trachea, and the bacteria were instilled slowly over 5 minutes using a circular motion to ensure the bacteria were distributed evenly. The skin was sutured, and the rats were given Ethiqua (buprenorphine extended-release injectable suspension; 0.65 mg/kg body weight) via a single subcutaneous injection for pain management during recovery.

4.3.5 Measurement of Arterial Blood Gases and Collection of Plasma

Rats were anesthetized via isoflurane (1-3%) and a transperitoneal approach was utilized to isolate the abdominal aorta and separate it from the inferior vena cava. The abdominal aorta was catheterized using a 24 g catheter, blood was drawn into a 1 mL syringe for arterial blood gas measurements (Stat Profile® Prime$^+$ Critical Care Analyzer, Nova Biomedical), and then blood was drawn into a 10 mL syringe for separation into

plasma (lithium heparin), an electrolyte panel (heparin), and analysis of complete blood counts with differential (EDTA). To isolate the plasma fraction, whole blood was centrifuged at 200 x g at 4º C for 10 minutes (Eppendorf 5910 R). Once separated, the plasma was removed and stored at -80º C.

4.3.6 Organ Harvesting

Male and female GSAP knockout rats and controls were anesthetized using isoflurane gas (1-3%). Once a surgical plane was achieved, as defined by the absence of a withdrawal reflex following toe and tail pinch, the rats were placed on their backs with their nose connected to the isoflurane tank via plastic tubing. Hair was removed from the abdominal and chest areas using hair clippers and hair removal paste. A midline incision was made using a #10 scalpel. Organs including spleen, liver, brain, lungs, heart, and thymus were isolated and removed. Organ wet weights were measured and recorded. Organs were then allowed to dry over 7 days. After 7 days, dry weights were measured and the wet to dry weight ratio was calculated. In separate experiments, the organs were removed and placed into conical tubes, flash frozen with liquid nitrogen, and stored at -80º C.

4.3.7 Echocardiography

A Vevo 3100 (VisualSonics, Toronto, ON, Canada) with a 30 MHz transducer (MX550D) was used to evaluate cardiac and pulmonary function. Spontaneously breathing rats were anesthetized with isoflurane (~1.5%, titrated as needed) in a 1:1 O_2 – air admixture. Heart rate, electrocardiogram, and respiration were continuously recorded

using the sensor- embedded exam pad, while cardiac and pulmonary ultrasound parameters were assessed, as described in detail previously [22].

4.3.8 Isolated Perfused Lung

Wild type and knockout rats were anesthetized using Nembutal (65 mg/kg body wt). Once a surgical plane was achieved, as defined by the absence of a withdrawal reflex following toe and tail pinch, rats were intubated and ventilated, a sternotomy was performed, and pulmonary artery and left ventricle/atrium catheters were placed. Heart and lungs were removed *en bloc* and suspended in a humidified chamber, where mechanical ventilation and flow were established. Rat lungs were perfused with buffer (in mmol/L: 119.0 NaCl, 4.7 KCl, 1.17 $MgSO_4$, 1.18 KH_2PO_4, 23 $NaHCO_3$, and 5.5 glucose) containing 4% bovine serum albumin and physiological (2.2 mmol/L) $CaCl_2$, plus 6% autologous whole blood. Lungs were perfused at 8 mL/minute in forward flow for 15 minutes to obtain an isogravimetric status and 250µL of PBS containing $ExoY^+$ (10^8) was introduced into the trachea. Kf was measured again 4 hours later.

4.3.9 Bronchoalveolar Lavage Fluid Collection and Analysis

Rats were infected with $ExoY^+$ (10^8) and monitored over 48 hours. Control and infected rats were then anesthetized with isoflurane gas (1-3%) and once a surgical plane was established, as determined by a negative toe and tail pinch reflex, the trachea was cannulated, and a sternotomy was performed, removing the heart and lungs *en bloc*. The cannula was connected to tubing attached to a 60 mL syringe that was adjusted to provide 25 cm H_2O filling pressure. PBS was allowed to flow into the lungs using the force of gravity until full (~10mL), at which point the tubing was disconnected and a syringe connected directly to the tracheal cannula to remove the PBS. This process was repeated

3 times to collect ~30 mL of BALF. BALF was quickly vortexed, and 1 mL was transferred into a separate tube for cell counting using a Countess 3 Cell Counter (ThermoFisher), and bacterial cell counting. The remaining BALF was centrifuged at 500 x g for 5-10 minutes. The supernatant was collected and sterilized via a 0.2 µm filter and frozen at -80° for later use. The remaining cell pellet was frozen at -80° C in full DMEM containing 20% FBS and 14% DMSO for analysis at a later date.

4.3.10 Measurement of Cytokines

Plasma collected from control and 48-hour ExoY$^+$ (10^8)-infected WT and KO rats was analyzed for inflammatory cytokines according to manufacturer instructions (BioLegend). The rat inflammation panel (13-plex with V-bottom Plate; #740401) was used for these studies.

4.3.11 Measurement of Aβ

Plasma and brain lysates were collected from control and 48-hour ExoY$^+$ (10^8)-infected WT and KO rats and were analyzed for 3 different species of beta amyloid (1-38, 1-40, and 1-42) according to manufacturer instructions (Meso Scale Discovery V-PLEX Aβ Peptide Panel 1 (4G8) Kit #K15199E-1).

4.3.12 Flow Cytometry

WT and KO rats were infected with ExoY$^+$ (10^8) over 48 hours. Control and infected rats were then anesthetized with isoflurane gas (1-3%) and once a surgical plane was established as determined by a negative toe and tail pinch reflex, the trachea was cannulated, and a sternotomy was performed, removing the heart and lungs *en bloc*. The cannula was connected to tubing attached to a 60 mL syringe that was adjusted to provide 25 cm H_2O filling pressure. PBS was allowed to flow into the lungs using the force of

gravity until full (~10mL), at which point the tubing was disconnected and a syringe connected directly to the tracheal cannula to remove the PBS. This process was repeated 3 times to collect ~30 mL of BALF. BALF was quickly vortexed, and 1 mL was transferred into a separate tube for cell counting using a cell countess. The remaining BALF was placed on ice and centrifuged at 500 x *g* for 10 minutes. Supernatant was collected, filter-sterilized with a 0.2 μm filter, and frozen at -20° C. The remaining cell pellet was resuspended in 1 mL PBS for use the same day, or frozen at -80° C in full DMEM containing 20% FBS and 14% DMSO for analysis later.

Frozen cells were thawed quickly at 37° C and put into a flow tube containing 3 mL of DMEM. Cells were pelleted at 1400 RPM for 7 minutes. DMEM was removed and the cell pellet was resuspended in PBS to a final 10^6 cell count per mL of PBS. Cells were centrifuged at 1300 RPM for 6 minutes and PBS was removed. Cells were resuspended in an antibody cocktail containing PE/Dazzle™ 594 anti-rat CD45 (Biolegend #202224; 0.2mg/ml), PE/Cyanine7 anti-rat CD11b/c (Biolegend #201818; 0.2mg/ml), mouse anti-rat CD43:RPE (Biorad #MCA54PE; 10uL/1million cells), mouse anti-rat CD68 (Biorad #MCA341R; 1mg/mL), BV605 mouse anti-rat RP-1 (BDBiosciences #743055; 0.2mg/mL), and mouse anti-rat His48 (ThermoFisher #11-0570-82; 0.5 mg/mL). BALF cells were incubated with the antibody cocktail away from light and on ice for 30 minutes. Three milliliters of PBS were added to the cells and antibody cocktail, quickly vortexed, and centrifuged at 1480 RPM for 7 minutes. PBS and antibody cocktail were aspirated, and the remaining cells were resuspended in fresh PBS for flow cytometric analysis. Fluorescence activated flow cytometry was performed

using a CytoFLEX S flow cytometer (Beckman Coulter) to sort cells, and the analysis was performed using FlowJo™ v10.8 Software (BD Life Sciences).

4.3.13 Compliance Curves

Rats ranging from 250-350 g were anesthetized using isoflurane gas (1-3%). Once a surgical plane was achieved as noted by lack of toe and tail pinch reflex, the heart and lungs were removed, and a tracheal tube inserted into the trachea and tied off. The tracheal tube was connected to tubing that was attached to the tip of a syringe that was filled with 30 mL of Formalin (10%). The syringe was attached to a stand. The syringe was raised to 5 mm and the stopcock was opened, allowing lung filling for 2 minutes at which point the stopcock was closed and the amount remaining in the syringe was noted. This procedure was repeated in 5 mm steps until a total pressure of 30 mm H_2O pressure was achieved.

4.3.14 Myocardial Infarction in the Open Chest Rat

Rats were infected with $ExoY^+$ (10^7) over 48 hours, as described above. At 48 hours, rats were anesthetized via intraperitoneal delivery of nembutal (65 mg/kg body weight) to a surgical plane, as determined by the absence of a toe pinch reflex. The right jugular vein was then catheterized, and anesthesia was maintained throughout the experimental period by intravenous delivery of nembutal. The left carotid artery was catheterized for measurement of blood pressure. A snare was placed around the left anterior descending branch of the left coronary artery, and the snare was tightened to

allow for ischemia for 30 minutes. After 30 minutes, the snare was removed to allow for 2 hours of reperfusion.

After the two-hour period, the heart was removed and mounted on a Langendorf apparatus and perfused at 100 mm Hg with normal saline through the aortic root. After 2 minutes of reperfusion, the coronary artery branch was reoccluded, and 2-9 μm fluorescent beads were infused into the heart. The heart was flash frozen in liquid nitrogen, cut into 2 mm transverse slices, and incubated for 8-10 minutes in triphenoltetrazolium chloride. The risk area was visualized as myocardium without fluorescent microspheres. All slices that included any tissue without fluorescent microspheres (the ischemic zones) were arranged in order from the base to the apex and sandwiched together between 2 glass plates spaced 2 mm apart. The border between the ischemic and normal tissue for each slice was traced with a fine tip marker on the top glass plate under a UV light. The mounted slices were then photographed on a blue background. Using an image editor, the ischemic zone for each slice in the resulting image was traced, copied, and pasted on a blue background color to form a new image having only the risk zones. Using the color threshold feature of the Image J program, the area of just the infarcts and then for the entire risk zones were both measured in the risk zone image. The percent infarction of the risk zone could then be calculated for the entire heart. The same color threshold settings for the infarct and for the entire risk zone were used for all the hearts.

4.3.15 Hippocampi Isolation and Long-Term Potentiation

Immediately after the harvest of peripheral organs, rat brain was obtained and kept in an ice-cold slushy sucrose-artificial cerebrospinal fluid (in mM): 70 sucrose, 80

NaCl, 2.5 KCl, 21.4 $NaHCO_3$, 1.25 NaH_2PO_4, 0.5 $CaCl_2$, 7 $MgCl_2$, 1.3 ascorbic acid, and 20 glucose. After 1 minute of incubation, the hippocampi were dissected out, placed onto an agar block, and sliced at 300 μm using a Leica VT1200s (Leica Instruments). Transverse hippocampal slices were placed into a holding chamber containing regular artificial cerebrospinal fluid (aCSF; in mM): 125 NaCl, 2.5 KCl, 21.5 $NaHCO_3$, 1.25 NaH_2PO_4, 2.0 $CaCl_2$, 1.0 $MgCl_2$, and 15 glucose. Slices were incubated for 30 minutes at 35°C and then for >1 hr at room temperature before they were transferred to an upright Leica microscope for field potential recording. All solutions were constantly equilibrated with carbogen (95% O_2 and 5% CO_2).

For hippocampal field potential recordings, hippocampal CA3 region was severed, and the brain slice was transferred to the recording chamber. Brain slices were superfused with aCSF at a flow rate of 1 mL/minute at room temperature. The perfusing aCSF contained SR95531 (2 μM) and CGP55845 (1 μM) to block inhibitory synaptic transmission. Brain slices were held in place with a harp slice anchor (Warner Instruments) and stimulating and recording glass electrodes were placed in the CA1 stratum radiatum, ~150 μm away from the somata, to stimulate the Schaffer collateral pathway. Stimulation was performed using an ISO-Flex stimulus isolation unit (A.M.P.I.), and recording was obtained using an EPC10 amplifier (HEKA Elektronik). Analog signals were further amplified 10x using an Axopatch amplifier (Axon Instrument) and digitized/filtered either at 20 kHz/5 kHz (for field and paired-pulse ratio

recordings) or 100 kHz/25 kHz (for input-output function recordings) using the Patchmater software (HEKA Elektronik).

At the beginning of recording for each brain slice, an input-output function was determined, and the excitatory postsynaptic potential amplitude was set at ~30% of maximum amplitude, followed by a series of paired-pulse ratio recordings, and then the field LTP. Paired-pulse stimulations, recorded every 10 seconds, were performed at 25, 50, 100, 200, and 400 ms inter-stimulus intervals, and five traces of each interval were averaged. For LTP studies, field excitatory postsynaptic potentials were evoked and recorded every 20 seconds, and a stable baseline of >10 minutes was established before a theta-burst stimulation consisting of three sweeps (a single burst consists of five stimuli delivered at 100 Hz and ten bursts delivered at 5 Hz per sweep) was delivered at 30 seconds intervals to induce synaptic potentiation. LTP was calculated from field potentials recorded at 55-60 minutes post the theta-burst stimulation and normalized to the baseline field potentials before the theta-burst stimulation.

Offline data analyses of electrophysiological recordings were performed using custom macros written in Igor Pro (WaveMatrics). As a general rule for this study, field excitatory postsynaptic potential amplitude was determined from the peak, and the slope was measured between 10 and 50% of the rising phase. The time-to-population spike was determined from the trace of the strongest electrical stimulus (i.e., 100 μA), and the groove was set as the lowest point (closest to the 0 baseline) between the two field excitatory postsynaptic peaks. LTP data were binned at 3-minute intervals to generate the summary field excitatory postsynaptic potential plot. Data are expressed as mean ± standard deviation or standard error of the mean and statistically compared as specified.

Figures were prepared in Igor Pro and/or Prism (GraphPad); data tabulation was done using Excel (Microsoft).

4.4 Discussion

Pneumonia is a common cause of end-organ dysfunction during, and in the aftermath of infection, yet the mechanism(s) responsible for end-organ dysfunction in this setting are poorly understood [35,36]. We have previously demonstrated that pneumonia elicits lung endothelial production of cytotoxic Aβ and tau, which induce end-organ dysfunction in the lung and brain [16-18,37]. These cytotoxins exhibit prion-like properties, meaning they are protease resistant, heat stable cytotoxins that are transmissible among cells and tissues and are self-propagating, i.e., they seed the production of new cytotoxic species [15,38]. While we have addressed the mechanisms responsible for infection-induced cytotoxic tau production within the lung microcirculation [15,17,22,32,33], the mechanisms responsible for increased cytotoxic Aβ production have not been reported. Here, we examined whether bacterial pneumonia acts through GSAP necessary to injure the lung, heart, and brain. Consistent with this idea, GSAP knockout rats exhibited preservation of alveolar-capillary barrier integrity in the lung, reduced susceptibility to ischemia-reperfusion injury in the heart, and improved hippocampal LTP following infection. Therefore, GSAP contributes to pneumonia-induced end-organ dysfunction.

Pneumonia is a direct cause of the ARDS. The ARDS is characterized by pulmonary edema and refractory hypoxemia, especially in the early stages of the ARDS [39]. Our studies illustrate a role for GSAP in both the pulmonary edema and hypoxemia that develop following infection. GSAP may contribute to disruption of the alveolar-

capillary barrier: (i) through an intracellular signaling function within the capillary endothelium and adjoining type I and type II pneumonocytes; (ii) by inhibiting Notch signaling; or, (iii) by promoting cytotoxic Aβ production. A signaling function of the 98-kD holoprotein and its 82- and 16-kD products is largely unexplored, aside from association of the 16-kD product with γ-secretase. Xu et al. [5] recently found the 16-kD GSAP interacts with ~80 proteins, including proteins involved in signal transduction, like protein phosphatases, and those involved in protein trafficking, lipid metabolism, and mitochondrial function. Future studies are needed to assess whether and how GSAP acutely impacts intracellular signaling events that disrupt the alveolar-capillary barrier.

Association of the 16-kD GSAP with γ-secretase increases γ-secretase coupling to amyloid precursor protein, while leaving the γ-secretase interaction with Notch unchanged[1,3,8]. It is unclear whether Notch signaling is enhanced in the alveolar-capillary membrane in the GSAP knockout rats. If so, then Notch signaling in the knockout rats may strengthen barrier integrity and promote repair [40,41]. Lung endothelium produces Aβ [15,17,23]. Amyloid concentrations are increased in the bronchoalveolar lavage fluid and plasma of pneumonia patients [18,38], and here, we observed increased $A\beta_{42}$ in the circulation of wild type rats and increased $A\beta_{42/40}$ ratios in both wild type and GSAP KO rats post-infection. Nonetheless, the increase in circulating amyloids during infection cannot be specifically attributed to their production by lung endothelium. As $A\beta_{40}$ and $A\beta_{42}$ can be cytotoxic to the host [23], these infection-elicited amyloids may be an independent cause of injury to the alveolar-capillary barrier. Amyloids can also have antimicrobial properties [11-15]. The post-translational or structural modifications of $A\beta_{40}$ and $A\beta_{42}$ that confer these distinct functions are unknown, and it is unclear whether

GSAP contributes to the production of antimicrobial versus cytotoxic Aβ variants. Future studies are warranted to establish whether GSAP contributes to the pathologic and/or antimicrobial properties of amyloids, including $A\beta_{40}$ and $A\beta_{42}$.

Neutrophil recruitment to the airway combats bacterial pneumonia. Once in the alveoli, neutrophils release proteases, oxidants, and in some cases, DNA (i.e., NETosis) essential to host antimicrobial defense [42]. However, protracted neutrophil activation in the airspace can also injure the alveolar-capillary membrane and interfere with lung repair [43,44]. Whereas GSAP did not impact the number of neutrophils in either the circulation or the airspace following infection, neutrophils recovered from the bronchoalveolar lavage fluid of the GSAP knockout rats were diverse and included cells with hyposegmented nuclei. The function of these distinct neutrophil populations has not been tested, yet the data suggest that GSAP may promote neutrophil maturation during bacterial infection, or alternatively, contribute to neutrophil nuclear segmentation. Hypersegmented nuclei possess high concentrations of lamin B2 interacting with high levels of lamin B receptor [45]. Genetic disruption of the lamin B receptor results in nuclear hyposegmentation [45]. At present, little is known about this nuclear developmental process, and it remains unclear how GSAP may contribute to nuclear segmentation. Immature neutrophils reportedly improve tissue repair, suggesting recruitment of these hyposegmented neutrophils to the airspace in GSAP knockout rats may portend improved long-term outcomes [46].

Pneumonia increases the risk of myocardial infarction. The mechanisms placing these patients at risk for myocardial infarction have largely been attributed to inflammation and the prothrombotic, procoagulant state that accompanies infection [47,48]. The proinflammatory environment increases the risk of plaque rupture in susceptible

patients resulting in ST-elevation myocardial infarction (STEMI), while hypoxemia, poor tissue perfusion, and increased myocardial oxygen demand promote the risk of demand ischemia leading to non-ST-elevation myocardial infarction (non-STEMI) [49]. The current treatment for STEMI is to remove the coronary embolus by angioplasty or thrombolysis, but this can seldom be performed before a significant amount of the ischemic zone infarcts. A number of factors are thought to contribute to the cell death after a transient period of coronary ischemia, including apoptosis, necroptosis, mitochondrial-mediated necrosis, pyroptosis, ferroptosis, and autophagic cell death [50]. Blockade of any of the above has been reported to make the heart more resistant to infarction. Similarly, activation of any of them will increase the infarct size. Infarcted myocardium cannot be regenerated so the strength of the heart, and thus the patient's prognosis, is dependent on how much muscle is killed by infarction. We assessed susceptibility to infarction following ischemia-reperfusion injury at baseline and during infection. In wild type rats, infection substantially increased the extent of myocardial infarction. Whereas GSAP was not incriminated in the mechanism of myocardial infarction in the uninfected heart, infection greatly increased the infarct size in our model, and surprisingly, that increase was found to be completely GSAP-dependent. Which, if any, of the aforementioned processes was involved in the increased vulnerability is unknown, but the fact that it is GSAP-dependent should aid in future studies seeking to resolve the mechanism.

GSAP is expressed in all brain regions, and via its influence on Aβ production, it has been incriminated in Alzheimer's disease pathology [1]. Yet, the role of GSAP in hippocampal information processing has not been determined. Our results support a central role for GSAP in four stages of information processing. First, GSAP promotes a

larger fiber volley response, meaning it contributes to a larger presynaptic action potential recruitment. Second, GSAP increases the paired-pulse ratio indicating a reduction in neurotransmitter release from CA3 neurons. Third, for any given presynaptic stimulation, GSAP reduces the post-synaptic response. Fourth, GSAP dampens post-synaptic neuronal hyperexcitability. Therefore, GSAP facilitates the presynaptic input while governing strength of the postsynaptic output, collectively increasing E-LTP and limiting L-LTP. This input-output tuning is consistent with the idea that distinct GSAP mechanisms control CA3 and CA1 activity, respectively. For example, GSAP's interaction with γ-secretase in CA3 neurons may optimize Aβ production and release, which in turn, provides negative feedback inhibition of both pre- and postsynaptic neurons. GSAP may also directly impact the post-synaptic response by orchestrating signaling events that occur through second messenger networks, trafficking of ion channels, and preservation of mitochondrial function, either in CA1 cells or other associated neuronal and/or glial cells [5]. Future studies are needed to assess the Aβ-dependent and independent role of GSAP in neurotransmission.

Pneumonia acutely increases the risk for delirium, and it is a cause of incident dementia [25]. Pneumonia promotes the accumulation of cytotoxic amyloids and tau within the cerebrospinal fluid within 48 hours of infection [17,22]. These cytotoxic amyloid and tau variants impair hippocampal information processing, and over time, they reduce CA1 dendritic spine density [16,18,37]. How infection is sensed, leading to the generation of cytotoxic Aβ variants, remains poorly understood. Here, we show that infection dramatically impairs neurotransmission in two ways. First, while infection does not affect the presynaptic action potential it decreases the paired-pulse ratio characteristic of an

increase in the neurotransmitter release probability from CA3 neurons. Second, it increases postsynaptic excitability. Collectively, this disruption in neurotransmission coincides with a reduction in LTP. It is notable that the infection-induced increase in neurotransmitter release probability and postsynaptic hyperexcitability are dependent upon GSAP. In the absence of GSAP, hippocampal neurons have higher release probability and are more hyperexcitable, and lung infection does not further increase these responses. In contrast, infection-induced inhibition of LTP is mostly GSAP-independent, because the amount of inhibition in the presence or absence of GSAP expression was generally comparable. Thus, it is most likely that the infection-induced suppression of LTP is due to cytotoxic tau variants, as demonstrated in our prior study [22], whereas postsynaptic hyperexcitability is GSAP dependent. The extent to which hyperexcitability contributes to suppressed LTP over time following infection remains to be determined. While we did not perceive any overt phenotypical behavioral deviations in the novel GSAP knockout rat, the role of GSAP in animal behavior and learning and memory remains to be studied.

In conclusion, we provide evidence that bacterial pneumonia requires GSAP to orchestrate the molecular events underlying end-organ dysfunction in the lung, heart, and brain. These data reveal a cardinal role for GSAP in innate immunity, as part of the host-pathogen response, and provide evidence for its involvement in end-organ dysfunction secondary to bacterial pneumonia and the ARDS. Future studies are needed to determine

the extent to which these GSAP-dependent mechanisms act through its regulation of the amyloidogenic pathway or result from other GSAP-dependent signaling events.

4.5 Acknowledgements and Funding Sources

The authors thank Dr. Michele Schuler and Leigh Ann Wiggins for their assistance in animal breeding and animal husbandry, Dr. Scott Neidich from Meso Scale Discovery for his assistance implementing amyloid measurements, and Rachel Rodenberg, PhD candidate in the department of Microbiology and Immunology for her insightful conversations regarding neutrophil biology. This work was supported by an American Heart Association predoctoral fellowship (PRE34381066, MG) and the Health and Human Services, including HL66299 (TS, RB, MA), HL148069 (TS, RB, MA), HL140182 (ML, TS, RB), HL160988 (JYL, TS), OD026560 (AMG), HL116264 (AMG), AG058780 (ARN), W81XWH2110161 (MA), W81XWH2110669 (MA), OD010944 (MA), S10OD025089 (MA), HL118334 (JPA), HL147512 (SV), HL007778 (SV), and VCOM-LA-BL (SV).

4.6 References

1 He, G., Luo, W., Li, P., Remmers, C., Netzer, W. J., Hendrick, J., Bettayeb, K., Flajolet, M., Gorelick, F., Wennogle, L. P. & Greengard, P. γ-Secretase Activating Protein is a Therapeutic Target for Alzheimer's Disease. *Nature* **467**, 95-98 (2010). https://doi.org:10.1038/nature09325

2 Chu, J., Li, J. G., Hoffman, N. E., Stough, A. M., Madesh, M. & Pratico, D. Regulation of γ-Secretase Activating Protein by the 5Lipoxygenase: In Vitro and In Vivo Evidence. *Sci Rep* **5**, 11086 (2015). https://doi.org:10.1038/srep11086

3 Chu, J., Li, J. G., Joshi, Y. B., Giannopoulos, P. F., Hoffman, N. E., Madesh, M. & Pratico, D. γ Secretase-Activating Protein is a Substrate for Caspase-3: Implications for Alzheimer's Disease. *Biol Psychiatry* **77**, 720-728 (2015). https://doi.org:10.1016/j.biopsych.2014.06.003

4 Chang, J. C., Xu, P., Wong, E., Flajolet, M., Li, Y. M. & Greengard, P. GSAP Regulates Amyloid β Production Through Modulation of Amyloid Precursor Protein Trafficking. *bioRxviv* Preprint at https://www.biorxiv.org/content/10.1101/2020.11.12.379313v1.full (2020)**.**

5 Xu, P., Chang, J. C., Zhou, X., Wang, W., Bamkole, M., Wong, E., Bettayeb, K., Jiang, L. L., Huang, T., Luo, W., Xu, H., Nairn, A. C., Flajolet, M., Ip, N. Y., Li, Y. M. & Greengard, P. GSAP Regulates Lipid Homeostasis and Mitochondrial Function Associated with Alzheimer's Disease. *J Exp Med* **218**, e20202446 (2021). https://doi.org:10.1084/jem.20202446

6 Jin, C., Wang, J., Wang, Y., Jia, B., Guo, X., Yang, G., Xu, P., Greengard, P., Zhou, R. & Shi, Y. Modulation of Amyloid Precursor Protein Cleavage by γ-Secretase Activating Protein Through Phase Separation. *Proc Natl Acad Sci* **119**, e2122292119 (2022). https://doi.org:10.1073/pnas.2122292119

7 Wong, E., Liao, G. P., Chang, J. C., Xu, P., Li, Y. M. & Greengard, P. GSAP Modulates γ-Secretase Specificity by Inducing Conformational Change in PS1. *Proc Natl Acad Sci* **116**, 6385-6390 (2019). https://doi.org:10.1073/pnas.1820160116

8 Hussain, I., Fabregue, J., Anderes, L., Ousson, S., Borlat, F., Eligert, V., Berger, S., Dimitrov, M., Alattia, J. R., Fraering, P. C. & Beher, D. The Role of γ-Secretase Activating Protein (GSAP) and Imatinib in the Regulation of γ-Secretase Activity and Amyloid-β Generation. *J Biol Chem* **288**, 2521-2531 (2013). https://doi.org:10.1074/jbc.M112.370924

9 Fagerberg, L., Hallstrom, B. M., Oksvold, P., Kampf, C., Djureinovic, D., Odeberg, J., Habuka, M., Tahmasebpoor, S., Danielsson, A., Edlund, K., Asplund, A., Sjostedt, E., Lundberg, E., Szigyarto, C. A., Skogs, M., Takanen, J. O., Berling, H., Tegel, H., Mulder, J., Nilsson, P., Schwenk, J. M., Lindskog, C., Danielsson, F., Mardinoglu, A., Sivertsson, A., von Feilitzen, K., Forsberg, M., Zwahlen, M., Olsson, I., Navani, S., Huss, M., Nielsen, J., Ponten, F. & Uhlen, M. Analysis of the Human Tissue-Specific Expression by Genome-Wide Integration of Transcriptomics and Antibody-Based Proteomics. *Mol Cell Proteomics* **13**, 397-406 (2014). https://doi.org:10.1074/mcp.M113.035600

10 Pavliukeviciene, B., Zentelyte, A., Jankunec, M., Valiuliene, G., Talaikis, M., Navakauskiene, R., Niaura, G. & Valincius, G. Amyloid β oligomers Inhibit Growth of Human Cancer Cells. *PLoS One* **14**, e0221563 (2019). https://doi.org:10.1371/journal.pone.0221563

11 Eimer, W. A., Vijaya Kumar, D. K., Navalpur Shanmugam, N. K., Rodriguez, A. S., Mitchell, T., Washicosky, K. J., Gyorgy, B., Breakefield, X. O., Tanzi, R. E. & Moir, R. D. Alzheimer's Disease-Associated β-Amyloid is Rapidly Seeded by Herpesviridae to Protect Against Brain Infection. *Neuron* **99**, 56-63.e3 (2018). https://doi.org:10.1016/j.neuron.2018.06.030

12 Kumar, D. K., Choi, S. H., Washicosky, K. J., Eimer, W. A., Tucker, S., Ghofrani, J., Lefkowitz, A., McColl, G., Goldstein, L. E., Tanzi, R. E. & Moir, R. D. Amyloid-β Peptide Protects Against Microbial Infection in Mouse and Worm Models of Alzheimer's Disease. *Sci Transl Med* **8**, 340ra72 (2016). https://doi.org:10.1126/scitranslmed.aaf1059

13 Moir, R. D., Lathe, R. & Tanzi, R. E. The Antimicrobial Protection Hypothesis of Alzheimer's Disease. *Alzheimers Dement* **14**, 1602-1614 (2018). https://doi.org:10.1016/j.jalz.2018.06.3040

14 Soscia, S. J., Kirby, J. E., Washicosky, K. J., Tucker, S. M., Ingelsson, M., Hyman, B., Burton, M. A., Goldstein, L. E., Duong, S., Tanzi, R. E. & Moir, R. D. The Alzheimer's Disease-Associated Amyloid β-Protein is an Antimicrobial Peptide. *PLoS One* **5**, e9505 (2010). https://doi.org:10.1371/journal.pone.0009505

15 Voth, S., Gwin, M., Francis, C. M., Balczon, R., Frank, D. W., Pittet, J. F., Wagener, B. M., Moser, S. A., Alexeyev, M., Housley, N., Audia, J. P., Piechocki, S., Madera, K., Simmons, A., Crawford, M. & Stevens, T. Virulent *Pseudomonas aeruginosa* Infection Converts Antimicrobial Amyloids into Cytotoxic Prions. *FASEB J* **34**, 9156-9179 (2020). https://doi.org:10.1096/fj.202000051RRR

16 Scott, A. M., Jager, A. C., Gwin, M., Voth, S., Balczon, R., Stevens, T. & Lin, M. T. Pneumonia-Induced Endothelial Amyloids Reduce Dendritic Spine Density in Brain Neurons. *Sci Rep* **10**, 9327 (2020). https://doi.org:10.1038/s41598-020-66321-1

17 Balczon, R., Pittet, J. F., Wagener, B. M., Moser, S. A., Voth, S., Vorhees, C. V., Williams, M. T., Bridges, J. P., Alvarez, D. F., Koloteva, A., Xu, Y., Zha, X. M., Audia, J. P., Stevens, T. & Lin, M. T. Infection-Induced Endothelial Amyloids Impair Memory. *FASEB J* **33**, 10300-10314 (2019). https://doi.org:10.1096/fj.201900322R

18 Lin, M. T., Balczon, R., Pittet, J. F., Wagener, B. M., Moser, S. A., Morrow, K. A., Voth, S., Francis, C. M., Leavesley, S., Bell, J., Alvarez, D. F. & Stevens, T. Nosocomial Pneumonia Elicits an Endothelial Proteinopathy: Evidence for a Source of Neurotoxic Amyloids in Critically Ill Patients. *Am J Respir Crit Care Med* **198**, 1575-1578 (2018). https://doi.org:10.1164/rccm.201801-0060LE

19 Sevigny, J., Chiao, P., Bussiere, T., Weinreb, P. H., Williams, L., Maier, M., Dunstan, R., Salloway, S., Chen, T., Ling, Y., O'Gorman, J., Qian, F., Arastu, M., Li, M., Chollate, S., Brennan, M. S., Quintero-Monzon, O., Scannevin, R. H., Arnold, H. M., Engber, T., Rhodes, K., Ferrero, J., Hang, Y., Mikulskis, A., Grimm, J., Hock, C., Nitsch, R. M. & Sandrock, A. The Antibody Aducanumab Reduces Aβ Plaques in Alzheimer's Disease. *Nature* **537**, 50-56 (2016). https://doi.org:10.1038/nature19323

20 Troncone, L., Luciani, M., Coggins, M., Wilker, E. H., Ho, C. Y., Codispoti, K. E., Frosch, M. P., Kayed, R. & Del Monte, F. Aβ Amyloid Pathology Affects the Hearts of Patients with Alzheimer's Disease: Mind the Heart. *J Am Coll Cardiol* **68**, 2395-2407 (2016). https://doi.org:10.1016/j.jacc.2016.08.073

21 Sonkar, V. K., Kulkarni, P. P. & Dash, D. Amyloid β Peptide Stimulates Platelet Activation Through RhoA-dependent Modulation of Actomyosin Organization. *FASEB J* **28**, 1819-1829 (2014). https://doi.org:10.1096/fj.13-243691

22 Balczon, R., Lin, M. T., Lee, J. Y., Abbasi, A., Renema, P., Voth, S. B., Zhou, C., Koloteva, A., Michael Francis, C., Sodha, N. R., Pittet, J. F., Wagener, B. M., Bell, J., Choi, C. S., Ventetuolo, C. E. & Stevens, T. Pneumonia Initiates a Tauopathy. *FASEB J* **35**, e21807 (2021). https://doi.org:10.1096/fj.202100718R

23 Balczon, R., Morrow, K. A., Leavesley, S., Francis, C. M., Stevens, T. C., Agwaramgbo, E., Williams, C., Stevens, R. P., Langham, G., Voth, S., Cioffi, E. A., Weintraub, S. E. & Stevens, T. Cystatin C Regulates the Cytotoxicity of Infection-Induced Endothelial-Derived β-Amyloid. *FEBS Open Bio* **10**, 2464-2477 (2020). https://doi.org:10.1002/2211-5463.12997

24 Torres, A., Cilloniz, C., Niederman, M. S., Menéndez, R., Chalmers, J. D., Wunderink, R. G. & van der Poll, T. Pneumonia. *Nat Rev Dis Prim* **7**, 25 (2021). https://doi.org:10.1038/s41572-021-00259-0

25 Pandharipande, P. P., Girard, T. D., Jackson, J. C., Morandi, A., Thompson, J. L., Pun, B. T., Brummel, N. E., Hughes, C. G., Vasilevskis, E. E., Shintani, A. K., Moons, K. G., Geevarghese, S. K., Canonico, A., Hopkins, R. O., Bernard, G. R., Dittus, R. S., Ely, E. W. & Investigators, BRAIN-ICU Investigators. Long-Term Cognitive Impairment After Critical Illness. *N Engl J Med* **369**, 1306-1316 (2013). https://doi.org:10.1056/NEJMoa1301372

26 Hopkins, R. O. & Jackson, J. C. Assessing Neurocognitive Outcomes After Critical Illness: Are Delirium and Long-Term Cognitive Impairments Related? *Curr Opin Crit Care* **12**, 388-394 (2006). https://doi.org:10.1097/01.ccx.0000244115.24000.f5

27 Mebazaa, A., Casadio, M. C., Azoulay, E., Guidet, B., Jaber, S., Levy, B., Payen, D., Vicaut, E., Resche-Rigon, M. & Gayat, E. Post-ICU Discharge and Outcome: Rationale and Methods of the French and European Outcome Registry in Intensive Care Units (FROG-ICU) Observational Study. *BMC Anesthesiol* **15**, 143 (2015). https://doi.org:10.1186/s12871-015-0129-2

28 Wagener, B. M., Anjum, N., Christiaans, S. C., Banks, M. E., Parker, J. C., Threet, A. T., Walker, R. R., Isbell, K. D., Moser, S. A., Stevens, T., Alexeyev, M. F., Audia, J. P., Richter, W., Hardy, K. S., Saleh, L. A., Morgan, C. & Pittet, J. F. Exoenzyme Y Contributes to End-Organ Dysfunction Caused by *Pseudomonas aeruginosa* Pneumonia in Critically Ill Patients: An Exploratory Study. *Toxins* **12**, 369 (2020). https://doi.org:10.3390/toxins12060369

29 Musher, D. M., Abers, M. S. & Corrales-Medina, V. F. Acute Infection and Myocardial Infarction. *N Engl J Med* **380**, 171-176 (2019). https://doi.org:10.1056/NEJMra1808137

30 Davydow, D. S., Hough, C. L., Levine, D. A., Langa, K. M. & Iwashyna, T. J. Functional Disability, Cognitive Impairment, and Depression after Hospitalization for Pneumonia. *Am J Med* **126**, 615-624.e5 (2013). https://doi.org:10.1016/j.amjmed.2012.12.006

31 Beckert, U., Wolter, S., Hartwig, C., Bahre, H., Kaever, V., Ladant, D., Frank, D. W. & Seifert, R. ExoY from *Pseudomonas aeruginosa* is a Nucleotidyl Cyclase with Preference for cGMP and cUMP Formation. *Biochem Biophys Res Commun* **450**, 870-874 (2014). https://doi.org:10.1016/j.bbrc.2014.06.088

32 Morrow, K. A., Seifert, R., Kaever, V., Britain, A. L., Sayner, S. L., Ochoa, C. D., Cioffi, E. A., Frank, D. W., Rich, T. C. & Stevens, T. Heterogeneity of Pulmonary Endothelial Cyclic Nucleotide Response to *Pseudomonas aeruginosa* ExoY Infection. *Am J Physiol Lung Cell Mol Physiol* **309**, L1199-L1207 (2015). https://doi.org:10.1152/ajplung.00165.2015

33 Ochoa, C. D., Alexeyev, M., Pastukh, V., Balczon, R. & Stevens, T. *Pseudomonas aeruginosa* Exotoxin Y is a Promiscuous Cyclase that Increases Endothelial Tau Phosphorylation and Permeability. *J Biol Chem* **287**, 25407-25418 (2012). https://doi.org:10.1074/jbc.M111.301440

34 Yahr, T. L., Vallis, A. J., Hancock, M. K., Barbieri, J. T. & Frank, D. W. ExoY, An Adenylate Cyclase Secreted by the *Pseudomonas aeruginosa* Type III System. *Proc Natl Acad Sci U S A* **95**, 13899-13904 (1998). https://doi.org:10.1073/pnas.95.23.13899

35 Dela Cruz, C. S., Wunderink, R. G., Christiani, D. C., Cormier, S. A., Crothers, K., Doerschuk, C. M., Evans, S. E., Goldstein, D. R., Khatri, P., Kobzik, L., Kolls, J. K., Levy, B. D., Metersky, M. L., Niederman, M. S., Nusrat, R., Orihuela, C. J., Peyrani, P., Prince, A. S., Ramirez, J. A., Ridge, K. M., Sethi, S., Suratt, B. T., Sznajder, J. I., Tsalik, E. L., Walkey, A. J., Yende, S., Aggarwal, N. R., Caler, E. V. & Mizgerd, J. P. Future Research Directions in Pneumonia. NHLBI Working Group Report. *Am J Respir Crit Care Med* **198**, 256-263 (2018). https://doi.org:10.1164/rccm.201801-0139WS

36 Martin, T. R., Zemans, R. L., Ware, L. B., Schmidt, E. P., Riches, D. W. H., Bastarache, L., Calfee, C. S., Desai, T. J., Herold, S., Hough, C. L., Looney, M. R., Matthay, M. A., Meyer, N., Parikh, S. M., Stevens, T. & Thompson, B. T. New Insights into Clinical and Mechanistic Heterogeneity of the Acute Respiratory Distress Syndrome: Summary of the Aspen Lung Conference 2021. *Am J Respir Cell Mol Biol* **67**, 284-308 (2022). https://doi.org:10.1165/rcmb.2022-0089WS

37 Choi, C. S., Gwin, M., Voth, S., Kolb, C., Zhou, C., Nelson, A. R., deWeever, A., Koloteva, A., Annamdevula, N. S., Murphy, J. M., Wagener, B. M., Pittet, J. F., Lim, S. S., Balczon, R., Stevens, T. & Lin, M. T. Cytotoxic Tau Released from Lung Microvascular Endothelial Cells Upon Infection with *Pseudomonas aeruginosa* Promotes Neuronal Tauopathy. *J Biol Chem* **298**, 101482 (2022). https://doi.org:10.1016/j.jbc.2021.101482

38 Balczon, R., Morrow, K. A., Zhou, C., Edmonds, B., Alexeyev, M., Pittet, J. F., Wagener, B. M., Moser, S. A., Leavesley, S., Zha, X., Frank, D. W. & Stevens, T. *Pseudomonas aeruginosa* Infection Liberates Transmissible, Cytotoxic Prion Amyloids. *FASEB J* **31**, 2785-2796 (2017). https://doi.org:10.1096/fj.201601042RR

39 ARDS Definition Task Force, Ranieri, V. M., Rubenfeld, G. D., Thompson, B. T., Ferguson, N. D., Caldwell, E., Fan, E., Camporota, L. & Slutsky, A. S. Acute Respiratory Distress Syndrome: The Berlin Definition. *JAMA* **307**, 2526-2533 (2012). https://doi.org:10.1001/jama.2012.5669

40 Cai, W., Shen, K., Ji, P., Jia, Y., Han, S., Zhang, W., Hu, X., Yang, X., Han, J. & Hu, D. The Notch Pathway Attenuates Burn-Induced Acute Lung Injury in Rats by Repressing Reactive Oxygen Species. *Burns Trauma* **10**, tkac008 (2022). https://doi.org:10.1093/burnst/tkac008

41 Fischer, A. & Braga, V. M. M. Vascular Permeability: Flow-Mediated, Non-Canonical Notch Signalling Promotes Barrier Integrity. *Curr Biol* **28**, R119-R121 (2018). https://doi.org:10.1016/j.cub.2017.11.065

42 Brinkmann, V. & Zychlinsky, A. Entering the Neutrophil Trap. *Nat Rev Immunol* **21**, 615 (2021). https://doi.org:10.1038/s41577-021-00614-y

43 Lefrancais, E., Mallavia, B., Zhuo, H., Calfee, C. S. & Looney, M. R. Maladaptive Role of Neutrophil Extracellular Traps in Pathogen-Induced Lung Injury. *JCI Insight* **3**, e98178 (2018). https://doi.org:10.1172/jci.insight.98178

44 Yipp, B. G., Kim, J. H., Lima, R., Zbytnuik, L. D., Petri, B., Swanlund, N., Ho, M., Szeto, V. G., Tak, T., Koenderman, L., Pickkers, P., Tool, A. T. J., Kuijpers, T. W., van den Berg, T. K., Looney, M. R., Krummel, M. F. & Kubes, P. The Lung is a Host Defense Niche for Immediate Neutrophil-Mediated Vascular Protection. *Sci Immunol* **2**, eaam8929 (2017). https://doi.org:10.1126/sciimmunol.aam8929

45 Manley, H. R., Keightley, M. C. & Lieschke, G. J. The Neutrophil Nucleus: An Important Influence on Neutrophil Migration and Function. *Front Immunol* **9**, 2867 (2018). https://doi.org:10.3389/fimmu.2018.02867

46 Peiseler, M. & Kubes, P. More Friend than Foe: The Emerging Role of Neutrophils in Tissue Repair. *Clin Invest* **129**, 2629-2639 (2019). https://doi.org:10.1172/JCI124616

47 Putot, A., Chague, F., Manckoundia, P., Cottin, Y. & Zeller, M. Post-Infectious Myocardial Infarction: New Insights for Improved Screening. *J Clin Med* **8** 827 (2019). https://doi.org:10.3390/jcm8060827

48 Corrales-Medina, V. F., Alvarez, K. N., Weissfeld, L. A., Angus, D. C., Chirinos, J. A., Chang, C. C., Newman, A., Loehr, L., Folsom, A. R., Elkind, M. S., Lyles, M. F., Kronmal, R. A. & Yende, S. Association Between Hospitalization for Pneumonia and Subsequent Risk of Cardiovascular Disease. *JAMA* **313**, 264-274 (2015). https://doi.org:10.1001/jama.2014.18229

49 Thygesen, K., Alpert, J. S., Jaffe, A. S., Chaitman, B. R., Bax, J. J., Morrow, D. A., White, H. D. & Executive Group on Behalf of the Joint European Society of Cardiology (ESC) /American College of Cardiology (ACC) /American Heart Association (AHA) /World Heart Federation (WHF) Task Force for the Universal Definition of Myocardial Infarction. Fourth Universal Definition of Myocardial Infarction (2018). *Circulation* **138**, e618-e651 (2018). https://doi.org:10.1161/CIR.0000000000000617

50 Mishra, P. K., Adameova, A., Hill, J. A., Baines, C. P., Kang, P. M., Downey, J. M., Narula, J., Takahashi, M., Abbate, A., Piristine, H. C., Kar, S., Su, S., Higa, J. K., Kawasaki, N. K. & Matsui, T. Guidelines for Evaluating Myocardial Cell Death. *Am J Physiol Heart Circ Physiol* **317**, H891-H922 (2019). https://doi.org:10.1152/ajpheart.00259.2019

CHAPTER V

SUMMARY AND FUTURE DIRECTIONS

The field of HAP has significantly advanced in the past 30 years, with improved medical care for the critically ill. With more patients than ever before recovering from HAP and returning home, new and previously unknown complications have become apparent in these patients. End-organ damage seen in ICU HAP survivors extends to many different organ systems, including the brain, heart, lungs, muscles, and the innate immune system, and has become a major point of interest[1-12]. While pneumonia is a common cause of end-organ dysfunction, the mechanisms underlying these dysfunctions are not yet understood.

Patients that recover from HAP often have significant neurocognitive impairments, increased risk of heart attacks and strokes, neuromuscular weakness as well as a decrease in their quality of life[2,5,6,11,13]. Aβ and tau have been of significant interest in the field of dementia due to their involvement with Alzheimer's disease, but the role of these proteins in the end organ dysfunction seen in the aftermath of critical illness is poorly understood[14-17]. While it is known that the pulmonary endothelium produces and secretes Aβ and tau during bacterial pneumonia, the relevance of the release of these proteins after the infection has cleared is understudied[18-22]. Here, we looked at the role of GSAP, a protein involved in the production of Aβ, as a contributor to not only the

severity of bacterial pneumonia, but the contribution it plays in the end-organ damage seen in the aftermath of pneumonia.

To study the effects of GSAP on the response to bacterial pneumonia, we generated a novel GSAP knockout rat and used a *P. aeruginosa* model to induce pneumonia. Our studies indicate a previously unknown role for GSAP in the pulmonary edema and hypoxemia that follows infection, neutrophil maturation, infarction size following ischemia reperfusion injury after infection, infection-induced increase in neurotransmitter release probability, and post-synaptic hyperexcitability.

The presence of GSAP appears to be detrimental in the lung and heart after bacterial infection but not in the brain. The short-term measurements of learning and memory in these animals showed that the presence of GSAP is a positive regulator of LTP, both before and after infection, as it acts to prevent post-synaptic hyperexcitability of CA1 neurons. This is significant because hyperexcitability of neurons leads to an increase in secretion of cytotoxic proteins like Aβ and tau, which in turn causes more hyperexcitability. This hyperexcitability occurs through calcium dysregulation and glutamate and glutamate receptors, namely the NMDAR, and leads to mitochondrial dysfunction and cell death[23-26]. The specific role that GSAP is playing in mitigating the damaging and potentially lethal effects of the Aβ that is produced and secreted during bacterial infection needs to be further addressed. Multiphoton imaging with fluorescent calcium indicators in live rats would allow us to analyze the location of neuronal activity in real time with single-action potential accuracy as well as visualizing the location of Aβ plaques[27-29]. This could help tease out the otherwise convoluted impact of GSAP on suppression of potentially excitotoxic hyperexcitability. Further investigation needs to be

done on the long-term impacts of GSAP on learning and memory after recovery from bacterial pneumonia to determine if the protection seen is merely transient. Seeing as many survivors of HAP experience neurocognitive dysfunction, it would be interesting to look at the impacts of GSAP on the pre- and post- pneumonia anxiety, depressive, and addiction behaviors in our animals. Many studies have been done to access the presence and rates of addiction in the aftermath of critical illness, namely opioid addiction, but I have yet to find any on the presence or likelihood of developing addictions or addictive behaviors (non-opioid related) in survivors of critical illness.

Neuromuscular weakness as well as a decrease in physical quality of life is seen in many that recover from critical illness[5,6,11]. Neuromuscular weakness can be caused by sodium and calcium channel abnormalities, calcium dysregulation, and/or mitochondrial dysfunction among other things[5,6,11]. GSAP was recently shown to interact with 80 different proteins involved in lipid metabolism, mitochondrial function, and protein phosphorylation[30]. The mitochondria regulate lipid transport, metabolism, and storage. Mitochondrial bioenergetic dysfunction and lipid accumulation in skeletal muscle leads to myopathy and muscle weakness[31,32]. The role GSAP plays in the development and severity of neuromuscular weakness in survivors of critical illness should be explored due to the many connections between GSAP and proteins that are involved in the causes of neuromuscular weakness. Behavioral tests including the elevated body swing test, the beam balance test, the ladder-climbing test, and the forelimb grip force should be done on our rats before and after recovery from pneumonia to access the contribution or lack thereof GSAP to neuromuscular weakness.

The findings laid out in this dissertation are many and significant and have set the stage for further discoveries on the role GSAP plays in many physiologic and pathologic states.

5.1 References

1 Angus, D. C., Carlet, J. & 2002 Brussels Roundtable Participants. Surviving Intensive Care: A Report From The 2002 Brussels Roundtable. *Intensive Care Med* **29**, 368-377 (2003). https://doi.org:10.1007/s00134-002-1624-8

2 Corrales-Medina, V. F., Alvarez, K. N., Weissfeld, L. A., Angus, D. C., Chirinos, J. A., Chang, C. C., Newman, A., Loehr, L., Folsom, A. R., Elkind, M. S., Lyles, M. F., Kronmal, R. A. & Yende, S. Association Between Hospitalization for Pneumonia and Subsequent Risk of Cardiovascular Disease. *JAMA* **313**, 264-274 (2015). https://doi.org:10.1001/jama.2014.18229

3 Davidson, T. A., Caldwell, E. S., Curtis, J. R., Hudson, L. D. & Steinberg, K. P. Reduced Quality of Life in Survivors of Acute Respiratory Distress Syndrome Compared with Critically Ill Control Patients. *JAMA* **281**, 354-360 (1999). https://doi.org:10.1001/jama.281.4.354

4 de Azevedo, J. R., Montenegro, W. S., Rodrigues, D. P., de C. Souza, S. C., Araujo, V. F., de Paula, M. P., Prazeres, P. H., da Luz Leitão, A. & Mendonça, A. V. Long-Term Cognitive Outcomes Among Unselected Ventilated and Non-Ventilated ICU Patients. *J Intensive Care* **5**, 18 (2017). https://doi.org:10.1186/s40560-017-0213-4

5 Fan, E., Dowdy, D. W., Colantuoni, E., Mendez-Tellez, P. A., Sevransky, J. E., Shanholtz, C., Himmelfarb, C. R., Desai, S. V., Ciesla, N., Herridge, M. S., Pronovost, P. J. & Needham, D. M. Physical Complications in Acute Lung Injury Survivors: A Two-Year Longitudinal Prospective Study. *Crit Care Med* **42**, 849-859 (2014). https://doi.org:10.1097/CCM.0000000000000040

6 Fletcher, S. N., Kennedy, D. D., Ghosh, I. R., Misra, V. P., Kiff, K., Coakley, J. H. & Hinds, C. J. Persistent Neuromuscular and Neurophysiologic Abnormalities in Long-Term Survivors of Prolonged Critical Illness. *Crit Care Med* **31**, 1012-1016 (2003). https://doi.org:10.1097/01.CCM.0000053651.38421.D9

7 Griffiths, J., Hatch, R. A., Bishop, J., Morgan, K., Jenkinson, C., Cuthbertson, B. H. & Brett, S. J. An Exploration of Social and Economic Outcome and Associated Health-Related Quality of Life After Critical Illness in General Intensive Care Unit Survivors: A 12-Month Follow-Up Study. *Crit Care* **17**, R100 (2013). https://doi.org:10.1186/cc12745

8 Gunst, J. Recovery from Critical Illness-Induced Organ Failure: The Role of Autophagy. *Crit Care* **21** (2017). https://doi.org:10.1186/s13054-017-1786-y

9 Jackson, J. C., Pandharipande, P. P., Girard, T. D., Brummel, N. E., Thompson, J. L., Hughes, C. G., Pun, B. T., Vasilevskis, E. E., Morandi, A., Shintani, A. K., Hopkins, R. O., Bernard, G. R., Dittus, R. S., Ely, E. W., Bringing to Light the Risk & Incidence of Neuropsychological Dysfunction in ICU Survivors (BRAIN-ICU) Study Investigators (2014). Depression, Post-Traumatic Stress Disorder, and Functional Disability in Survivors of Critical Illness in the BRAIN-ICU Study: A Longitudinal Cohort Study. *Lancet Respir Med* **2**, 369-379 (2014). https://doi.org:10.1016/S2213-2600(14)70051-7

10 Mehlhorn, J., Freytag, A., Schmidt, K., Brunkhorst, F. M., Graf, J., Troitzsch, U., Schlattmann, P., Wensing, M. & Gensichen, J. Rehabilitation Interventions for Postintensive Care Syndrome: A Systematic Review. *Crit Care Med* **42**, 1263-1271 (2014). https://doi.org:10.1097/CCM.0000000000000148

11 Needham, D. M., Wozniak, A. W., Hough, C. L., Morris, P. E., Dinglas, V. D., Jackson, J. C., Mendez-Tellez, P. A., Shanholtz, C., Ely, E. W., Colantuoni, E., Hopkins, R. O. & National Institutes of Health NHLBI ARDS Network (2014). Risk Factors for Physical Impairment After Acute Lung Injury in a National, Multicenter Study. *Am J Respir Crit Care Med* **189**, 1214-1224 (2014). https://doi.org:10.1164/rccm.201401-0158OC

12 Pandharipande, P. P., Girard, T. D., Jackson, J. C., Morandi, A., Thompson, J. L., Pun, B. T., Brummel, N. E., Hughes, C. G., Vasilevskis, E. E., Shintani, A. K., Moons, K. G., Geevarghese, S. K., Canonico, A., Hopkins, R. O., Bernard, G. R., Dittus, R. S., Ely, E. W. & BRAIN-ICU Study Investigators (2013) Long-Term Cognitive Impairment After Critical Illness. *N Engl J Med* **369**, 1306-1316 (2013). https://doi.org:10.1056/NEJMoa1301372

13 Davydow, D. S., Hough, C. L., Levine, D. A., Langa, K. M. & Iwashyna, T. J. Functional Disability, Cognitive Impairment, and Depression After Hospitalization for Pneumonia. *Am J Med* **126**, 615-624.e5 (2013). https://doi.org:10.1016/j.amjmed.2012.12.006

14 Chen, G. F., Xu, T. H., Yan, Y., Zhou, Y. R., Jiang, Y., Melcher, K. & Xu, H. E. Amyloid β: Structure, Biology and Structure-Based Therapeutic Development. *Acta Pharmacologica Sinica* **38**, 1205-1235 (2017). https://doi.org:10.1038/aps.2017.28

15 Murphy, M. P. & LeVine, H., 3rd. Alzheimer's Disease and the β-Amyloid Peptide. *J Alzheimers Dis* **19**, 311-323 (2010). https://doi.org:10.3233/JAD-2010-1221

16 Prasansuklab, A. & Tencomnao, T. Amyloidosis in Alzheimer's Disease: The Toxicity of Amyloid Beta (Aβ), Mechanisms of its Accumulation and Implications of Medicinal Plants for Therapy. *J Evid Based Complementary Altern Med* **2013**, 413808

17 Younkin, S. G. The Role of Aβ42 in Alzheimer's Disease. *J Physiol Paris* **92**, 289-292 (1998). https://doi.org:10.1016/S0928-4257(98)80035-1

18 Balczon, R., Lin, M. T., Lee, J. Y., Abbasi, A., Renema, P., Voth, S. B., Zhou, C., Koloteva, A., Michael Francis, C., Sodha, N. R., Pittet, J. F., Wagener, B. M., Bell, J., Choi, C. S., Ventetuolo, C. E. & Stevens, T. Pneumonia Initiates a Tauopathy. *FASEB J* **35**, e21807 (2021). https://doi.org:10.1096/fj.202100718R

19 Balczon, R., Morrow, K. A., Zhou, C., Edmonds, B., Alexeyev, M., Pittet, J. F., Wagener, B. M., Moser, S. A., Leavesley, S., Zha, X., Frank, D. W. & Stevens, T. *Pseudomonas aeruginosa* Infection Liberates Transmissible, Cytotoxic Prion Amyloids. *FASEB J* **31**, 2785-2796 (2017). https://doi.org:10.1096/fj.201601042RR

20 Balczon, R., Pittet, J. F., Wagener, B. M., Moser, S. A., Voth, S., Vorhees, C. V., Williams, M. T., Bridges, J. P., Alvarez, D. F., Koloteva, A., Xu, Y., Zha, X. M., Audia, J. P., Stevens, T. & Lin, M. T. Infection-Induced Endothelial Amyloids Impair Memory. *FASEB J* **33**, 10300-10314 (2019). https://doi.org:10.1096/fj.201900322R

21 Balczon, R., Prasain, N., Ochoa, C., Prater, J., Zhu, B., Alexeyev, M., Sayner, S., Frank, D. W. & Stevens, T. *Pseudomonas aeruginosa* Exotoxin Y-Mediated Tau Hyperphosphorylation Impairs Microtubule Assembly in Pulmonary Microvascular Endothelial Cells. *PLoS One* **8**, e74343 (2013). https://doi.org:10.1371/journal.pone.0074343

22 Voth, S., Gwin, M., Francis, C. M., Balczon, R., Frank, D. W., Pittet, J. F., Wagener, B. M., Moser, S. A., Alexeyev, M., Housley, N., Audia, J. P., Piechocki, S., Madera, K., Simmons, A., Crawford, M. & Stevens, T. Virulent *Pseudomonas aeruginosa* Infection Converts Antimicrobial Amyloids into Cytotoxic Prions. *FASEB J* **34**, 9156-9179 (2020). https://doi.org:10.1096/fj.202000051RRR

23 Busche, M. A. & Konnerth, A. Impairments of Neural Circuit Function in Alzheimer's Disease. *Philos Trans R Soc Lond B Biol Sci* **371**, 20150429 (2016). https://doi.org:10.1098/rstb.2015.0429

24 Busche, M. A., Wegmann, S., Dujardin, S., Commins, C., Schiantarelli, J., Klickstein, N., Kamath, T. V., Carlson, G. A., Nelken, I. & Hyman, B. T. Tau Impairs Neural Circuits, Dominating Amyloid-β Effects, in Alzheimer Models In Vivo. *Nat Neurosci* **22**, 57-64 (2019). https://doi.org:10.1038/s41593-018-0289-8

25 Toniolo, S., Sen, A. & Husain, M. Modulation of Brain Hyperexcitability: Potential New Therapeutic Approaches in Alzheimer's Disease. *Int J Mol Sci* **21**, 9318 (2020). https://doi.org:10.3390/ijms21239318

26 Targa Dias Anastacio, H., Matosin, N. & Ooi, L. Neuronal Hyperexcitability in Alzheimer's Disease: What are the Drivers Behind this Aberrant Phenotype? *Transl Psychiatry* **12**, 257 (2022). https://doi.org:10.1038/s41398-022-02024-7

27 Busche, M. A., Eichhoff, G., Adelsberger, H., Abramowski, D., Wiederhold, K. H., Haass, C., Staufenbiel, M., Konnerth, A. & Garaschuk, O. Clusters of Hyperactive Neurons Near Amyloid Plaques in a Mouse Model of Alzheimer's Disease. *Science* **321**, 1686-1689 (2008). https://doi.org:10.1126/science.1162844

28 Stosiek, C., Garaschuk, O., Holthoff, K. & Konnerth, A. In Vivo Two-Photon Calcium Imaging of Neuronal Networks. *Proc Natl Acad Sci U S A* **100**, 7319-7324 (2003). https://doi.org:10.1073/pnas.1232232100

29 Eichhoff, G., Busche, M. A. & Garaschuk, O. In Vivo Calcium Imaging of the Aging and Diseased Brain. *Eur J Nucl Med Mol Imaging* **35**, S99-S106 (2008). https://doi.org:10.1007/s00259-007-0709-6

30 Xu, P., Chang, J. C., Zhou, X., Wang, W., Bamkole, M., Wong, E., Bettayeb, K., Jiang, L. L., Huang, T., Luo, W., Xu, H., Nairn, A. C., Flajolet, M., Ip, N. Y., Li, Y. M. & Greengard, P. GSAP Regulates Lipid Homeostasis and Mitochondrial Function Associated with Alzheimer's Disease. *J Exp Med* **218**, e20202446 (2021). https://doi.org:10.1084/jem.20202446

31 Debashree, B., Kumar, M., Keshava Prasad, T. S., Natarajan, A., Christopher, R., Nalini, A., Bindu, P. S., Gayathri, N. & Srinivas Bharath, M. M. Mitochondrial Dysfunction in Human Skeletal Muscle Biopsies of Lipid Storage Disorder. *J Neurochem* **145**, 323-341 (2018). https://doi.org:10.1111/jnc.14318

32 Falabella, M., Vernon, H. J., Hanna, M. G., Claypool, S. M. & Pitceathly, R. D. S. Cardiolipin, Mitochondria, and Neurological Disease. *Trends Endocrinol Metab* **32**, 224-237 (2021). https://doi.org:10.1016/j.tem.2021.01.006

BIOGRAPHICAL SKETCH

Name of Author: Meredith S. Gwin

Graduate and Undergraduate Schools Attended:

Coastal Alabama Community College, Bay Minette, Alabama

University of Mobile, Mobile, Alabama

University of South Alabama, Mobile, Alabama

Degrees Awarded:

Coastal Alabama Community College
Associate of Arts, Liberal Arts, summa cum laude 2014
Associate of Science, General Studies, summa cum laude 2014

University of Mobile
Bachelor of Science., Pre-Professional Biology with a minor in Chemistry, summa cum laude 2016

University of South Alabama
Doctor of Philosophy., Basic Medical Science, Physiology and Cell Biology, Center for Lung Biology

Awards and Honors:

1. The University of South Alabama College of Medicine Dean's Predoctoral Fellowship #00541R 04/01/2018-12/31/2018

2. American Heart Association Predoctoral Fellowship #19PRE34380166 01/01/2019-12/31/2020

Publications:

1. Scott AM, Jager AC, **Gwin MS**, Voth S, Balczon R, Stevens T, Lin MT. Pneumonia-Induced Endothelial Amyloids Reduce Dendritic Spine Density in Brain Neurons. *Sci Rep*. 2020 Jun 9;10(1):9327. doi: 10.1038/s41598-020-66321-1. PMID: 32518286; PMCID: PMC7283224.
2. Voth S, **Gwin MS**, Francis CM, Balczon R, Frank DW., Pittet JF, Wagener BM, Moser SA, Alexeyev M, Housley N, Audia JP, Piechocki S, Madera K, Simmons A, Crawford M, Stevens T. Virulent *Pseudomonas aeruginosa* Infection Converts Antimicrobial Amyloids into Cytotoxic Prions. *FASEB J*. 2020 Jul;34(7):9156-9179. doi: 10.1096/fj.202000051RRR. Epub 2020 May 15. PMID: 32413239; PMCID: PMC7383673.
3. Lee JY, Stevens RP, Kash M, Alexeyev MF, Balczon R, Zhou C, Renema P, Koloteva A, Kozhukhar N, Pastukh V, **Gwin MS**, Voth S, deWeever A, Wagener BM, Pittet JF, Eslaamizaad Y, Siddiqui W, Nawaz T, Clarke C, Fouty BW, Audia JP, Alvarez DF, Stevens T. Carbonic Anhydrase IX and Hypoxia Promote Rat Pulmonary Endothelial Cell Survival during Infection. *Am J Respir Cell Mol Biol.* 2021 Dec;65(6):630-645. doi: 10.1165/rcmb.2020-0537OC. PMID: 34251286; PMCID: PMC8641799.

4. Choi CS, **Gwin MS**, Voth S, Kolb C, Zhou C, Nelson AR, deWeever A, Koloteva A, Annamdevula NS, Murphy JM, Wagener BM, Pittet JF, Lim SS, Balczon R, Stevens T, Lin MT. Cytotoxic Tau Released from Lung Microvascular Endothelial Cells upon Infection with *Pseudomonas aeruginosa* Promotes Neuronal Tauopathy. *J Biol Chem*. 2022 Jan;298(1):101482. doi: 10.1016/j.jbc.2021.101482. Epub 2021 Dec 8. PMID: 34896150; PMCID: PMC8718960.

5. **Gwin MS,** Alexeyev MF, Geurts AM, Lee JY, Zhou C, Yang X-M, Cohen MV, Downey JM, Barrington RA, Spadafora D, Audia JP, Frank DW, Voth S, Pastukh VV, Bell J, Ayers L, Tambe DT, Nelson AR, Balczon R, Lin MT, Stevens T. Gamma Secretase Activating Protein Promotes End-Organ Dysfunction After Bacterial Pneumonia. *AJP Lung. Resubmitted March 2023*

6. Lee JY, Stevens RP, Pastukh VV, Pastukh VM, Kozhukhar N, Alexeyev MF, Reisz JA, Nerguizian D, D'Alessandro A, Koloteva A, **Gwin MS**, Roberts JT, Borchert GM, Wagener BM, Pittet JF, Graham BB, Stenmark KR, and Stevens T. PFKFB3 Inhibits Fructose Metabolism in Pulmonary Microvascular Endothelial Cells. *Am. J. Respir. Cell Mol. Resubmitted April 2023*